5-2013

Tuning Sol-Gel Phase Diagrams of Doubly Thermosensitive Hydrophilic Diblock Copolymers in Water

Naixiong Jin
njin@utk.edu

To the Graduate Council:

I am submitting herewith a dissertation written by Naixiong Jin entitled "Tuning Sol-Gel Phase Diagrams of Doubly Thermosensitive Hydrophilic Diblock Copolymers in Water." I have examined the final electronic copy of this dissertation for form and content and recommend that it be accepted in partial fulfillment of the requirements for the degree of Doctor of Philosophy, with a major in Chemistry.

<div align="right">Bin Zhao, Major Professor</div>

We have read this dissertation and recommend its acceptance:

Mark D. Dadmun, Charles S. Feigerle, Wei He

<div align="right">Accepted for the Council:
<u>Dixie L. Thompson</u></div>

<div align="right">Vice Provost and Dean of the Graduate School</div>

(Original signatures are on file with official student records.)

Tuning Sol-Gel Phase Diagrams of Doubly Thermosensitive Hydrophilic Diblock Copolymers in Water

A Dissertation

Presented for the

Doctor of Philosophy Degree

The University of Tennessee, Knoxville

Naixiong Jin

May 2013

Acknowledgements

Abstract

This dissertation presents the synthesis of stimuli-responsive hydrophilic diblock copolymers and the study of their behavior in water under various conditions. The polymers were made by "living"/controlled radical polymerization. Chapter 1 presents a background of this dissertation. Chapters 2-4 describe a family of doubly thermosensitive diblock copolymers with a small amount of carboxylic acid groups incorporated into either one or both blocks. The lower critical solution temperature (LCST) of the weak acid-containing block increases with increasing pH due to the ionization of carboxylic acid. Chapter 5 presents the preparation of pH-sensitive diblock copolymer micelle-embedded agarose hydrogels.

Chapter 2 describes the synthesis and solution behavior of poly(methoxytri(ethylene glycol) acrylate-*co*-acrylic acid)-*b*-poly(ethoxydi(ethylene glycol) acrylate) (P(TEGMA-*co*-AA)-*b*-PDEGEA)). PTEGMA and PDEGEA are thermosensitive polymers with LCSTs of 58 and 9 °C [degree Celsius], respectively, in water. A 20 wt% aqueous solution of P(TEGMA-*co*-AA)-*b*-PDEGEA with pH of 3.11 underwent transitions from a free-flowing liquid, to a free-standing gel, to a hot liquid, and to a cloudy mixture upon heating. The $T_{\text{sol-gel}}$ [sol-to-gel transition temperature] and $T_{\text{gel-sol}}$ [gel-to-sol transition temperature] are closely related to the LCSTs of the two blocks. Upon raising pH, the $T_{\text{gel-sol}}$ increased, while the $T_{\text{sol-gel}}$ remained the same. Accordingly, only the upper boundary of the sol-gel phase diagram shifted upward.

Chapter 3 presents the tuning of $T_{\text{sol-gel}}$ of moderately concentrated aqueous solutions of doubly thermosensitive diblock copolymers by incorporating a small amount of AA groups into the lower LCST block and changing the solution pH. The AA content had a

significant effect on the pH dependence of $T_{\text{sol-gel}}$. Chapter 4 shows that by incorporating a small amount of carboxylic acid groups into both blocks of a doubly thermosensitive diblock copolymer, the C-shaped sol-gel phase diagram can be readily and reversibly shifted by changing the solution pH.

Chapter 5 presents the fabrication of pH-sensitive diblock copolymer micelle-embedded agarose hydrogels. The gel properties were not significantly affected by the incorporation of the micelles even when the polymer concentration reached 5 mg/g. The pH-induced release of the payload from the core of micelles in a hybrid gel was studied. Chapter 6 presents conclusions and future work.

Table of Contents

List of Tables

List of Schemes

List of Figures

List of Abbreviations

AA: Acrylic acid

AIBN: 2,2'-Azobis(2-methylpropionitrile)

ATRP: Atom transfer radical polymerization

tBA: *tert*-Butyl acrylate

bcc: Body-centered cubic

CGC: Critical gelation concentration

CMT: Critical micellization temperature

CTA: Chain transfer agent

DEGEA: Ethoxydi(ethylene glycol) acrylate (or: di(ethylene glycol) ethyl ether acrylate)

D_h: Hydrodynamic diameter

DMF: *N,N*-Dimethylformamide

DLS: Dynamic light scattering

DP: Degree of polymerization

DPAEMA: 2-(*N,N*-Diisopropylamino)ethyl methacrylate

DSC: Differential scattering calorimetry

fcc: Face-centered cubic

GPC: Gel permeation chromatography

hcp: Hexagonal close-packing

HMTETA: 1,1,4,7,10,10-Hexamethyltriethylenetetramine

^{1}H NMR: Proton nuclear magnetic resonance spectroscopy

kDa: kilodaltons

KHP: Potassium hydrogen phthalate

LCST: Lower critical solution temperature

MEI: Maximum emission intensity

M_n: Number average molecular weight

PBS: Phosphate buffered saline

PDEGEA: Poly(ethoxydi(ethylene glycol) acrylate)

PDI: Polydispersity index

PDPAEMA: Poly(2-(*N*,*N*-diisopropylamino)ethyl methacrylate)

PEO: Poly(ethylene oxide)

PEO-*b*-PDPAEMA: Poly(ethylene oxide)-*b*-poly(2-(*N*,*N*-diisopropylamino)ethyl

methacrylate)

PEO-*b*-PPO-b-PEO: Poly(ethylene oxide)-*b*-poly(propylene oxide)-*b*-poly(ethylene

oxide)

PEO-*b*-P(TEGEA-*co*-NBA): Poly(ethylene oxide)-*b*-poly(ethoxytri(ethylene glycol)

acrylate-*co*-*o*-nitrobenzyl acrylate)

PPO: Poly(propylene oxide)

PTEGEA: Poly(ethoxytri(ethylene glycol) acrylate)

PTEGMA: Poly(methoxytri(ethylene glycol) acrylate)

PTEGMA-*b*-PDEGEA: Poly(methoxytri(ethylene glycol) acrylate)-*b*-

poly(ethoxydi(ethylene glycol) acrylate)

PTEGMA-*b*-P(DEGEA-*co*-AA): Poly(methoxytri(ethylene glycol) acrylate)-*b*-

poly(ethoxydi(ethylene glycol) acrylate-*co*-acrylic acid)

PTEGMA-*b*-P(DEGEA-*co-t*BA): Poly(methoxytri(ethylene glycol) acrylate)-*b*-poly(ethoxydi(ethylene glycol) acrylate-*co-tert*-butyl acrylate)

P(TEGMA-*co*-AA)-*b*-PDEGEA: Poly(methoxytri(ethylene glycol) acrylate-*co*-acrylic acid)-*b*-poly(ethoxydi(ethylene glycol) acrylate)

P(TEGMA-*co*-AA)-*b*-P(DEGEA-*co*-AA): Poly(methoxytri(ethylene glycol) acrylate-*co*-acrylic acid)-*b*-poly(ethoxydi(ethylene glycol) acrylate-*co*-acrylic acid))

P(TEGMA-*co-t*BA)-*b*-PDEGEA: Poly(methoxytri(ethylene glycol) acrylate-*co-tert*-butyl acrylate)-*b*-poly(ethoxydi(ethylene glycol) acrylate)

P(TEGMA-*co-t*BA)-*b*-P(DEGEA-*co-t*BA): Poly(methoxytri(ethylene glycol) acrylate-*co-tert*-butyl acrylate)-*b*-poly(ethoxydi(ethylene glycol) acrylate-*co-tert*-butyl acrylate)

RAFT: Reversible addition-fragmentation chain transfer (polymerization)

SAXS: Small-angle X-ray scattering

SEC: Size exclusion chromatography

$T_{clouding}$: Clouding temperature

TEGMA: Methoxytri(ethylene glycol) acrylate (or: tri(ethylene glycol) methyl ether acrylate)

TFA: Trifluoroacetic acid

$T_{gel-sol}$: Gel-to-sol transition temperature

THF: Tetrahydrofuran

$T_{\text{sol-gel}}$: Sol-to-gel transition temperature

Chapter 1. Introduction

Diblock copolymers can self-associate into, often spherical, micelles in a selective solvent with the solvophobic block forming the core and the solvophilic block forming the corona.[1,2] In a moderately concentrated solution, micelles are packed into an ordered structure, leading to the formation of a gel.[1-25] As a result, the free-flowing solution is transformed into a free-standing micellar gel. The sol-to-gel and gel-to-sol transitions of diblock copolymer solutions, especially aqueous solutions of thermosensitive block copolymers, have been intensively studied in the past decades and have found technological uses, e.g., in controlled drug delivery and tissue engineering.[26-29]

Poly(ethylene oxide) (PEO)-based block copolymers have gained considerable attention, particularly PEO-*b*-poly(propylene oxide)-*b*-PEO (PEO-*b*-PPO-*b*-PEO) triblock copolymers.[1-3,12-25,30] Above critical gelation concentration, aqueous solutions of PEO-*b*-PPO-*b*-PEO undergo a sol-gel-sol transition upon heating. The sol-to-gel transition is caused by the micelles packing into an ordered structure with increasing temperature. The gel-to-sol transition results from the shrinking of the PEO corona at higher temperatures. The hard gel boundary in this type of phase diagram is usually a C-shaped curve. Besides PEO-*b*-PPO-*b*-PEO, other block copolymers capable of forming micellar gels in water have been synthesized. For example, the PPO blocks can be replaced with other polymers, such as poly(1,2-butylene oxide) (PBO),[15] poly(L-lactic acid) (PLLA)[28] or (DL-lactic acid-*co*-glycolic acid) (PLGA).[31] Recently, Aoshima et al. synthesized a series of non-PEO-based thermosensitive block copolymers by living cationic polymerization , such as poly(2-(2-ethoxy)ethoxyethyl vinyl ether)-*b*-poly(2-methoxyethyl vinyl ether) (PEOEOVE-*b*- PMOVE).[32-35]

Recently, aqueous block copolymer micellar gels that can respond to more than one external stimulus have gained great interest.[29,36-43] Considerable effort has been invested on temperature- and pH-sensitive block copolymers because these two stimuli are relatively easy to control. These block copolymers were usually prepared in one of three ways, by growing pH-responsive blocks from or introducing pH-sensitive groups to the chain ends of an ABA triblock thermosensitive copolymer,[36-41,44,45] or by reacting pyromellitic dianhydride with PEO-*b*-PPO-*b*-PEO to introduce carboxylic acid groups at the junction points,[42] or by synthesizing multiblock copolymers composed of PEO and poly(amino urethane).[46,47]

Although the aqueous gels formed from these block copolymers can respond to both temperature and pH changes and have found practical uses in drug release and other biomedical applications, the molecular mechanisms underlying the sol-to-gel and gel-to-sol transitions are unclear and no attempts have been made to elucidate the gel structures. This is because the phase behaviors of multi-block copolymers composed of pH-sensitive blocks and thermosensitive blocks in water are very complicated. The introduction of pH-sensitive groups to the chain ends of PEO-*b*-PPO-*b*-PEO allows the gels to respond to pH variations, but again it is unclear how the ionization of end groups affects the LCST of the thermosensitive PPO block and the solubility of PEO (the LCST of PEO approaches the normal boiling point of water when the molecular weight is > 10,000 g/mol).

To address this issue, a series of well-defined diblock copolymers were developed. They are composed of two thermosensitive polymers possessing well-defined LCSTs, with either one or both of the blocks containing a small number of pH-responsive groups.

The sol-to-gel, gel-to-sol, or both transition temperatures can be tuned separately or simultaneously by changing the pH of the solution.

References

1. Hamley, I. W. *Block Copolymers in Solution: Fundamentals and Applications*, John Wiley & Sons: Chichester, 2005.

2. Hamley, I. W. *The Physics of Block Copolymers*, Oxford University Press: Oxford, 1998.

3. Hamley, I. W. *Phil. Trans. R. Soc. Lond. A* **2001**, *359*, 1017-1044.

4. Watanabe, H.; Kotaka, T.; Hashimoto, T.; Shibayama, M.; Kawai, H. *J. Rheology* **1982**, *26*, 153-179.

5. Shibayama, M.; Hashimoto, T.; Kawai, H. *Macromolecules* **1983**, *16*, 16-28.

6. Hashimoto, T.; Shibayama, M.; Kawai, H.; Watanabe, H.; Kotaka, T. *Macromolecules* **1983**, *16*, 361-371.

7. McConnell, G. A.; Gast, A. P.; Huang, J. S.; Smith, S. D. *Phys. Rev. Lett.* **1993**, *71*, 2102-2105.

8. Hanley, K. J.; Lodge, T. P.; Huang, C.-I. *Macromolecules* **2000**, *33*, 5918-5931.

9. Lodge, T. P.; Pudil, B.; Hanley, K. J. *Macromolecules* **2002**, *35*, 4707-4717.

10. Lodge, T. P.; Hanley, K. J.; Pudil, B.; Alahapperuma, V. *Macromolecules* **2003**, *36*, 816-822.

11. Willet, N.; Gohy, J. F.; Lei, L. C.; Heinrich, M.; Auvray, L.; Varshney, S.; Jérôme, R.; Leyh, B. *Angew. Chem. Int. Ed.* **2007**, *46*, 7988-7992.

12. Luo, Y. Z.; Nicholas, C. V.; Attwood, D.; Collett, J. H.; Price, C.; Booth, C. *Colloid Polym. Sci.* **1992**, *270*, 1094-1105.

13. Hvidt, S.; Jørgensen, E. B.; Schillén, K.; Brown, W. *J. Phys. Chem.* **1994**, *98*, 12320-12328.

14. Kelarakis, A.; Mingvanish, W.; Daniel, C.; Li, H.; Havredaki, V.; Booth, C.; Hamley, I. W.; Ryan, A. J. *Phys. Chem. Chem. Phys.* **2000**, *2*, 2755-2763.

15. Li, H.; Yu, G. -E.; Price, C.; Booth, C.; Hecht, E.; Hoffmann, H. *Macromolecules* **1997**, *30*, 1347-1354.

16. Deng, N.-J.; Luo, Y.-Z.; Tanodekaew, S.; Binham, N.; Attwood, D.; and Booth, C. *J. Polym. Sci. Part B: Polym. Phys.* **1995**, *33*, 1085-1096.

17. Mingvanish, W.; Mai, S.-M.; Heatley, F.; Booth, C.; Attwood, D. *J. Phys. Chem. B.* **1999**, *103*, 11269-11274.

18. Hamley, I. W.; Pople, J. A.; Fairclough, J. P. A.; Ryan, A. J.; Booth, C.; Yang, Y.-W. *Macromolecules* **1998**, *31*, 3906-3911.

19. Hamley, I. W.; Daniel, C.; Mingvanish, W.; Mai, S.-M.; Booth, C.; Messe, L.; Ryan, A. J. *Langmuir* **2000**, *16*, 2508-2514.

20. Mortensen, K.; Brown, W.; Norden, B. *Phys. Rev. Lett.* **1992**, *68*, 2340-2343.

21. Mortensen, K. *Europhys. Lett.* **1992**, *19*, 599-604.

22. Alexandridis, P.; Hatton, T. A. *Colloids and Surfaces A: Physicochem. Eng. Aspects* **1995**, *96*, 1-46.

23. Alexandridis, P.; Olsson, U.; Kindman, B. *Langmuir* **1997**, *12*, 23-34.

24. Wanka, G.; Hoffmann, H.; Ulbricht, W. *Macromolecules* **1994**, *27*, 4145-4159.

25. Zhou, Z; Chu, B. *Macromolecules* **1994**, *27*, 2025-2033.

26. Gil, E.S.; Hudson, S.M. *Prog. Polym. Sci.* **2004**, *29*, 1173-1222.

27. Bromberg, L.E.; Ron, E.S. *Adv. Drug. Deliv. Rev.* **1998**, *31*, 197-221.

28. Jeong, B.; Bae, Y.H.; Lee, D.S.; Kim, S.W.; *Nature* **1997**, *388*, 860-862.

29. He, C. L.; Kim, S. W.; Lee, D. S. *J. Controlled Release* **2008**, *127*, 189-207.

30. Jiang, X.G.; Lavender, C.A.; Woodcock, J.W.; Zhao, B. *Macromolecules* **2008**, *41*, 2632-2643.

31. Jeong, B.; Bae, Y,H.; Kim, S.W. *Macromolecules* **1999**, *32*, 7064-7069.

32. Aoshima, S.; Sugihara, S. *J. Polym. Sci. Part A: Polym. Chem.* **2000**, *38*, 3962-3965.

33. Aoshima, S.; Sugihara, S.; Shibayama, M.; Kanaoka, S. *Macromol. Symp.* **2004**, *215*, 151-163.

34. Sugihara, S. Kanaoka, S.; Aoshima, S. *J. Polym. Sci. Part A: Polym. Chem.* **2004**, *42*, 2601-2611.

35. Sugihara, S.; Kanaoka, S.; Aoshima, S. *Macromolecules* **2005**, *38*, 1919-1927.

36. Anderson, B. C.; Cox, S. M.; Bloom, P. D.; Sheares, V. V.; Mallapragada, S. K. *Macromolecules* **2003**, *36*, 1670-1676.

37. Determan, M. D.; Cox, J. P.; Seifert, S.; Thiyagarajan, P.; Mallapragada, S. K. *Polymer* **2005**, *46*, 6933-6946.

38. Shim, W. S.; Yoo, J. S.; Bae, Y. H.; Lee, D. S. *Biomacromolecules* **2005**, *6*, 2930-2934.

39. Shim, W. S.; Kim, S. W.; Lee, D. S. *Biomacromolecules* **2006**, *7*, 1935-1941.

40. Dayananda, K.; Pi, B. S.; Kim, B. S.; Park, T. G.; Lee, D. S. *Polymer* **2007**, *48*, 758-762.

41. Park, S. Y.; Lee, Y.; Bae, K. H.; Ahn, C. H.; Park, T. G. *Macromol. Rapid Commun.* **2007**, *28*, 1172-1176.

42. Suh, J. M.; Bae, S. J.; Jeong, B. *Adv. Mater.* **2005**, *17*, 118-120.

43. Joo, M. K.; Park, M. H.; Choi, B. G.; Jeong, B. *J. Mater. Chem.* **2009**, *19*, 5891-5905.

44. Determan, M. D.; Guo, L.; Thiyagarajan, P.; Mallapragada, S. K. *Langmuir* **2006**, *22*,

1469-1473.

45. Shim, W.S.; Kim, J. H.; Park, H.; Kim, K.; Kwon, I. C.; Lee, D. S. *Biomaterials* **2006**, *27*, 5178-5185.

46. Dayananda, K.; He, C. L.; Park, D. K.; Park, T. G.; Lee, D. S. *Polymer* **2008**, *49*, 4968-4973.

47. Huynh, D. P.; Nguyen, M. K.; Kim, B. S.; Lee, D. S. *Polymer* **2009**, *50*, 2565-2571.

Chapter 2. Tuning Thermally Induced Gel-to-Sol Transition of Aqueous Solution of Multi-Responsive Hydrophilic Diblock Copolymer Poly(methoxytri(ethylene glycol) acrylate-*co*-acrylic acid)-*b*-poly(ethoxydi(ethylene glycol) acrylate)

Abstract

   This chapter presents the synthesis of a hydrophilic diblock copolymer composed of two distinct thermosensitive polymers with one block containing a small amount of carboxylic acid groups, poly(methoxytri(ethylene glycol) acrylate-*co*-acrylic acid)-*b*-poly(ethoxydi(ethylene glycol) acrylate) (P(TEGMA-*co*-AA)-*b*-PDEGEA)), and the study of thermo-induced sol-gel-sol transitions of its moderately concentrated aqueous solutions at various pH values. The diblock copolymer was obtained by the removal of *tert*-butyl groups of P(TEGMA-*co-tert*-butyl acrylate)-*b*-PDEGEA, which was synthesized by reversible addition fragmentation chain transfer polymerization. PTEGMA and PDEGEA are thermosensitive polymers with lower critical solution temperatures (LCSTs) of 58 and 9 °C, respectively, in water. The incorporation of a small amount of carboxylic acid groups into PTEGMA allowed the LCST of the P(TEGMA-*co*-AA) block to be tuned by changing the solution pH. We found that a 20 wt% aqueous solution of P(TEGMA-*co*-AA)-*b*-PDEGEA with pH of 3.11 (measured at 0 °C) underwent multiple phase transitions upon heating, from a clear, free-flowing liquid (< 19 °C), to a clear, free-standing gel (19 to 39 °C), to a clear, free flowing hot liquid (40 to 55 °C), and a cloudy mixture ($\geq$ 56 °C). With the increase of pH, the gel-to-sol transition ($T_{\text{gel-sol}}$) and the clouding temperature (T_{clouding}) of the sample shifted to higher values, while the sol-to-gel transition temperature ($T_{\text{sol-gel}}$) remained the same. These transitions and the tunability of $T_{\text{gel-sol}}$ stemmed from the thermosensitive properties of the two blocks of the diblock copolymer and the pH dependence of the LCST of P(TEGMA-*co*-AA), which were confirmed by differential scanning calorimetry and dynamic light scattering studies. Using the vial inversion test method, we further mapped out the C-

shaped sol-gel phase diagrams of (PTEGMA-*co*-AA)-*b*-PDEGEA in water in the moderate concentration range at three different pH values (3.11, 4.49, and 5.25, all measured at 0 °C). While the lower temperature boundaries overlapped, the upper temperature boundary shifted upward and the critical gelation concentration decreased with the increase of pH. In contrast, the sol-gel phase diagram of PTEGMA-*b*-PDEGEA, which contained no pH-responsive groups, showed no changes in $T_{\text{sol-gel}}$, $T_{\text{gel-sol}}$, and T_{clouding} with pH.

2.1 Introduction

Owing to the intriguing transitions between free-flowing liquids and free-standing gels and the associated changes in rheological properties, stimuli-induced reversible formation of aqueous micellar gels of block copolymers has received considerable interest.[1-3] Compared with chemically crosslinked hydrogels, these responsive micellar gels, especially those triggered by temperature changes, can be more advantageous for certain applications because of the in situ sol-gel transition.[1-3] For example, Jeong et al. reported injectable drug delivery systems based on aqueous solutions of block copolymers of poly(ethylene glycol) (PEO) and polylactide that can undergo cooling-induced sol-gel transitions.[3] The polymer solutions were loaded with a model drug in the sol state at an elevated temperature. Upon subcutaneous injection and cooling to the body temperature, the polymer solutions formed gels instantaneously that subsequently acted as matrices for sustained release of drug molecules.

Generally, there are two types of stimuli-responsive aqueous block copolymer micellar gels: 3-dimensional network gels, in which one block, e.g., the central block of an ABA triblock copolymer, forms bridges among micellar cores of other blocks,[1a,4] and physically jammed micellar gels, in which discrete spherical micelles of block copolymers are packed into an ordered structure.[1-3,5,6] Representative examples of the latter include aqueous gels of PEO-*b*-poly(propylene oxide)-*b*-PEO (PEO-*b*-PPO-*b*-PEO) triblock copolymers.[1,5] PPO is a thermosensitive water-soluble polymer exhibiting a lower critical solution temperature (LCST) in water at ~ 15 °C.[1,7] Above the LCST, PEO-*b*-PPO-*b*-PEO self-assembles into micelles with the dehydrated PPO blocks associated into the core and PEO blocks forming the corona. At a sufficiently high concentration,

i.e., above the critical gelation concentration (CGC), the aqueous solution of PEO-*b*-PPO-*b*-PEO undergoes sol-gel-sol transitions upon heating. The sol-gel phase diagram at low/moderate concentrations is usually a C-shaped curve.[1] It has been established that the sol-to-gel transition, corresponding to the lower temperature boundary in the phase diagram, is driven by the enhancement of micellization and the ordering of micelles with the increase of temperature, while the gel-to-sol transition, corresponding to the upper boundary, results from the shrinking of PEO at elevated temperatures. The ordered structures of micelles in the gel state have been confirmed by small-angle X-ray and neutron scattering studies.[1]

Besides PEO-*b*-PPO-*b*-PEO triblock copolymers, other block copolymers that can form thermosensitive micellar gels in water have also been reported.[2-4,6,8,9] For example, Aoshima et al. synthesized a series of well-defined vinyl ether block copolymers composed of two or more thermosensitive blocks with different LCSTs by living cationic polymerization.[9] They observed that 20 wt% aqueous solutions of these block copolymers underwent multi-stage transitions from clear liquids to transparent gels, to hot clear liquids, and phase separated opaque mixtures upon heating. The sol-to-gel and gel-to-sol transitions are closely related to the LCSTs of the thermosensitive blocks.

Our lab is especially interested in the active control of unimer-micelle and sol-gel transitions of thermosensitive hydrophilic block copolymers in water. The strategy used is to incorporate a small amount of stimuli-responsive groups into thermosensitive blocks of block copolymers such that the LCSTs of the thermosensitive blocks can be modified by applying an external stimulus.[10] These doubly responsive block copolymers can undergo multiple micellization and dissociation transitions in dilute aqueous solutions

13

and multiple sol-gel-sol transitions in moderately concentrated solutions in response to environmental variations. For example, Jiang et al. synthesized thermo- and light-responsive PEO-*b*-poly(ethoxytri(ethylene glycol) acrylate-*co*-*o*-nitrobenzyl acrylate) (PEO-*b*-P(TEGEA-*co*-NBA)) by atom transfer radical polymerization.[10a] PTEGEA is a thermosensitive polymer with an LCST of 36 °C in water and *o*-nitrobenzyl group is known to undergo a photo-cleavage reaction when exposed to 365 nm UV light.[11] The block copolymer dissolved molecularly in a 0.2 wt% aqueous solution when the temperature was below 25 °C and self-assembled into micelles at elevated temperatures. Upon UV irradiation, the *o*-nitrobenzyl groups were cleaved and the LCST of the thermosensitive block was increased, causing the micelles to dissociate. Further raising the temperature induced the formation of micelles again.[10a] At a polymer concentration of 20 wt%, multiple sol-gel-sol transitions were achieved.[10c] Such doubly responsive block copolymers are expected to offer more advantages for some potential applications compared with those that respond to only one external stimulus.

This chapter describes the synthesis of a well-defined hydrophilic diblock copolymer composed of two distinct thermosensitive polymers with the higher LCST block containing a small amount of carboxylic acid groups, poly(methoxytri(ethylene glycol) acrylate-*co*-acrylic acid)-*b*-poly(ethoxydi(ethylene glycol) acrylate) (P(TEGMA-*co*-AA)-*b*-PDEGEA), and the study of thermo-induced sol-gel-sol transitions of its moderately concentrated aqueous solutions at various pH values. PTEGMA and PDEGEA are thermosensitive water-soluble polymers with LCSTs of 58 and 9 °C, respectively, which belong to a new class of thermosensitive polymers with a short oligo(ethylene glycol) pendant from each repeat unit.[12] The block copolymer was prepared by reversible

14

addition-fragmentation chain transfer polymerization (RAFT)[13] and post-polymerization modification (Scheme 2.1). The incorporation of a small amount of carboxylic acid groups into PTEGMA allowed the LCST of the P(TEGMA-*co*-AA) block to be tuned by changing the solution pH. We show that the moderately concentrated aqueous solutions of this multi-responsive diblock copolymer undergo sol-gel-sol transitions upon heating and the gel-to-sol transition can be continuously tuned by adjusting the solution pH. It should be noted here that thermo- and pH-sensitive block copolymer aqueous gels have been reported in the literature.[14-17] The block copolymers used in those studies were usually prepared by either growing pH-sensitive blocks from or introducing pH-responsive groups onto the chain ends of an ABA triblock copolymer that can form thermoreversible gels in water (e.g., PEO-*b*-PPO-*b*-PEO).[14-16] Other types of multiblock copolymers were also employed.[17] We emphasize here that our thermo- and pH-sensitive polymer is a diblock copolymer and our block copolymer design, via the incorporation of a small amount of pH-responsive functional groups randomly distributed in one block, is different, which allows the LCST to be readily tuned.

2.2 Experimental Section

2.2.1 Materials

Anisole (99%, anhydrous) and trifluoroacetic acid (99%) were purchased from Acros and used as received. Hexanes, diethyl ether, 1.0 M KOH solution (volumetric standard solution), and 1.0 M HCl solution (volumetric standard solution) were obtained from Fisher Scientific. Di(ethylene glycol) ethyl ether acrylate (or ethoxydi(ethylene glycol) acrylate, DEGEA, ≥ 90 %, Aldrich) and *tert*-butyl acrylate (*t*BA, 99%, Fisher Scientific)
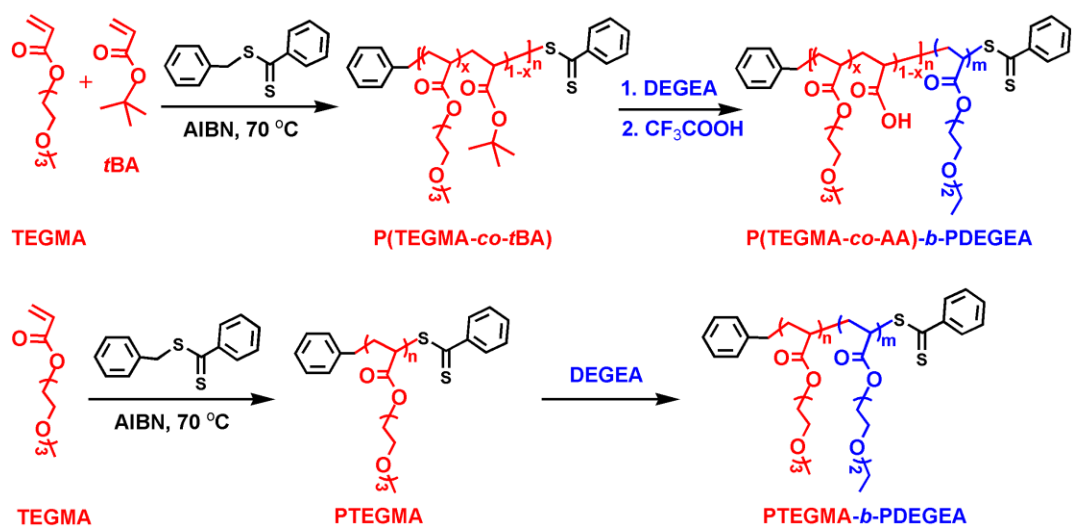
Scheme 2.1 Synthesis of P(TEGMA-*co*-AA)-*b*-PDEGEA and PTEGMA-*b*-PDEGEA

were dried over calcium hydride overnight, distilled under reduced pressure, and stored in a refrigerator prior to use. Methoxytri(ethylene glycol) acrylate (TEGMA) was synthesized according to the procedure described in the literature.[12f] 2,2'-Azobis(2-methylpropionitrile) (AIBN, 98%, Aldrich) was recrystallized in ethanol twice and dried under high vacuum at room temperature. The purified AIBN was then dissolved in N,N-dimethylformamide (DMF, extra dry, Acros) to make a solution with a concentration of 3.95 wt%. Benzyl dithiobenzoate, a chain transfer agent (CTA) used in RAFT, was synthesized according to a literature procedure [18] and the molecular structure was confirmed by ^{1}H and ^{13}C NMR spectroscopy. 20 mM aqueous potassium hydrogen phthalate (KHP) buffers were made by dissolving KHP in Milli-Q water and the pH values were adjusted by adding either a 1.0 M aqueous KOH or a 1.0 M aqueous HCl solution. All pH values in this work were measured with a pH meter (Accumet AB15 pH meter from Fisher Scientific, calibrated with pH = 4.01, 7.00, and 10.01 standard buffer solutions) in an ice/water bath (0 °C). All other solvents and chemicals were purchased from either Aldrich or Fisher and used without further treatment.

2.2.2 Characterization

Size exclusion chromatography (SEC) was carried out at room temperature using PL-GPC 20 (an integrated GPC system from Polymer Laboratories, Inc.) with a refractive index detector, one PLgel 5 μm guard column (50 × 7.5 mm), and two PLgel 5 μm mixed-C columns (each 300 × 7.5 mm, linear range of molecular weight from 200 to 2,000,000 Da according to Polymer Laboratories, Inc.). The data were processed using Cirrus^{TM} GPC/SEC software (Polymer Laboratories). Tetrahydrofuran was used as a carrier solvent at a flow rate of 1.0 mL/min. Polystyrene standards (Polymer

Laboratories, Inc.) were employed for calibration. The ^{1}H NMR (300 MHz) spectra were recorded on a Varian Mercury 300 NMR spectrometer.

2.2.3 Synthesis of Macro-CTA PTEGMA by RAFT

Below is a procedure for the synthesis of macro-CTA PTEGMA by RAFT. Benzyl dithiobenzoate (27.1 mg, 0.111 mmol), AIBN (40.8 mg of a solution of AIBN in DMF with a concentration of 39.5 mg/g, 0.0098 mmol), TEGMA (11.529 g, 52.8 mmol), and anisole (12.98 g) were added into a 50 mL two-necked flask. The mixture was stirred to form a homogeneous solution and degassed by three freeze-pump-thaw cycles. An aliquot was taken for ^{1}H NMR spectroscopy analysis. The polymerization was started by placing the flask in a 70 °C oil bath, and was monitored by ^{1}H NMR spectroscopy and SEC analysis. After the reaction proceeded for 325 min, the flask was removed from the oil bath and a sample was taken for the determination of the monomer conversion. The reaction mixture was diluted with THF and precipitated in hexanes. The polymer was then dissolved in THF (10 mL) and precipitated in a mixture of hexane and diethyl ether (v : v = 60 : 40, 200 mL). This process was repeated two more times. The polymer was then dried in vacuum and obtained as a very viscous liquid. SEC analysis results (polystyrene standards): $M_{n,SEC}$ = 24.5 kDa, polydispersity index (PDI) = 1.15. The DP of the polymer was calculated from the monomer conversion and the monomer-to-CTA ratio. The peaks located in the range of 4.0 - 4.5 ppm, which were from -CH_2OOC- of monomer TEGMA and the TEGMA units in the copolymer, were used as internal standard. The conversion was calculated from the integral values of the peaks from 5.8 to 5.9 ppm (CHH=CH- from TEGMA monomer) at t = 0 min and 325 min. The calculated DP was 166.

18

2.2.4 Synthesis of Diblock Copolymer PTEGMA-*b*-PDEGEA by RAFT Using Macro-CTA PTEGMA

PTEGMA (1.429 g, 0.0394 mmol), AIBN (21.6 mg of a solution of AIBN in DMF with a concentration of 39.5 mg/g, 0.0052 mmol), DEGEA (5.284 g, 28.1 mmol), and anisole (13.76 g) were added into a 50 mL two-necked flask. The mixture was degassed by three freeze-pump-thaw cycles. A sample was taken for ^{1}H NMR spectroscopy analysis and the flask was placed in a 70 °C oil bath. The polymerization was monitored by ^{1}H NMR spectroscopy and SEC analysis. After 325 min, the polymerization was stopped by removing the flask from the oil bath and diluting the mixture with THF. The polymer solution was precipitated in hexanes. The polymer was then dissolved in THF (15 mL) and precipitated in a mixture of hexane and diethyl ether (v : v = 60 : 40, 200 mL). This process was repeated two more times. The polymer was dried in vacuum. SEC results (polystyrene standards): $M_{n,SEC}$ = 41100 Da; PDI = 1.23. The composition of the block copolymer was determined from the ^{1}H NMR spectrum. The number of DEGEA units in the block copolymer was calculated using the integral values of the peak from 4.4 to 4.0 ppm (-CH_2OOC- of TEGMA and DEGEA units) and the peaks from 1.3 to 1.1 ppm (-CH$_2$CH_3 of DEGEA units). The obtained number of DEGEA units was 106.

2.2.5 Synthesis of Macro-CTA P(TEGMA-*co*-*t*BA) by RAFT

Benzyl dithiobenzoate (21.4 mg, 0.088 mmol), 2,2′-azobis(2-methylpropionitrile) (AIBN, 34.6 mg of a solution of AIBN in DMF with a concentration of 3.95 wt%, 0.0083 mmol), *tert*-butyl acrylate *(t*BA, 0.297 g, 2.32 mmol), TEGMA (9.469 g, 43.4 mmol), and anisole (10.25 g) were added into a 50 mL two-necked flask. The mixture was stirred under a nitrogen atmosphere and degassed by three freeze-pump-thaw cycles. A sample

was taken for ^{1}H NMR spectroscopy analysis, and the flask was placed in a 70 °C oil bath. The reaction was monitored by ^{1}H NMR spectroscopy and SEC analysis. After the polymerization proceeded for 255 min, the flask was removed from the oil bath and a sample was taken immediately for the determination of the monomer conversion by ^{1}H NMR spectroscopy. The reaction mixture was diluted with THF and precipitated in hexanes. The polymer was then dissolved in THF (10 mL) and precipitated in a mixture of hexane and diethyl ether (v : v = 60 : 40, 200 mL). This process was repeated an additional two times. The polymer was then dried in vacuum. SEC analysis results (polystyrene standards): $M_{n,SEC}$ = 28100 Da; polydispersity index (PDI) = 1.17. The DP of the copolymer was calculated from the monomer conversion and the monomer-to-CTA ratio. The peaks located in the range of 4.0 - 4.5 ppm, which were from -CH_2OOC-of monomer TEGMA and the TEGMA units in the copolymer, were used as internal standard. The conversion was calculated from the integral values of the peaks from 5.7 to 5.9 ppm (CHH=CH- from both TEGMA and tBA monomers) at t = 0 min and 255 min. The calculated DP was 194.

2.2.6 Synthesis of Diblock Copolymer P(TEGMA-*co*-*t*BA)-*b*-PDEGEA by RAFT Using Macro-CTA PTEGMA

P(TEGMA-*co*-*t*BA) (2.834 g, 0.0686 mmol), AIBN (34.8 mg of a solution of AIBN in DMF with a concentration of 3.95 wt%, 0.0084 mmol), DEGEA (9.083 g, 48.3 mmol), and anisole (21.84 g) were added into a 50 mL two-necked flask. The mixture was stirred under a nitrogen atmosphere and then degassed by three freeze-pump-thaw cycles. A sample was taken for ^{1}H NMR spectroscopy analysis, and the flask was placed in a 70 °C oil bath. SEC and ^{1}H NMR spectroscopy were used to monitor the reaction progress.

20

After the polymerization proceeded for 190 min, the polymerization was stopped by removing the flask from the oil bath and diluting the mixture with THF. The polymer solution was precipitated in hexanes. The polymer was then dissolved in THF (15 mL) and precipitated in a mixture of hexane and diethyl ether (v : v = 60 : 40, 200 mL). This process was repeated an additional two times. The block copolymer was then dried in vacuum and analyzed by ^{1}H NMR spectroscopy and SEC. SEC results (polystyrene standards): $M_{n,SEC}$ = 42300 Da; PDI = 1.20. The composition of the block copolymer was determined from the ^{1}H NMR spectrum. The obtained numbers of DEGEA, TEGMA, and tBA units were 95, 183 and 11, respectively.

2.2.7 Removal of t-Butyl Groups of P(TEGMA-co-tBA)-b-PDEGEA

P(TEGMA-co-tBA)-b-PDEGEA (2.505 g, $M_{n,SEC}$ = 42300 Da, PDI = 1.20) was dissolved in dry dichloromethane (10 mL) in a 20 mL vial. After the addition of trifluoroacetic acid (2.34 g), the reaction mixture was stirred at room temperature for 48 h. The volatiles were then removed by the use of a rotavapor. The residue was dissolved in 100 mL dichloromethane and the volatiles were evaporated again by a rotavapor. This process was repeated an additional two times to remove as much trifluoroacetic acid as possible. The polymer was then dissolved in THF (10 mL) and precipitated in a mixture of hexane and diethyl ether (v/v = 50:50, 100 mL) three times. After drying in vacuum, the polymer was obtained as a pink viscous liquid (2.30 g, yield: 92%). The successful removal of $tert$-butyl group was evidenced by the disappearance of the $tert$-butyl peak located at 1.4 ppm in the ^{1}H NMR spectrum.

2.2.8 Preparation of 20 wt% Aqueous Solution of PTEGMA-*b*-PDEGEA

The block copolymer was added into a pre-weighed vial (inner diameter: 20 mm). The vial was then placed in a large flask and dried in high vacuum at 55 ºC for 12 h. The mass of the dried polymer inside the vial was 0.485 g. Milli-Q water (1.940 g) was added into the vial. The mixture was then sonicated in an ice/water ultrasonic bath (Fisher Scientific Model B200 Ultrasonic Cleaner) to dissolve the block copolymer. The vial was then stored in a refrigerator (~ 4 ºC) overnight to ensure that a homogeneous solution was formed.

2.2.9 Preparation of 20 wt% Aqueous Solution of P(TEGMA-*co*-AA)-*b*-PDEGEA

P(TEGMA-*co*-AA)-*b*-PDEGEA was added into a pre-weighed vial (inner diameter: 20 mm). The vial was then placed in a large flask and dried under high vacuum at 55 °C for 12 h. The mass of the dried polymer inside the vial was 0.584 g. Milli-Q water (2.334 g) was added into the vial. The mixture was then sonicated in an ice/water ultrasonic bath (Fisher Scientific Model B200 Ultrasonic Cleaner) to dissolve the polymer. The vial was then stored in a refrigerator (~ 4 °C) overnight and a homogeneous solution was obtained.

2.2.10 Rheological Measurements

Rheological experiments were conducted using a stress-controlled rheometer (TA Instruments Model TA AR 2000ex). A cone-plate geometry with a cone diameter of 20 mm and an angle of 2 ° (truncation 52 μm) was employed; the temperature was controlled by the bottom Peltier plate. In each measurement, 90 μL of a polymer solution was loaded onto the plate by a micropipette. The solvent trap was filled with water and a solvent trap cover was used to minimize water evaporation. Dynamic viscoelastic properties (dynamic storage modulus G' and loss modulus G'') of a polymer solution

were measured by oscillatory shear experiments performed at a fixed frequency of 1 Hz in a heating ramp at a heating rate of 1 °C/min. The frequency dependences of *G'* and *G''* of a polymer solution at selected temperatures were obtained by frequency sweep tests from 0.1 to 100 Hz. A strain amplitude of $\gamma = 0.2\%$ was used in all dynamic tests to ensure that the deformation was within the linear viscoelastic regime. The flow properties (shear stress-shear rate curves) of a polymer solution at selected temperatures were measured by a shear rate ramp from 0 to 600 s^{-1} for duration of 6 min. The apparent viscosities of a polymer solution at different temperatures were measured by a temperature ramp experiment performed at a heating rate of 3 °C/min and a shear rate of 10 s^{-1}.

2.2.11 Polarized Light Microscopy Experiments

Polarized light microscopy experiments were conducted on a Leica (DM LB2) polarized light microscope coupled with a Mettler hot stage (FP-90). The 20 wt% aqueous solution of P(TEGMA-*co*-AA)-*b*-PDEGEA was added into a thin (0.5 mm) quartz demountable cell. The temperature of the cell was controlled by a Mettler hot stage (FP-90).

2.2.12 Small-Angle X-Ray Scattering Experiments

Small-angle X-ray scattering data were collected on a Bruker NanoStar equipped with a rotating anode X-ray generator and a Vantec 2000 area detector. Copper K_α radiation ($\lambda = 1.5418$ Å) was used. The 20 wt% aqueous solution of P(TEGMA-*co*-AA)-*b*-PDEGEA was loaded into a quartz capillary sample holder, which was then inserted into a cooling/heating stage. The temperature of the cooling/heating stage was controlled by a Materials Research Instruments TCPUP temperature controller. The scattering data for

the samples were corrected by subtracting the background which was recorded from the same sample holder using deionized water. The calibration was performed using silver behenate as the standard sample.

2.2.13 Differential Scanning Calorimetry Study of Thermo-Induced Phase Transitions of Aqueous Solutions of P(TEGMA-*co*-AA)-*b*-PDEGEA

Differential scanning calorimetry analysis of polymer solutions was conducted on a TA Q-1000 DSC instrument that was calibrated with sapphire disks. Approximately 20 mg of a 20 wt% polymer solution was loaded into a pre-weighed aluminum hermetic pan and sealed carefully. A heating rate of 1 °C/min was used to obtain the thermograms with an empty pan as reference.

2.2.14 Dynamic Light Scattering Studies

Dynamic light scattering (DLS) studies of aqueous solutions of P(TEGMA-*co*-AA)-*b*-PDEGEA were conducted with a Brookhaven Instruments BI-200SM goniometer equipped with a PCI BI-9000AT digital correlator, a temperature controller, and a solid-state laser (model 25-LHP-928-249, $\lambda = 633$ nm) at a scattering angle of 90°. Three 0.02 wt% solutions of P(TEGMA-*co*-AA)-*b*-PDEGEA in 20 mM KHP aqueous buffers with pH values of 3.11, 4.49, and 5.25, respectively, were made. The solutions were filtered into borosilicate glass tubes with an inner diameter of 7.5 mm using Millipore hydrophilic PTFE filters (0.2 μm pore size) and the tubes were sealed with PE stoppers. The glass tube was placed in the cell holder of the light scattering instrument and gradually heated. At each temperature, the solution was equilibrated for 20 min prior to data recording. The time intensity-intensity correlation functions were analyzed with a Laplace inversion program (CONTIN).

2.2.15 Determination of Sol-Gel-Sol-Cloudy Phase Diagrams of Diblock Copolymers in Water by the Vial Inversion Test and Visual Examination

A glass vial that contained an aqueous solution of a diblock copolymer with a known concentration was placed in the water bath of a Fisher Scientific Isotemp refrigerated circulator. The inner diameter of the vial was 20 mm. The temperature was gradually increased. At each temperature, the solution was equilibrated for 20 min before the vial was held in a tilted or inverted position for 5 s to visually examine if the solution was a mobile liquid or an immobile gel under its own weight. The temperature at which the solution changed from a mobile to an immobile state (or vice versus) was taken as the sol-to-gel (or gel-to-sol) transition temperature. The clouding temperature was determined by visual examination. Polymer solutions with different concentrations were obtained by adding a predetermined amount of water into the vial or evaporating water from the solution; their sol-to-gel/gel-to-sol transition temperatures and clouding temperatures were determined by the vial inversion method and visual examination.

2.3 Results and Discussion

2.3.1 Synthesis of P(TEGMA-*co*-AA)-*b*-PDEGEA and PTEGMA-*b*-PDEGEA

P(TEGMA-*co*-AA)-*b*-PDEGEA, a diblock copolymer composed of two distinct thermosensitive polymers with the higher LCST PTEGMA block containing a small amount of carboxylic acid groups, was prepared by RAFT and subsequent removal of *t*-butyl groups using trifluoroacetic acid (Scheme 2.1). The macro-CTA P(TEGMA-*co*-*t*BA) was synthesized by the copolymerization of TEGMA and *t*BA with a molar ratio of 100 : 5.3 at 70 °C in anisole using benzyl dithiobenzoate as chain transfer agent and

AIBN as initiator. P(TEGMA-*co-t*BA) was then used for the synthesis of the diblock copolymer. Figure 2.1a shows the SEC traces of P(TEGMA-*co-t*BA) and P(TEGMA-*co-t*BA)-*b*-PDEGEA. The peak completely shifted to the high molecular weight side and remained narrow. The polydispersity index (PDI) of the diblock copolymer using polystyrene calibration was 1.20. Figure 2.1b shows the ^{1}H NMR spectrum of P(TEGMA-*co-t*BA)-*b*-PDEGEA. The numbers of TEGMA, *t*BA, and DEGEA units in the block copolymer were calculated using the integral values of the peak from 4.4 to 4.0 ppm (-CH_2OOC- of TEGMA and DEGEA units), the peak from 2.5 to 2.1 ppm (-CH$_2$CH- of TEGMA, DEGEA and *t*BA units), and the peaks from 1.3 to 1.1 ppm (-CH$_2$CH_3 of DEGEA units) along with the DP of macro-CTA P(TEGMA-*co-t*BA) (DP = 194). The obtained numbers of TEGMA, *t*BA, and DEGEA units were 183, 11, and 95, respectively. The molar ratio of TEGMA and *t*BA units in the copolymer was 100 : 6.0, close to the feed ratio of 100 : 5.3 in the synthesis of macro-CTA P(TEGMA-*co-t*BA). The *t*-butyl groups of P(TEGMA-*co-t*BA)-*b*-PDEGEA were then removed by using trifluoroacetic acid, yielding the targeted thermo- and pH-sensitive diblock copolymer, P(TEGMA-*co*-AA)-*b*-PDEGEA. This was confirmed by ^{1}H NMR spectroscopy analysis; the *t*-butyl peak located at 1.4 ppm disappeared after the reaction (Figure 2.1c). The block copolymer was then used for micellar gel study. For comparison, PTEGMA-*b*-PDEGEA, which did not contain pH-responsive groups, was also synthesized by RAFT (Scheme 2.1). The SEC traces of PTEMGA and PTEGMA-*b*-PDEGEA and ^{1}H NMR spectrum of PTEGMA-*b*-PDEGEA are showed in Figure 2.2a and 2.2b. The characterization data for the polymers used in this work are summarized in Table 2.1.
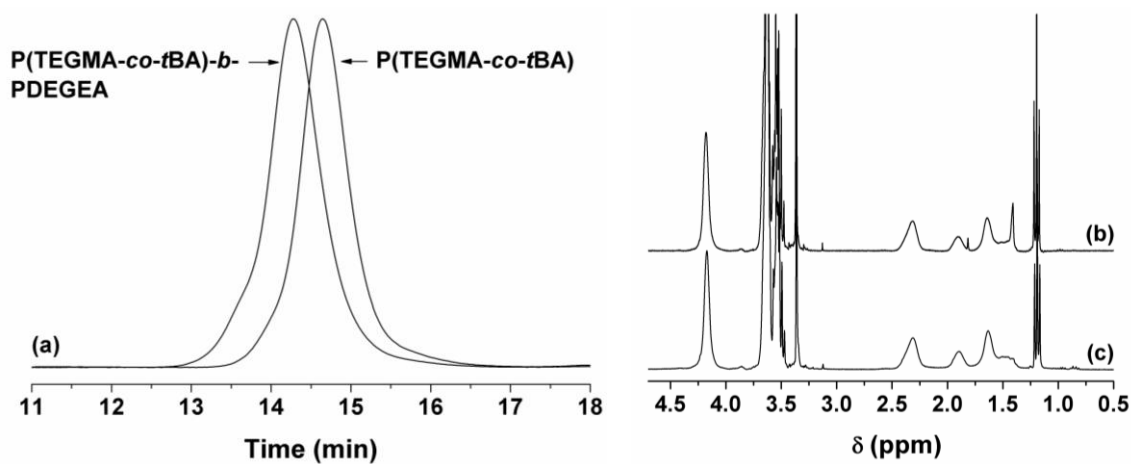
Figure 2.1 (a) Size exclusion chromatography traces of macro-CTA P(TEGMA-*co-t*BA) and diblock copolymer P(TEGMA-*co-t*BA)-*b*-PDEGEA, and ^{1}H NMR spectra of P(TEGMA-*co-t*BA)-*b*-PDEGEA (b) and P(TEGMA-*co*-AA)-*b*-PDEGEA (c). P(TEGMA-*co*-AA)-*b*-PDEGEA was prepared from P(TEGMA-*co-t*BA)-*b*-PDEGEA using trifluoroacetic acid to remove the *t*-butyl groups. CDCl$_3$ was used as solvent in ^{1}H NMR spectroscopy analysis.
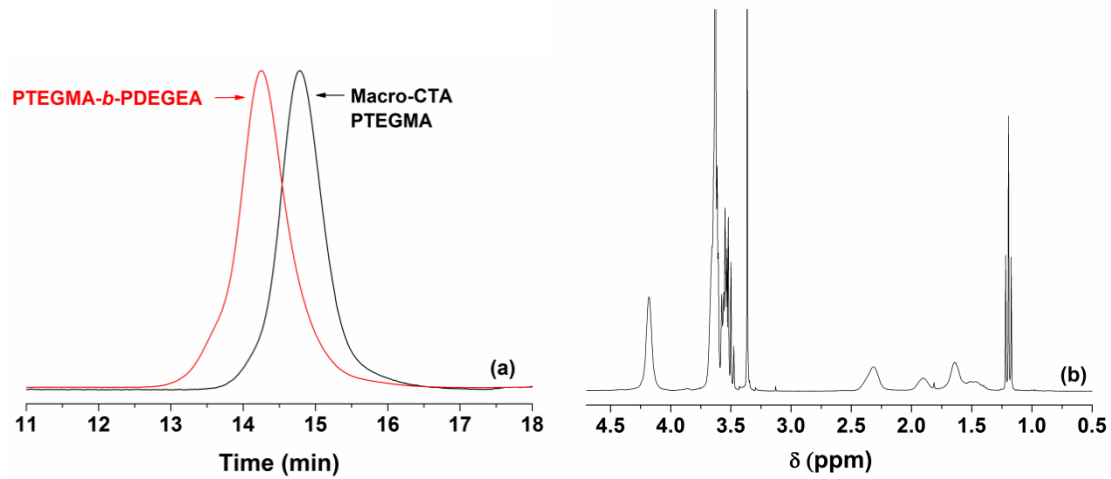
Figure 2.2 (a) Size exclusion chromatography traces of macro-CTA PTEGMA and diblock copolymer PTEGMA-*b*-PDEGEA, and (b) ^{1}H NMR spectra of PTEGMA-*b*-PDEGEA. CDCl$_3$ was used as solvent in ^{1}H NMR spectroscopy analysis.

Table 2.1 Characterization Data for P(TEGMA-*co*-*t*BA), P(TEGMA-*co*-*t*BA)-*b*-PDEGEA, P(TEGMA-*co*-AA)-*b*-PDEGEA, PTEGMA, and PTEGMA-*b*-PDEGEA.

Polymer [a]	$M_{n,SEC}$ (Da), PDI [b]	$n_{TEGMA} : n_{tBA \, (or \, AA)} : n_{DEGEA}$ [c]
P(TEGMA-*co*-*t*BA)	28100, 1.17	183 : 11 : 0
P(TEGMA-*co*-*t*BA)-*b*-PDEGEA	42300, 1.20	183 : 11 : 95
P(TEGMA-*co*-AA)-*b*-PDEGEA	NA	183 : 11 : 95
PTEGMA	24500, 1.15	166 : 0 : 0
PTEGMA-*b*-PDEGEA	41100, 1.23	166 : 0 : 106

[a] P(TEGMA-*co*-*t*BA), PTEGMA, P(TEGMA-*co*-*t*BA)-*b*-PDEGEA, and PTEGMA-*b*-PDEGEA were synthesized by RAFT; P(TEGMA-*co*-AA)-*b*-PDEGEA was obtained from P(TEGMA-*co*-*t*BA)-*b*-PDEGEA by the removal of *t*-butyl groups using trifluoroacetic acid. [b] the values of $M_{n,SEC}$ and PDI of polymers were determined by size exclusion chromatography using polystyrene calibration. [c] The degrees of polymerization of macro-CTAs P(TEGMA-*co*-*t*BA) and PTEGMA were calculated from the monomer conversion and monomer-to-CTA ratio. The numbers of TEGMA, *t*BA, and DEGMA units in the copolymers were determined from ^{1}H NMR spectra along with the use of the DPs of macro-CTAs.

2.3.2 Thermo-Induced Sol-Gel-Sol-Cloudy Transitions of 20 wt% Aqueous Solution of P(TEGMA-*co*-AA)-*b*-PDEGEA with pH of 3.11

A 20 wt% aqueous solution of P(TEGMA-*co*-AA)-*b*-PDEGEA was made by dissolving the polymer in Milli-Q water and the pH of the solution at 0 °C was 3.11.[19] To test the thermo-induced sol-gel-sol transitions, we gradually heated the solution from 8 °C. At each temperature, the sample was equilibrated for 20 min before the vial was tilted or inverted to visually examine if the sample was a free-flowing liquid or an immobile micellar gel under its own weight. As shown in Figure 2.3, the sample was a free-flowing liquid at 15 °C. With the increase of temperature, the sample turned into a clear gel at 19 °C, which was 10 °C higher than the cloud point of PDEGEA (Figure 2.3b shows the sample at 30 °C). Further increasing the temperature to 40 °C, the solution began to flow under its own weight when tilted but remained clear, indicating a transition from the gel to a sol (Figure 2.3c shows the sample at 45 °C). The block copolymer solution remained clear until the temperature reached 56 °C, at which point it turned cloudy (Figure 2.3d). This clouding temperature was very close to the cloud point of PTEGMA in water at a concentration of 0.5 wt% (58 °C).[12f] The sample stayed cloudy after that (Figure 2.3e shows the picture of the sample at 74 °C). Evidently, the sol-to-gel and the clear-to-cloudy transition temperatures were close to the LCSTs of the two component blocks of P(TEGMA-*co*-AA)-*b*-PDEGEA.

2.3.3 Rheological Properties of 20 wt% Aqueous Solution of P(TEGMA-*co*-AA)-*b*-PDEGEA with pH of 3.11

Rheological measurements were conducted to characterize the thermo-induced sol-gel/gel-sol transitions of the 20 wt% aqueous solution of P(TEGMA-*co*-AA)-*b*-PDEGEA
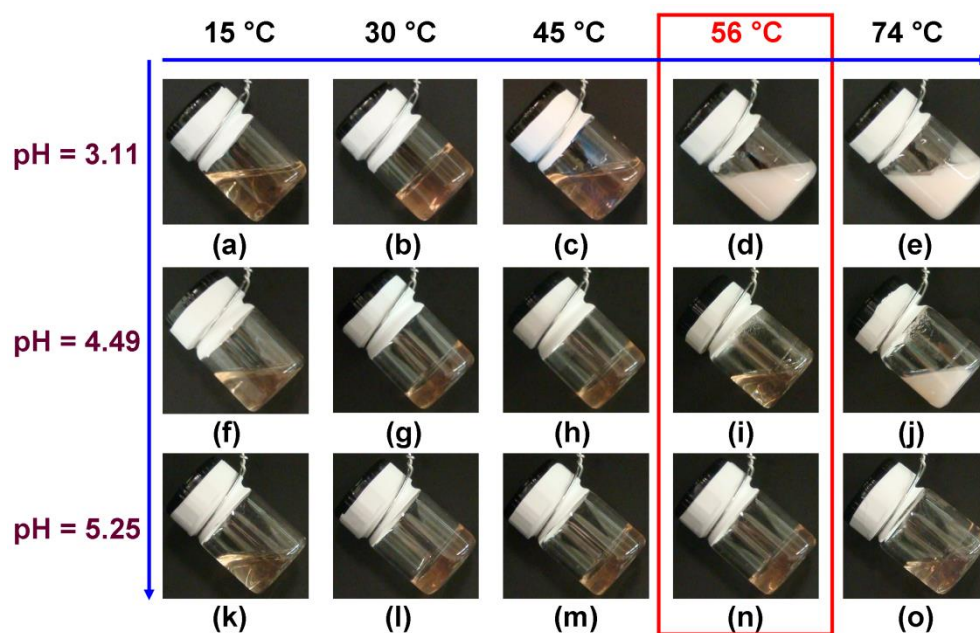
Figure 2.3 Digital optical pictures of 20 wt% aqueous solutions of P(TEGMA-*co*-AA)-*b*-PDEGEA at pH = 3.11 (the 1st row), 4.49 (the 2nd row), and 5.25 (the 3rd row), and T = 15 °C (the 1st column, a, f, k), 30 °C (the 2nd column, b, g, l), 45 °C (the 3rd column, c, h, m), 56 °C (the 4th column, d, i, n), and 74 °C (the 5th column, e, j, o).

with pH of 3.11 and the gel property. Figure 2.4a shows the dynamic storage modulus G' and loss modulus G'' of the sample as a function of temperature collected from an oscillatory shear experiment, which was performed at a fixed frequency of 1 Hz in a heating ramp at a heating rate of 1 °C/min. A strain amplitude of $\gamma = 0.2$ % was used to ensure that the measurements were taken in the linear viscoelastic regime. Below ~ 15 °C, both G' and G'' were very small. When the temperature was raised above 15 °C, G' and G'' increased quickly and G' became larger than G'' at ~ 21 °C, suggesting that the sample turned into a gel. In the temperature range of 23 to 37 °C, the G' was greater than G'' by at least one order of magnitude. Moreover, the G' was nearly independent of frequency. These are characteristics of gels. Above 37 °C, G' and G'' began to decrease and a sharp drop was observed for both moduli at ~ 39 °C. The crossover points of the two curves are commonly used as indicators of sol-to-gel ($T_{\text{sol-gel}}$) and gel-to-sol transitions ($T_{\text{gel-sol}}$).[1,20] Thus, with this method, the $T_{\text{sol-gel}}$ and the $T_{\text{gel-sol}}$ were 21.1 and 40.8 °C, respectively, which were close to those determined by the vial inversion method (19 and 40 °C).

The difference in the rheological property of the sample below and above $T_{\text{sol-gel}}$ can also be seen from the results of frequency sweep experiments (Figure 2.5). At 16 °C, which was below the $T_{\text{sol-gel}}$, G' scaled with the second power of oscillation frequency f, while G'' increased linearly with f (Figure 2.5a). This is the typical rheological behavior of a viscoelastic fluid.[9d,20] At 25 °C, G' was essentially independent of f and G'' varied slightly with a minimum appearing at an intermediate frequency (Figure 2.5b). In addition, G' was about one order of magnitude larger than G'' in the frequency range of 0.1 to ~ 50 s^{-1}. These are the characteristics of elastic solids with a cubic structure,[1,21]
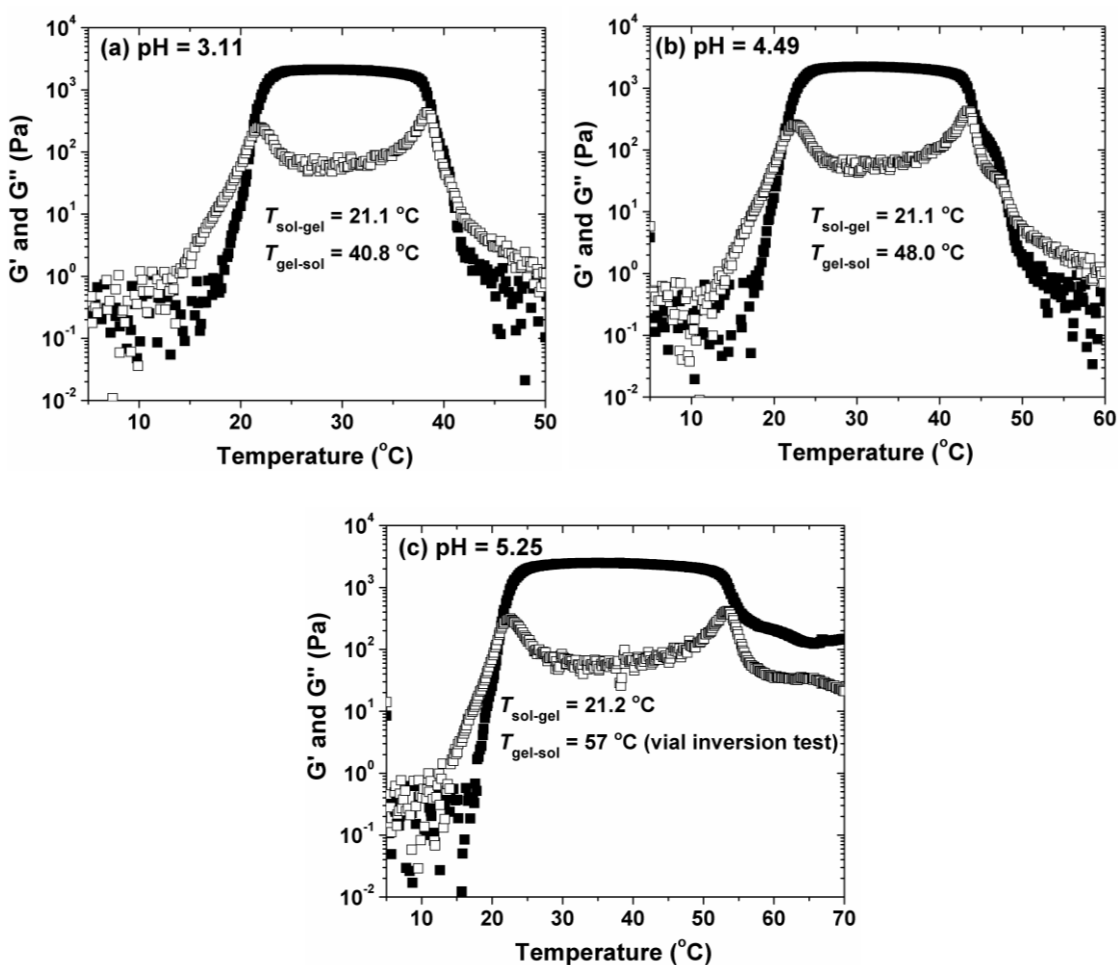
Figure 2.4 Plot of dynamic storage modulus *G'* (black solid square) and loss modulus *G''* (black hollow square) of 20.0 wt% aqueous solution of P(TEGMA-*co*-AA)-*b*-PDEGEA with pH of (a) 3.11, (b) 4.49, and (c) 5.25 versus temperature. The data were collected from oscillatory shear experiments performed in a heating ramp using a heating rate of 1 °C/min, a strain amplitude of 0.2%, and a frequency of 1 Hz.
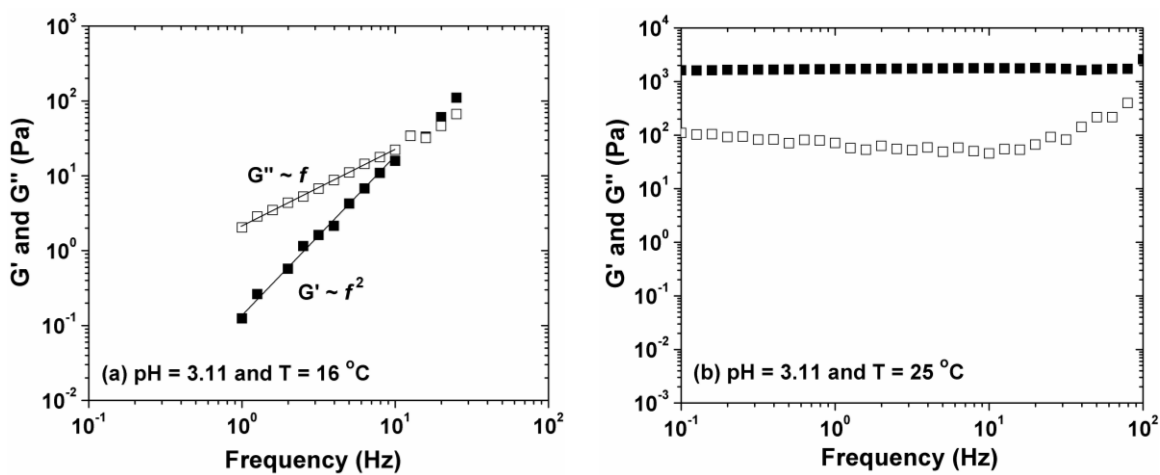
Figure 2.5 Frequency dependences of dynamic storage modulus *G'* (black solid square) and dynamic loss modulus *G''* (black solid square) of the 20 wt% aqueous solution of P(TEGMA-*co*-AA)-*b*-PDEGEA with pH of 3.11 at (a) 16 and (b) 25 °C. A strain amplitude of 0.2% was used in the frequency sweep experiments.

which is also supported by the polarized light microscopy result. In the gel zone, the sample was completely dark under a polarized light microscope with crossed polarizers, demonstrating that the gel was optically isotropic.

Figure 2.6a shows the flow curves (plots of shear stress versus shear rate) of the sample with pH of 3.11, 4.49, and 5.25 at various temperatures. At 10, 12, and 15 °C, the shear stress σ was proportional to the shear rate $d\gamma/dt$, indicating that the sample behaved as a Newtonian liquid. From 25 – 39 °C, the sample exhibited plastic flow behavior;[9d] after the initial resistance was overcome, the shear stress increased linearly with the shear rate. At 50 °C, the sample again behaved as a Newtonian liquid. These observations were consistent with the results from visual examination and dynamic viscoelastic measurements. The temperature dependence of apparent viscosity of the sample collected at a shear rate of 10 s^{-1} is displayed in Figure 2.7. When the temperature was below 13 °C, the viscosity was ≤ 0.05 Pa•s and there was essentially no change from 5 to 13 °C. A sharp increase was observed at ~ 20 °C, which was around the $T_{\text{sol-gel}}$ (19 °C by visual examination and 21.1 °C from rheological measurement). After reaching the highest value, 6.45 Pa•s, at 27 °C, the apparent viscosity began to decrease with the further increase of temperature. At 55 °C, the apparent viscosity was only 0.051 Pa•s. The transition temperatures determined from Figure 2.5b, $T_1 = 17$ °C and $T_2 = 42$ °C, matched reasonably well with those from the vial inversion test and the rheological measurement.

2.3.4 pH Effect on Sol-Gel-Sol-Cloudy Transitions of 20 wt% Aqueous Solution of P(TEGMA-*co*-AA)-*b*-PDEGEA

The LCST of a thermosensitive water-soluble polymer that contains a small amount of weak acid groups is known to depend on the solution pH.[22] With the increase of pH,
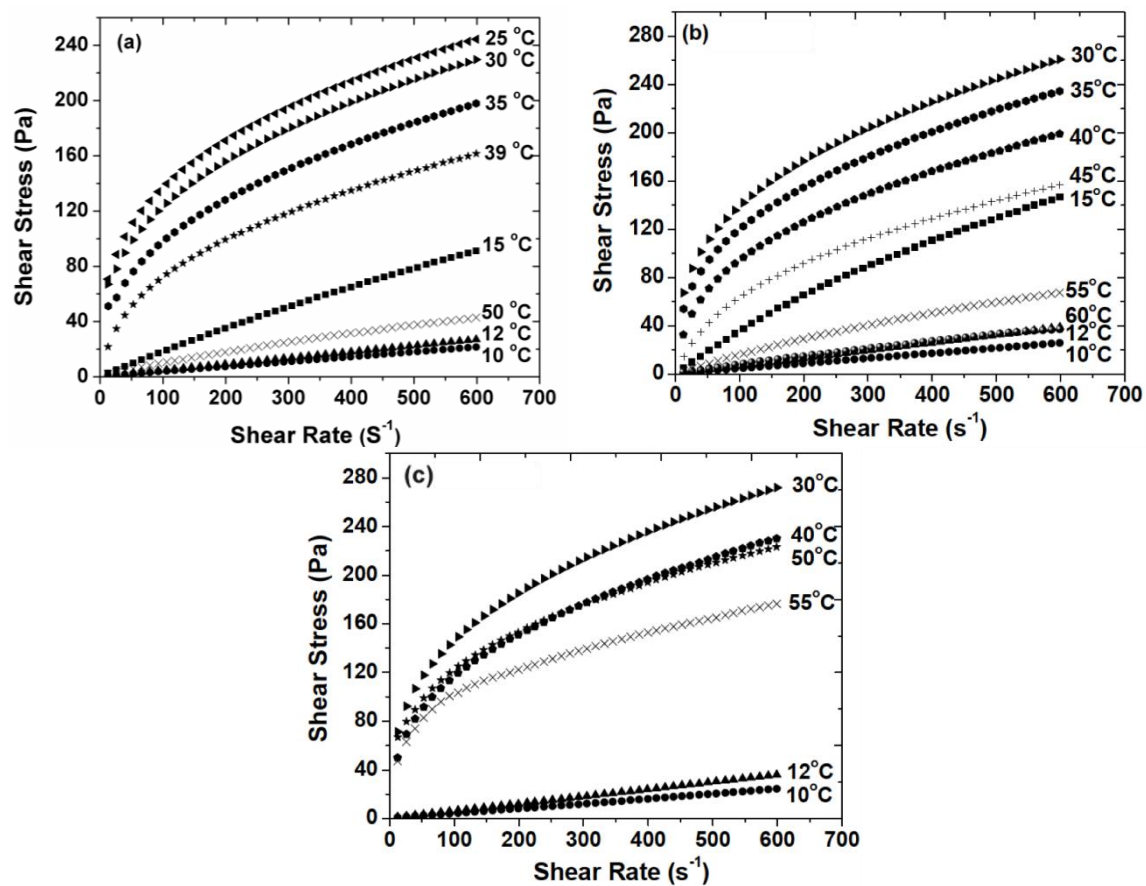
Figure 2.6 Flow curves of the 20 wt% aqueous solution of P(TEGMA-*co*-AA)-*b*-PDEGEA with pH of (a) 3.11, (b) 4.49, and (c) 5.25 at various temperatures.
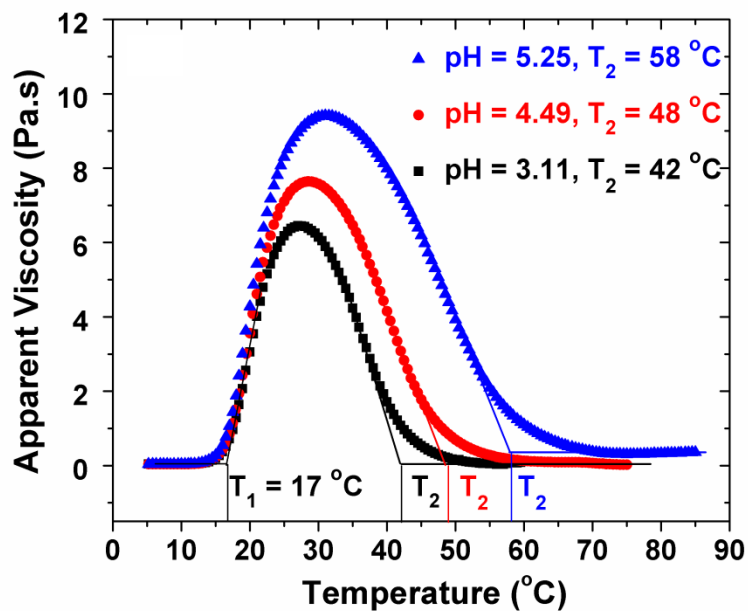
Figure 2.7 Apparent viscosity of the sample as a function of temperature at pH of 3.11 (solid black square), 4.49 (solid red circle), and 5.25 (blue solid triangle), collected at a shear rate of 10 s^{-1} and a heating rate of 3 °C/min.

the weak acid groups ionize, making the polymer more hydrophilic and thus increasing the LCST. For the diblock copolymer studied here, the higher LCST block contained 5.7 mol% of AA. To study the pH effects on sol-gel-sol transitions, clouding temperature, and gel property, we raised the pH of the 20 wt% aqueous solution of P(TEGMA-*co*-AA)-*b*-PDEGEA in a stepwise fashion by injecting a 1.0 M KOH solution. Each time, the sample was sonicated in an ice/water bath for 2 min to ensure that the solution was homogeneous and the pH was measured at 0 °C.

Figure 2.8 shows the $T_{\text{sol-gel}}$, $T_{\text{gel-sol}}$, and T_{clouding} of the sample, determined by visual examination, as a function of pH.[19] The $T_{\text{sol-gel}}$ remained at 19 °C throughout the studied pH range (3.11 − 6.04), consistent with the expected as the $T_{\text{sol-gel}}$ of the sample was governed by the thermosensitive property of the lower LCST block − the PDEGEA block that did not contain any pH-sensitive groups. In contrast, the $T_{\text{gel-sol}}$ and the T_{clouding} increased with the increase of pH. Initially, the $T_{\text{gel-sol}}$ changed slowly with pH, from 40 °C at pH = 3.11 to 47 °C at pH 4.49. Above pH = 4.49, the increase became faster; in 1.6 pH units, the $T_{\text{gel-sol}}$ jumped up by 30 °C ($T_{\text{gel-sol}}$ = 77 °C at pH = 6.04). Interestingly, the T_{clouding} went up with pH more sharply than the $T_{\text{gel-sol}}$. The difference between $T_{\text{gel-sol}}$ and T_{clouding} became larger with the increase of pH, from 16 °C at pH = 3.11, to 25 °C at pH 4.23, and to 40 °C at pH = 4.81. At pH of 5.08, the clouding temperature was not observed in the studied temperature range (up to 97 °C). To confirm that the tunability of $T_{\text{gel-sol}}$ and T_{clouding} arose from the pH dependence of the LCST of P(TEGMA-*co*-AA), we measured the cloud points of P(TEGMA-*co*-AA), which was obtained from macro-CTA P(TEGMA-*co*-*t*BA) by the removal of *t*-butyl groups, in 10 mM aqueous KHP buffers with various pH values at a concentration of 0.5 wt%. The cloud point of P(TEGMA-*co*-
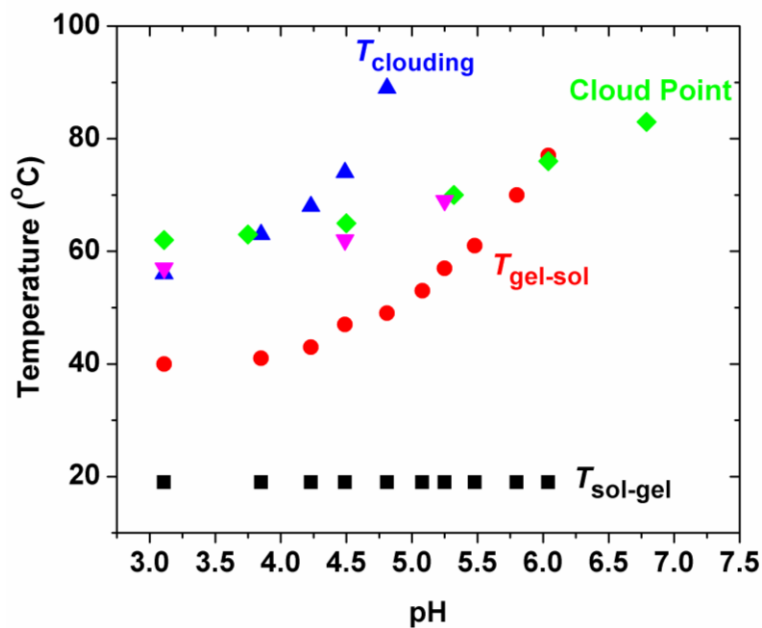
Figure 2.8 Sol-to-gel transition temperature ($T_{sol\text{-}gel}$, black solid square), gel-to-sol transition temperature ($T_{gel\text{-}sol}$, red solid circle), and clouding temperature ($T_{clouding}$, blue solid triangle) of the 20 wt% aqueous solution of P(TEGMA-*co*-AA)-*b*-PDEGEA as a function of pH as well as the pH dependences of the cloud point of random copolymer P(TEGMA-*co*-AA) at a concentration of 0.5 wt% in the 10 mM KHP aqueous buffer (green solid diamond) and the clouding temperature of P(TEGMA-*co*-AA)-*b*-PDEGEA at a concentration of 0.02 wt% in the 20 mM KHP aqueous buffer (pink solid triangle).

AA) in the dilute aqueous solution increased smoothly from 62 °C at pH = 3.11 to 83 °C at pH = 6.79 (Figure 2.8). However, the increase was slower compared with the $T_{\text{gel-sol}}$ and the T_{clouding}. Figure 2.8 also shows that the $T_{\text{gel-sol}}$ is closely related to but not solely determined by the LCST of P(TEGMA-*co*-AA). The PEO type thermosensitive water-soluble polymers are known to undergo shrinking, though small, with the increase of temperature.[1,23] The gel-to-sol transition occurred when the effective volume of micelles dropped below the critical value for the gelation.

The pH effect on gel-to-sol and clouding transitions of the 20 wt% aqueous solution of P(TEGMA-*co*-AA)-*b*-PDEGEA can be easily seen from the pictures of the sample in Figure 2.3. At 45 °C, the sample was a free-flowing clear sol when the pH was 3.11 (Figure 2.3c) but became a free-standing, clear gel at pH = 4.49 (Figure 2.3h). Interestingly, three distinct states, cloudy sol (Figure 2.3d), clear sol (Figure 2.3i), and clear gel (Figure 2.3n), were observed at 56 °C under the three different pH values.

The dynamic rheological properties of the samples at pH values of 4.49 and 5.25 were investigated and the data are shown in Figure 2.4. Consistent with the results from the visual examination, the values of $T_{\text{sol-gel}}$ at pH of 4.49 and 5.25 were the same as that at pH = 3.11. With the increase of pH from 3.11 to 4.49, the gel zone clearly became wider and the $T_{\text{gel-sol}}$ shifted to a higher temperature (48.0 °C). For the pH of 5.25, although the G' and G'' curves did not cross over each other at elevated temperatures,[24] the plateau zone of G' was significantly broader than those at pH values of 3.11 and 4.49, indicating that the $T_{\text{gel-sol}}$ shifted to a higher temperature ($T_{\text{gel-sol}}$ = 57 °C by visual examination). Interestingly, we also found that the maximum value of G' increased with the increase of pH, from 2119 Pa at pH = 3.11, to 2231 Pa at pH = 4.49, and 2469 Pa at pH of 5.25. This

is likely because the ionization of carboxylic acid groups at higher pH values causes the volume fraction of micelles to increase and thus the micelles are more jammed in the gel state, resulting in higher G' values.

The pH effect can also be seen from the flow curves of the sample at three different pH values (Figure 2.6). At 50 °C, the solution with the original pH of 3.11 was a Newtonian liquid (Figure 2.6a), while at pH = 5.25 it exhibited a plastic flow behavior at the same temperature (Figure 2.6c). Similarly, at 55 °C, the sample was a free flowing liquid at pH = 4.49 (Figure 2.6b) but became a gel with a finite yield stress at pH = 5.25 (Figure 2.6c). Besides the viscosity data for pH = 3.11, Figure 2.7 also shows the plots of apparent viscosity versus temperature for pH = 4.49 and 5.25. The three curves overlapped on the left side and the T_1 defined in the figure was essentially identical for three pH values, indicating that the pH change had a negligible effect on the $T_{sol-gel}$ of the sample, consistent with the results in Figures 2.4 and 2.8. Noticeable differences were observed on the right sides of the curves; T_2 shifted to higher temperatures with the increase of pH, from 42 °C at pH = 3.11, to 48 °C for pH = 4.49, and 58 °C for pH = 5.25. These temperatures were close to the corresponding gel-to-sol transitions by visual examination (40, 47, and 57 °C, respectively). Moreover, the highest value of the apparent viscosity increased with the pH and also appeared at a higher temperature, from 6.45 Pa•s at 27 °C for pH = 3.11, to 7.64 Pa•s observed at 28.5 °C for pH = 4.49, and to 9.41 Pa•s that appeared at 31 °C for pH = 5.25. These observations suggested that the gel was slightly harder at a higher pH value, in agreement with the observation from dynamic viscoelastic measurements that the maximum value of G' increased slightly with the increase of the solution pH.

2.3.5 Differential Scanning Calorimetry and Dynamic Light Scattering Studies of pH Effects on Solution Behavior of P(TEGMA-*co*-AA)-*b*-PDEGEA

The observed solution behavior of the 20 wt% aqueous solution of P(TEGMA-*co*-AA)-*b*-PDEGEA stemmed from the thermosensitive properties of the two blocks and the pH dependence of the LCST of P(TEGMA-*co*-AA). Below the LCST of PDEGEA (LCST$_{PDEGEA}$), the block copolymer dissolved molecularly in water. Above the LCST$_{PDEGEA}$, the polymer molecules self-assembled into micelles with the dehydrated PDEGEA blocks associated into the core and the P(TEGMA-*co*-AA) blocks forming the corona. With the increase of temperature, more block copolymer molecules entered the micelles. When the effective volume of micelles exceeded a critical value, the solution turned into a gel. Like other PEO-type thermosensitive polymers,[1,23] the copolymer underwent shrinking at elevated temperatures. At a certain point, the volume fraction of micelles dropped below the critical value, triggering the transition from a clear gel to a clear sol. At an even higher temperature, the P(TEGMA-*co*-AA) blocks underwent a LCST transition and macroscopically, the clear sol turned into a cloudy mixture. When the solution pH was raised, the carboxylic acid groups ionized, causing the P(TEGMA-*co*-AA) block to be more hydrophilic. As a result, the LCST transition occurred at a higher temperature and so did the gel-to-sol transition and the clouding transition.

To look into the origin of the observed pH effects on sol-gel-sol-cloudy transitions, we conducted differential scattering calorimetry (DSC) analysis of the 20 wt% aqueous solution of P(TEGMA-*co*-AA)-*b*-PDEGEA and dynamic light scattering (DLS) studies of 0.02 wt% aqueous solutions of the block copolymer with three different pH values (3.11, 4.49, and 5.25). Figure 2.9a shows the DSC thermogram of the sample with pH of
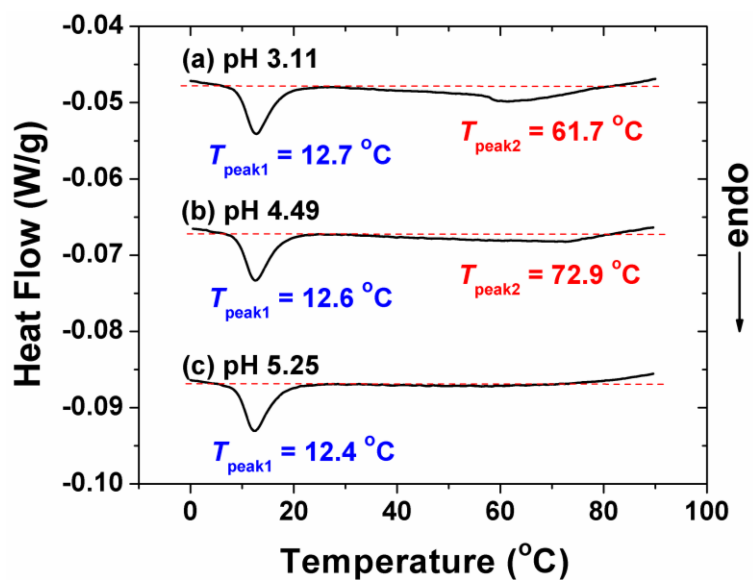
Figure 2.9 Differential scanning calorimetry thermograms of 20 wt% aqueous solutions of P(TEGMA-*co*-AA)-*b*-PDEGEA with pH of 3.11 (a), 4.49 (b), and 5.25 (c). The heating rate was 1 °C/min. For the sake of clarity, the thermograms were shifted vertically.

3.11. Two endothermic peaks were observed with the peak positions located at 12.7 and 61.7 °C, indicating that the transitions were entropically driven, consistent with the commonly accepted mechanism for the LCST behavior of thermosensitive water-soluble polymers.[9d,25] The two peaks, which were reasonably close to the $T_{\text{sol-gel}}$ (19 °C) and the T_{clouding} (56 °C) of the sample by visual examination, respectively, were attributed to the LCST transitions of the two thermosensitive blocks, PDEGEA and P(TEGMA-*co*-AA), of the block copolymer. While the peak at the lower temperature was relatively sharp, suggesting a strong phase transition, the one at the higher temperature was broad, a sign of a weaker phase transition. As discussed by Feil et al., the amount of structured water around a thermosensitive water-soluble polymer is a function of temperature and the LCST transition at a higher temperature tends to be broader and weaker.[22b]

With the increase of pH from 3.11 to 4.49 and 5.25, the peak of the PDEGEA block remained essentially at the same position as expected. For the sample with pH of 4.49, the endothermic peak position of the P(TEGMA-*co*-AA) block shifted to 72.9 °C and the transition became even broader (Figure 2.9b). This observation is in line with that reported by Urry.[26] The ionization of carboxylic acid groups introduced charges onto the thermosensitive block and disrupted the ordered structure of water molecules around the hydrophobic moieties. In addition, the random distribution of a small amount of carboxylic acid groups further enhanced the heterogeneity, resulting in a broader transition. The maximum peak position, 72.9 °C, was close to the clouding temperature, 74 °C, from visual examination. At pH of 5.25 (Figure 2.9c), the endothermic peak at the higher temperature was not observed in the studied temperature range. These results were consistent with the observations from the visual examination and rheological

44

measurements that the $T_{\text{sol-gel}}$ remained the same while the $T_{\text{gel-sol}}$ and T_{clouding} shifted to higher temperatures with the increase of pH, evidencing that the sol-gel-sol-cloudy transitions originated from the thermosensitive properties of the two blocks and the pH dependence of the LCST transition of the P(TEGMA-*co*-AA) block.

Figure 2.10 shows the DLS results. For the 0.02 wt% solution of P(TEGMA-*co*-AA)-*b*-PDEGEA in a 20 mM KHP aqueous buffer with pH of 3.11, below 14 °C, the scattering intensity was low and the apparent size was < 10 nm, indicating that the block copolymer dissolved molecularly in water. With the increase of temperature, the scattering intensity increased and micelles with an apparent hydrodynamic size of ~ 55 nm were observed in the temperature range of 15 to 55 °C. The critical micellization temperature (CMT) was 14 °C. When the temperature reached 57 °C, the scattering intensity jumped up dramatically and aggregates of > 1000 nm were found from the analysis; this temperature corresponded to the LCST transition of P(TEGMA-*co*-AA) and matched the T_{clouding} (56 °C) very well.

With the increase of pH from 3.11 to 4.49 and 5.25, the CMT did not change (Figure 2.10a). The second transition temperature at which large aggregates were observed shifted from 57 °C at pH = 3.11, to 62 °C at pH = 4.49, and 69 °C at pH = 5.25. Note that the increase of the clouding temperature of 0.02 wt% aqueous solutions of P(TEGMA-*co*-AA)-*b*-PDEGEA with pH was similar to that of 0.5 wt% aqueous solutions of P(TEGMA-*co*-AA), but quite different from the trend of 20 wt% aqueous solutions of P(TEGMA-*co*-AA)-*b*-PDEGEA (Figure 2.8). From the DSC and DLS results presented above, it is clear that the sol-gel-sol-cloudy transitions originated from the responsive properties of the two blocks.

45
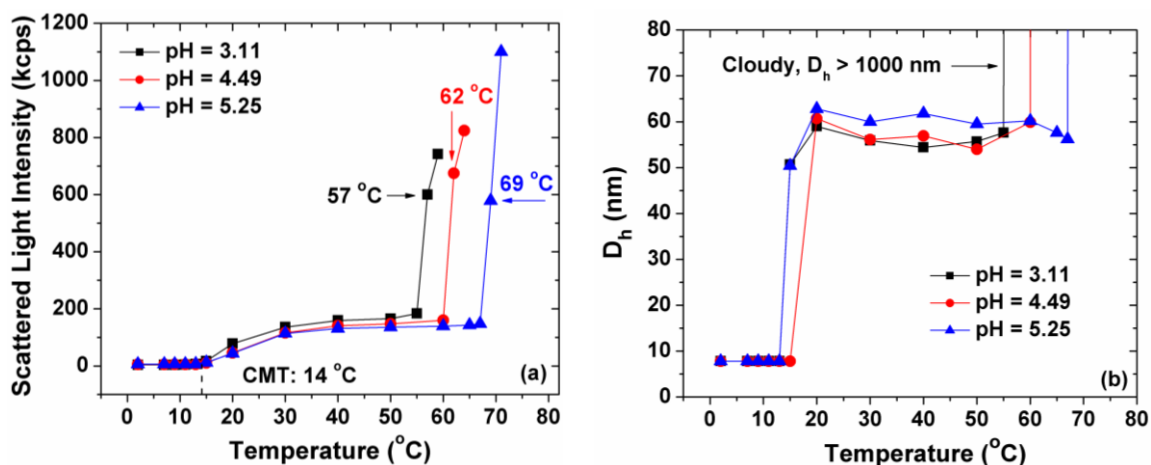
Figure 2.10 Scattering intensity at scattering angle of 90° (a) and apparent hydrodynamic size D_h (b), obtained from CONTIN analysis, as a function of temperature in a dynamic light scattering study of a 0.02 wt% solution of P(TEGMA-*co*-AA)-*b*-PDEGEA in a 20 mM aqueous KHP buffer with pH = 3.11 (black solid square), 4.49 (red solid circle), and 5.25 (blue solid triangle).

2.3.6 Sol-Gel-Sol Phase Diagrams of P(TEGMA-*co*-AA)-*b*-PDEGEA in Water at Moderate Concentrations

We further mapped out the sol-gel-sol phase diagrams for the moderately concentrated aqueous solutions of P(TEGMA-*co*-AA)-*b*-PDEGEA at three different pH values (pH = 3.11, 4.49, and 5.25).[19] The results are shown in Figure 2.11a and all three diagrams are C-shaped curves. It should be noted here that in the process of changing the polymer concentration by evaporating or adding water for the samples with pH of 3.11, we measured the pH value for each concentration and found that the pH was in the range of 3.07 - 3.11 when the polymer concentration was changed between 18 to 25 wt%. Thus, the effect of pH variations from the change of the polymer concentration on the sol-gel/gel-sol transitions should be quite small. One noticeable feature in Figure 2.11a is that the lower temperature boundaries for the three pH values overlapped while the upper temperature boundary shifted upward with the increase of pH. The gap between any two curves appeared to be either essentially independent of concentration or increase slightly with the increase of polymer concentration. Different from $T_{\text{sol-gel}}$ and $T_{\text{gel-sol}}$, the clouding temperature at a specific pH value did not change with the polymer concentration in the studied concentration range (T_{clouding} remained at 56 °C for pH of 3.11 and 74 °C for pH of 4.49). The fact that there was a difference between clouding temperature and $T_{\text{gel-sol}}$ indicates that the gel-to-sol transition was not entirely and directly governed by the LCST transition. The gel-to-sol transition occurred when the volume fraction of micelles dropped below the critical value. Although the continued dehydration of PDEGEA blocks in the micellar cores at elevated temperatures could contribute, we believe that the change in the micelle volume fraction mainly came from the shrinking of the corona blocks.

47
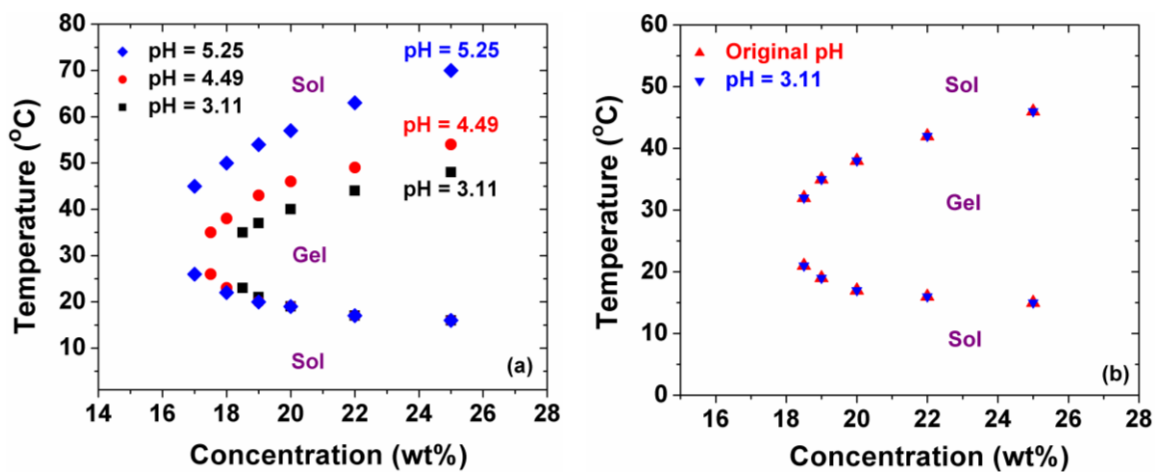
Figure 2.11 Sol-gel phase diagrams determined by the vial inversion test method for (a) P(TEGMA-*co*-AA)-*b*-PDEGEA in water at pH of 3.11 (black solid square), 4.49 (red solid circle), and 5.25 (blue solid diamond) and for (b) PTEGMA-*b*-PDEGEA in water at the original pH (red solid triangle) and pH of 3.11 (blue solid triangle).

Figure 2.11b shows the C-shaped sol-gel-sol phase diagram of PTEGMA-*b*-PDEGEA in the moderate concentration range at the original neutral pH value. To compare its solution behavior with that of P(TEGMA-*co*-AA)-*b*-PDEGEA, we injected a 1.0 M HCl aqueous solution to adjust the pH to 3.11 and determined the sol-gel-sol phase diagram. The two diagrams overlapped, indicating that the change of pH to 3.11 had no effect on the sol-gel-sol transitions as expected.

A second noticeable feature of Figure 2.11a is that the curve not only shifted upward but also extended into the lower concentration range with the increase of pH. That is, the critical gelation concentration (CGC) decreased with the increase of pH, from ~ 18 wt% at pH 3.11, to ~ 17 wt% at pH = 4.49, to ~ 16 wt% at pH = 5.25. This is reasonable because at a higher pH the carboxylic acid groups ionize, producing charges on the P(TEGMA-*co*-AA) block. Two scenarios can be envisioned.[27] (i) The micelle size increases slightly with the increase of pH because of the charge-charge interaction in the corona layer while the number of polymer molecules in each micelle stays about the same. (ii) The number of polymer molecules in each micelle decreases with the increase of pH while the apparent hydrodynamic size stays about the same or decreases slightly. Thus, more micelles would be present in the solution. Either of these two scenarios would lead to a greater volume fraction of micelles at a higher pH value.

Although the DLS studies of 0.02 wt% aqueous solutions of P(TEGMA-*co*-AA)-*b*-PDEGEA showed that the apparent diameter of micelles appeared to be larger at higher pH values (Figure 2.10b), the situation for the 20 wt% block copolymer solution might be different; this will be discussed in the next section.

2.3.7 Small-Angle X-Ray Scattering (SAXS) of Aqueous Micellar Gels of P(TEGMA-*co*-AA)-*b*-PDEGEA at 25 °C

Two-dimensional small-angle X-ray scattering (SAXS) experiments were conducted to determine the structures of the gels formed from the 20 wt% aqueous solutions of P(TEGMA-*co*-AA)-*b*-PDEGEA with pH values of 3.11, 4.49, and 5.25 at 25 °C. Note that all three samples were in the gel state at this temperature. The SAXS results are shown in Figure 2.12. Diffraction spots were clearly present in the diffraction patterns of the samples with pH of 4.49 and 5.25, indicating that the micelles were packed into an ordered structure. It is known that spherical particles are typically close-packed into a face-centered cubic (fcc) or a hexagonal close-packing lattice (hcp), with fcc as the slightly more stable structure.[28,29] Since the polarized light microscopy results showed that the gels were optically isotropic, the hcp lattice could be excluded. However, an fcc lattice cannot be applied alone to explain the diffraction spots in Figure 2.12. It is possible that the diffractions are generated by a mixture of two types of lattices. Therefore, we assume that both fcc and body-centered cubic (bcc) lattices are present in the gels. Based on the assumption that the strongest diffraction ring is attributed to fcc {111} and bcc {110}, essentially all the observed diffraction spots can be indexed, as shown in Figures 2.13 and 2.14. The successful indexation in turn validates our structural model. Note that {111} and {110} diffractions are indeed the strongest diffractions given by hard spheres that are packed in fcc and bcc lattices, respectively. The two diffraction peaks appear at the same q value when the two lattices arise from spheres with the same size.
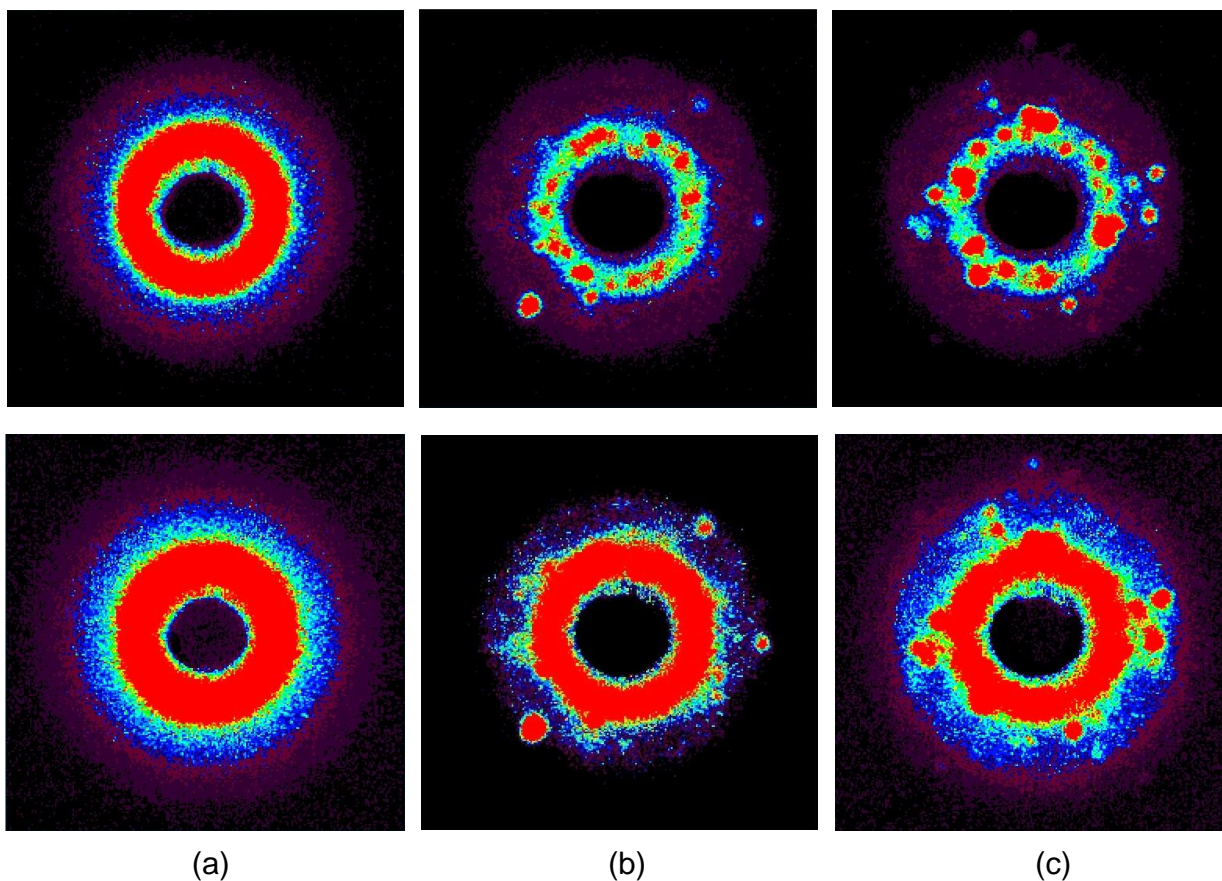
Figure 2.12 Two-dimensional small-angle X-ray diffraction patterns of 20 wt% aqueous solutions of P(TEGMA-*co*-AA)-*b*-PDEGEA with pH values of (a) 3.11, (b) 4.49, and (c) 5.25. The data were collected at 25 °C. The diffraction patterns in the second row were overexposed to show those weak diffraction spots.
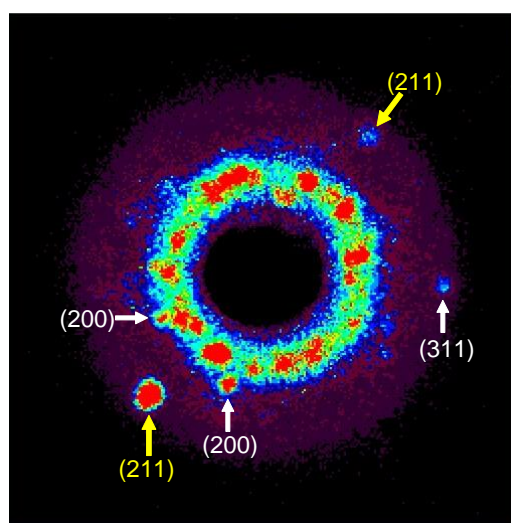
Figure 2.13 Two-dimensional small-angle X-ray diffraction patterns of a 20 wt% aqueous solution of P(TEGMA-*co*-AA)-*b*-PDEGEA with pH of 4.49 and the assignments of diffraction spots. The strong diffraction ring at the smallest angle is assigned to the fcc {111} and bcc {110} diffraction peaks, which are at the same position when the micelles are of the same size. Other diffraction spots are assigned to the fcc (yellow) and bcc (white) lattices. The indices are generated with the assumption that the lattices arise from the hard sphere-type packing of micelles with an adjacent micelle center-to-center distance of 45 nm.
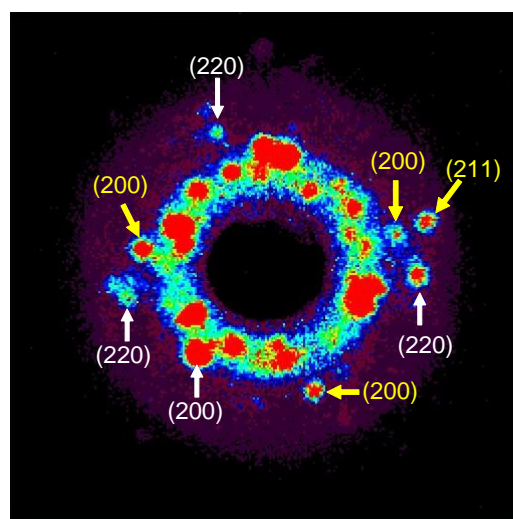
Figure 2.14 Two-dimensional small-angle X-ray diffraction pattern of a 20 wt% aqueous solution of P(TEGMA-*co*-AA)-*b*-PDEGEA with pH of 5.25 and the assignments of diffraction spots. The strong diffraction ring at the smallest angle was assigned to the fcc {111} and bcc {110} diffraction peaks, which are at the same position when the micelles are of the same size. Other diffraction spots are assigned to the fcc (yellow) or bcc (white) lattices. The indices are generated with the assumption that the lattices arising from the hard sphere-type packing of micelles with an adjacent micelle center-to-center distance of 44 nm.

After the diffraction spots are indexed, the center-to-center distance, D, of adjacent

micelles can be calculated using the following equations:

$$D = \frac{\sqrt{2}}{2}a \quad \text{for fcc lattice} \qquad \text{(Equation 1.1)}$$

$$D = \frac{\sqrt{3}}{2}a \quad \text{for bcc lattice} \qquad \text{(Equation 1.2)}$$

where a is the cell edge length. We use the term of "center-to-center distance of adjacent

micelles" instead of the size or diameter of micelles because the micelles could be

deformed/compressed when the volume fraction of micelles exceeds the critical value for

the physical jamming.

The appearance of diffraction spots in Figure 2.12b and 2.12c implies that the

crystalline domains of micelles are fairly large and likely only a small number of

crystallites are responsible for the generation of diffraction at a particular q value.

Therefore, spots instead of a ring are observed. The absence of clear diffraction spots in

Figure 2.12a may be attributed to the micelles packed in a crystalline fashion but in much

smaller crystallites or the micelles in a disorderd state. Figure 2.15 shows the one-

dimensional SAXS curves integrated from the 2D patterns in Figure 2.12 for the samples

with pH values of 3.11, 4.49, and 5.25. Since the shape of the one-dimensional small-

angle X-ray scattering curve of the sample with pH of 3.11 is quite similar to that with

pH of 5.25, it is more likely that the micelles at pH = 3.11 are also in the ordered state but

crystallites are very small. This is also supported by the similar rheological properties of

the gels at three pH values at 25 °C. With the assumption that the gel at pH of 3.11 also

consists of micelles packed in both fcc and bcc lattices, the corresponding center-to-

center distance between two adjacent micelles is also calculated. The strongest diffraction
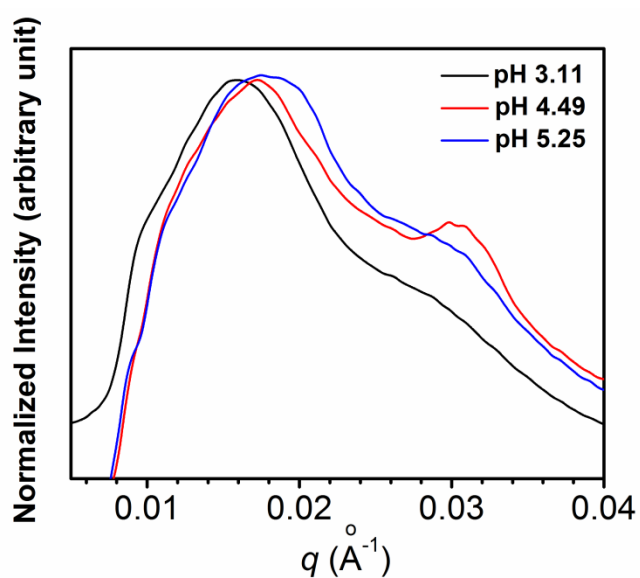
Figure 2.15 One-dimensional small-angle X-ray diffraction curves of 20 wt% aqueous solutions of P(TEGMA-*co*-AA)-*b*-PDEGEA with pH values of 3.11 (black), 4.49 (red) and 5.25 (blue) at 25 °C. The curves were integrated from 2-D diffraction patterns shown in Figure 2.12 and the intensity of the strongest peak in each curve is normalized to the same level. The normalized intensity is presented in a logarithm scale.

at q ≈ 0.016 Å^{-1} is attributed the fcc {111} and bcc {110} diffraction peaks. This yields a center-to-center distance between two adjacent micelles of 48 nm. Thus, it was 48 nm at pH = 3.11, 45 nm at pH = 4.49 (Figure 2.13), and 44 nm at pH = 5.25 (Figure 2.14). The results from SAXS studies suggested that the scenario in which both the micelle size and the number of polymer chains decrease with the increase of pH is more likely to be the case. That is, the micelle size decreased slightly but more micelles formed, resulting in a greater volume fraction of micelles in the gel. Since the CGC of a block copolymer in water is determined by the total volume of micelles, it is thus reasonable that the CGC decreases with the increase of pH. This could also explain the observations in rheological measurements for the samples at three pH values; micelles were more jammed in the gel state at higher pH values, giving rise to higher maximum G' values (Figure 2.4) and greater viscosities (Figure 2.7).

2.4 Conclusions

A well-defined multi-responsive hydrophilic diblock copolymer, P(TEGMA-*co*-AA)-*b*-PDEGEA, was successfully synthesized.[30] A 20 wt% aqueous solution of P(TEGMA-*co*-AA)-*b*-PDEGEA with pH of 3.11 underwent multiple phase transitions upon heating, from a clear, free-flowing liquid (< 19 °C), to a clear, free-standing gel (19 to 39 °C), to a clear, free flowing hot liquid (40 to 55 °C), and a cloudy mixture (≥ 56 °C). The data from rheological measurements corroborated the visual examination results. With the increase of pH, the $T_{gel-sol}$ and the $T_{clouding}$ of the sample shifted to higher temperatures, while the $T_{sol-gel}$ remained the same. The sol-gel-sol-cloudy transitions and the observed pH effects stemmed from the thermosensitive properties of the two blocks of the diblock

copolymer and the pH dependence of the LCST of P(TEGMA-*co*-AA), which were confirmed by DSC and DLS studies. We also determined the sol-gel-sol phase diagrams of (PTEGMA-*co*-AA)-*b*-PDEGEA in water in the moderate concentration range at three pH values (3.11, 4.49, and 5.25). While the lower temperature boundaries overlapped, the upper boundary shifted upward and the CGC decreased with the increase of pH. In contrast, the sol-gel-sol phase diagram of PTEGMA-*b*-PDEGEA, which contained no pH-responsive groups, showed no changes with pH. SAXS studies suggested that the micelles likely became smaller with the increase of pH and thus more micelles were present in the gel state. This work demonstrated that the sol-gel-sol-cloudy transitions of moderately concentrated aqueous solutions of a thermosensitive hydrophilic diblock copolymer can be tuned by incorporating a small amount of stimuli-responsive groups into a thermosensitive block and applying a 2nd external stimulus. This provides great flexibility for the design of stimuli-responsive reversible gels for potential applications.

References

1. (a) Hamley, I. W. *Block Copolymers in Solution: Fundamentals and Applications*, John Wiley & Sons: Chichester, 2005. (b) Hamley, I. W. *Phil. Trans. R. Soc. Lond. A* **2001**, *359*, 1017-1044.

2. (a) He, C. L.; Kim, S. W.; Lee, D. S. *J. Controlled Release* **2008**, *127*, 189-207. (b) Joo, M. K.; Park, M. H.; Choi, B. G.; Jeong, B. *J. Mater. Chem.* **2009**, *19*, 5891-5905. (c) Yu, L.; Ding, J. *Chem. Soc. Rev.* **2008**, *37*, 1473-1481. (d) Gil, E.S.; Hudson, S.M. *Prog. Polym. Sci.* **2004**, *29*, 1173-1222.

3. Jeong, B. M.; Bae, Y. H.; Lee, D. S.; Kim, S. W. *Nature* **1997**, *388*, 860-862.

4. (a) Li, C.; Tang, Y.; Armes, S. P.; Morris, C. J.; Rose, S. F.; Lloyd, A. W.; Lewis, A. L. *Biomacromolecules* **2005**, *6*, 994-999. (b) Li, C.; Buurma, N. J.; Haq, I.; Turner, C.; Armes, S. P. *Langmuir* **2005**, *21*, 11026-11033. (c) Madsen, J. Armes, S. P.; Lewis, A. L. *Macromolecules* **2006**, *39*, 7455-7457. (d) Kirkland, S. E.; Hensarling, R. M.; McConaught, S. D.; Guo, Y.; Jarrett, W. L.; McCormick, C. L. *Biomacromolecules* **2008**, *9*, 481-486. (e) Fechler, N.; Badi, N.; Schade, K.; Pfeifer, S.; Lutz, J.-F. *Macromolecules* **2009**, *42*, 33-36.

5. (a) Hvidt, S.; Jørgensen, E. B.; Schillén, K.; Brown, W. *J. Phys. Chem.* **1994**, *98*, 12320-12328. (b) Mortensen, K.; Brown, W.; Norden, B. *Phys. Rev. Lett.* **1992**, *68*, 2340-2343. (c) Mortensen, K. *Europhys. Lett.* **1992**, *19*, 599-604. (d) Alexandridis, P.; Hatton, T. A. *Colloids and Surfaces A: Physicochem. Eng. Aspects* **1995**, *96*, 1-46. (e) Wanka, G.; Hoffmann, H.; Ulbricht, W. *Macromolecules* **1994**, *27*, 4145-4159. (f) Zhou, Z; Chu, B. *Macromolecules* **1994**, *27*, 2025-2033.

6. (a) Li, H.; Yu, G. -E.; Price, C.; Booth, C.; Hecht, E.; Hoffmann, H. *Macromolecules*

1997, *30*, 1347-1354. (b) Alexandridis, P.; Olsson, U.; Kindman, B. *Langmuir* **1997**, *12*, 23-34. (c) Hamley, I. W.; Pople, J. A.; Fairclough, J. P. A.; Ryan, A. J.; Booth, C.; Yang, Y.-W. *Macromolecules* **1998**, *31*, 3906-3911. (d) Hamley, I. W.; Daniel, C.; Mingvanish, W.; Mai, S.-M.; Booth, C.; Messe, L.; Ryan, A. J. *Langmuir* **2000**, *16*, 2508-2514.

7. Liu, S.; Billingham, N. C.; Armes, S. P. *Angew. Chem. Int. Ed.* **2001**, *40*, 2328-2331.

8. (a) Lin, H. H.; Cheng, Y. L. *Macromolecules* **2001**, *34*, 3710-3715. (b) Motokawa, R.; Morishita, K.; Koizumi, S.; Nakahira, T.; Annaka, M. *Macromolecules* **2005**, *38*, 5748-5760. (c) Sugihara, S.; Hashimoto, K.; Okabe, S.; Shibayama, M.; Kanaoka, S.; Aoshima, S. *Macromolecules* **2004**, *37*, 336-343.

9. (a) Aoshima, S.; Sugihara, S. *J. Polym. Sci. Part A: Polym. Chem.* **2000**, *38*, 3962-3965. (b) Aoshima, S.; Sugihara, S.; Shibayama, M.; Kanaoka, S. *Macromol. Symp.* **2004**, *215*, 151-163. (c) Sugihara, S. Kanaoka, S.; Aoshima, S. *J. Polym. Sci. Part A: Polym. Chem.* **2004**, *42*, 2601-2611. (d) Sugihara, S.; Kanaoka, S.; Aoshima, S. *Macromolecules* **2005**, *38*, 1919-1927. (e) Aoshima, S.; Kanaoka, S. *Adv. Polym. Sci.* **2008**, *210*, 169-208.

10. (a) Jiang, X.G.; Lavender, C.A.; Woodcock, J.W.; Zhao, B. *Macromolecules* **2008**, *41*, 2632-2643. (b) Jiang X. G.; Zhao, B. *Macromolecules* **2008**, *41*, 9366-9375. (c) Jiang, X. G.; Jin, S; Zhong, Q. X.; Dadmun, M. D.; Zhao, B. *Macromolecules* **2009**, *42*, 8468-8476. (d) O'Lenick, T. G.; Jiang X. G.; Zhao, B. *Langmuir* **2010**, *26*, 8787–8796. (e) Woodcock, J. W.; Wright, R. A. E.; Jiang, X. G.; O'Lenick, T. G.; Zhao, B. *Soft Matter*, **2010**, *6*, 3325-3336. (f) O'Lenick, T. G.; Jin, N. X.; Woodcock, J. W.; Zhao, B. *J. Phys. Chem. B.* **2011**, *115*, 2870-2881.

11. (a) Zhao, B.; Viernes, N. O. L.; Moore, J. S.; Beebe, D. J. *J. Am. Chem. Soc.* **2002**, *124*, 5284-5285. (b) Zhao, B.; Moore, J. S.; Beebe, D. J. *Langmuir* **2003**, *19*, 1873-1879. (c) Jiang, J. Q.; Tong, X.; Morris, D.; Zhao. Y. *Macromolecules* **2006**, *39*, 4633-4640. (d) Zhao, Y. *J. Mater. Chem.* **2009**, *19*, 4887-4895.

12. (a) Han, S.; Hagiwara, M.; Ishizone, T. *Macromolecules* **2003**, *36*, 8312-8319. (b) Ishizone, T.; Seki, A.; Hagiwara, M.; Han, S.; Yokoyama, H.; Oyane, A.; Deffieux, A.; Carlotti, S. *Macromolecules* **2008**, *41*, 2963-2967. (c) Lutz, J.-F.; Hoth, A. *Macromolecules* **2006**, *39*, 893-896. (d) Lutz, J. F.; Weichenhan, K.; Akdemir, O.; Hoth, A. *Macromolecules* **2007**, *40*, 2503-2508. (e) Zhao, B.; Li, D. J.; Hua, F. J.; Green, D. R. *Macromolecules* **2005**, *38*, 9509-9517. (f) Hua, F. J.; Jiang, X. G.; Li, D. J.; Zhao, B. *J. Polym. Sci. Part A: Polym. Chem.* **2006**, *44*, 2454-2467. (g) Jiang, X. G.; Zhao, B. *J. Polym. Sci. Part A: Polym. Chem.* **2007**, *45*, 3707-3721. (h) Allcock, H. R.; Dudley, G. K. *Macromolecules* **1996**, *29*, 1313-131. (i) O'Lenick, T. G.; Jiang, X. M.; Zhao, B. *Polymer* **2009**, *50*, 4363-4371. (j) Li, D. J.; Zhao, B. *Langmuir* **2007**, *23*, 2208-2217. (k) Li, D. J.; Dunlap, J. R.; Zhao, B. *Langmuir* **2008**, 24, 5911-5918. (l) Jiang, X. M.; Wang, B. B.; Li, C. Y.; Zhao, B. *J. Polym. Sci. Part A: Polym. Chem.*, **2009**, *47*, 2853-2870. (m) Qiao, Z.-Y.; Du, F.-S.; Zhang, R.; Liang, D.-H.; Li, Z.-C. *Macromolecules* **2010**, *43*, 6485-6494.

13. (a) Chiefari, J.; Chong, Y. K.; Ercole, F.; Krstina, J.; Jeffery, J.; Le, T. P. T.; Mayadunne, R. T. A.; Meijs, G. F.; Moad, C. L.; Moad, G.; Rizzardo, E.; Thang, S. H. Macromolecules **1998**, 31, 5559-5562. (b) **Moad, G.; Rizzardo, E.; Thang, S. H.** *Acc. Chem. Res.* **2008**, *41*, **1133-1142.**

14. (a) Anderson, B. C.; Cox, S. M.; Bloom, P. D.; Sheares, V. V.; Mallapragada, S. K.

Macromolecules **2003**, *36*, 1670-1676. (b) Determan, M. D.; Cox, J. P.; Seifert, S.; Thiyagarajan, P.; Mallapragada, S. K. *Polymer* **2005**, *46*, 6933-6946. (c) Determan, M. D.; Guo, L.; Thiyagarajan, P.; Mallapragada, S. K. *Langmuir* **2006**, *22*, 1469-1473.

15. (a) Shim, W. S.; Yoo, J. S.; Bae, Y. H.; Lee, D. S. *Biomacromolecules* **2005**, *6*, 2930-2934. (b) Shim, W. S.; Kim, S. W.; Lee, D. S. *Biomacromolecules* **2006**, *7*, 1935-1941.

16. (a) Park, S. Y.; Lee, Y.; Bae, K. H.; Ahn, C. H.; Park, T. G. *Macromol. Rapid Commun.* **2007**, *28*, 1172-1176. (b) Suh, J. M.; Bae, S. J.; Jeong, B. *Adv. Mater.* **2005**, *17*, 118-120. (c) Joo, M. K.; Park, M. H.; Choi, B. G.; Jeong, B. *J. Mater. Chem.* **2009**, *19*, 5891-5905.

17. (a) Shim, W.S.; Kim, J. H.; Park, H.; Kim, K.; Kwon, I. C.; Lee, D. S. *Biomaterials* **2006**, *27*, 5178-5185. (b) Dayananda, K.; He, C. L.; Park, D. K.; Park, T. G.; Lee, D. S. *Polymer* **2008**, *49*, 4968-4973. (c) Huynh, D. P.; Nguyen, M. K.; Kim, B. S.; Lee, D. S. *Polymer* **2009**, *50*, 2565-2571.

18. Chong, Y. K.; Krstina, J.; Le, T. P. T.; Moad, G.; Postma, A.; Rizzardo, E.; Thang, S. H. *Macromolecules* **2003**, *36*, 2256-2272.

19. All pH values reported in this work were measured at 0 °C. We examined the effect of temperature on pH values of a 20 mM aqueous KHP buffer with pH of 3.32 at 0 °C and a 18 wt% aqueous solution of a different but similar thermo- and pH-sensitive diblock copolymer P(TEGMA-*co*-AA)-*b*-PDEGEA with pH of 3.05 at 0 °C. The pH values of these two solutions at 0, 25, 45, and 65 °C were measured. We found that the pH variations were < 0.1 for both solutions in the range of 0 − 65 °C. Details can

be found in Appendix A. In light of this observation, we believe that the temperature-induced pH variations should not affect our conclusions.

20. Noro, A.; Matshushita, Y.; Lodge, T. P. *Macromolecules* **2009**, *42*, 5802-5810.

21. Kossuth, M. B.; Morse, D. C.; Bates, F. S. *J. Rheol.* **1999**, *43*, 167-196.

22. (a) Yin, X.; Hoffman, A. S.; Stayton, P. S. *Biomacromolecules* **2006**, *7*, 1381-1385. (b) Feil, H.; Bae, Y. H.; Feijen, J.; Kim, S. W. *Macromolecules* **1993**, *26*, 2496-2500. (c) Bulmus, V.; Ding, Z.; Long, C. J.; Stayton, P. S.; Hoffman, A. S. *Bioconjugate Chem.* **2000**, *11*, 78-83. (d) Lokitz, B. S.; York, A. W.; Stempka, J. E.; Treat, N. D.; Li, Y.; Jarrett, W. L.; McCormick, C. L. *Macromolecules* **2007**, *40*, 6473-6480. (e) Yamamoto, S.-I.; Pietrasik, J.; Matyjaszewski, K. *Macromolecules* **2008**, *41*, 7013-7020. (f) Luo, C. H.; Liu, Y.; Li, Z. B. *Macromolecules* **2010**, *43*, 8101-8108.

23. Bai, Z. F.; Lodge, T. P. *J. Phys. Chem. B* **2009**, 113, 14151-14157.

24. The crossover of *G'* and *G''* curves was not observed on the high temperature side. We repeated the measurement several times and the results were reproducible. The reason was unclear.

25. Schild , H. G. *Prog. Polym. Sci.* **1992**, *17*, 163-249.

26. Urry, D. W. *J. Phys. Chem. B* **1997**, *101*, 11007-11028.

27. The third possible scenario is that both the number of polymer molecules in each micelle and the size of micelles increase with the increase of pH. This scenario is unlikely the case. The ionization of carboxylic acid groups at a higher pH would lead to the P(TEGMA-*co*-AA) block occupying a larger volume while the PDEGEA block stays the same, which should favor micelles with a larger curvature (a smaller size).

28. Woodcock, L. V. *Nature* **1997**, *385*, 141-143.

29. Bolhuis, P. G.; Frenkel, D.; Mau, S.-C.; Huse, D. A. *Nature* **1997**, *388*, 235-236.

30. The work presented in this Chapter has been published in *Macromolecules* as an article (*Macromolecules* **2011**, *44*, 3556-3566).

    http://pubs.acs.org/doi/abs/10.1021/ma200384k

Appendix A

for

Chapter 2. Tuning Thermally Induced Gel-to-Sol Transition of Aqueous Solution of Multi-Responsive Hydrophilic Diblock Copolymer Poly(methoxytri(ethylene glycol) acrylate-*co*-acrylic acid)-*b*-poly(ethoxydi(ethylene glycol) acrylate)

A.1 Temperature Effect on pH of a KHP Buffer with pH of 3.32 at 0 °C and a 18 wt% Aqueous Solution of a New Thermo- and pH-Sensitive Diblock Copolymer P(TEGMA-*co*-AA)-*b*-PDEGEA with pH of 3.05 at 0 °C

We examined the effect of temperature on pH values of a 20 mM aqueous buffer of potassium hydrogen phthalate (KHP) with pH of 3.32 at 0 °C and a 18 wt% aqueous solution of a different but similar thermo- and pH-sensitive diblock copolymer P(TEGMA-*co*-AA)-*b*-PDEGEA with pH of 3.05 at 0 °C. The precursor of this new diblock copolymer, P(TEGMA-*co*-*t*BA)-*b*-PDEGEA, had $M_{n,SEC}$ and PDI of 42800 Da and 1.19, respectively, and the numbers of TEGMA, *t*BA, and PDEGEA units in the copolymer were 151, 8, and 119, respectively. This block copolymer is similar to the one used in the present work. The pH values of the solutions at 0, 25, 45, and 65 °C were measured and are summarized in the following table.

The pH variations were ≤ 0.08 for the 20 mM KHP buffer in the temperature range of 0 – 65 °C, which is similar to that for the standard pH 4.01 buffer from Fisher (4.00 at 0 °C, 4.01 at 25 °C, 4.04 at 40 °C, and 4.09 at 60 °C). The pH variations of the 18 wt% aqueous solution of P(TEGMA-*co*-AA)-*b*-PDEGEA were ≤ 0.07. Both were less than 0.10. In light of this observation, we believe that the effect of temperature on pH values of moderately concentrated (17 – 25 wt%) aqueous block copolymer solutions should not affect the conclusions of the present work.

Table A1. Temperature Effect on pH Values of a 20 mM KHP Buffer and a 18 wt% Aqueous Solution of a New P(TEGMA-*co*-AA)-*b*-PDEGEA

Solution	pH at 0 °C	pH at 25 °C	pH at 45 °C	pH at 65 °C
20 mM KHP buffer	3.32	3.30	3.34	3.38
18 wt% aqueous solution of new P(TEGMA-*co*-AA)-*b*-PDEGEA	3.05	2.99	3.04	3.06

Chapter 3. Tuning Thermally Induced Sol-to-Gel Transitions of Aqueous Solutions of Doubly Thermosensitive Diblock Copolymers Poly(methoxytri(ethylene glycol) acrylate)-*b*-poly(ethoxydi(ethylene glycol) acrylate-*co*-acrylic acid)

Abstract

    This chapter describes a method to tune the sol-to-gel transitions of moderately concentrated aqueous solutions of doubly thermosensitive hydrophilic diblock copolymers that consist of two blocks exhibiting distinct lower critical solution temperatures (LCSTs) in water. A small amount of weak acid groups is statistically incorporated into the lower LCST block so that its LCST can be tuned by varying solution pH. Well-defined diblock copolymers, poly(methoxytri(ethylene glycol) acrylate-*b*-poly(ethoxydi(ethylene glycol) acrylate-*co*-acrylic acid)) (PTEGMA-*b*-P(DEGEA-*co*-AA)), were prepared by reversible addition fragmentation chain transfer polymerization and post-polymerization modification. PTEGMA and PDEGEA are thermosensitive water-soluble polymers with LCSTs of 58 and 9 °C, respectively, in water. A 25 wt% aqueous solution of PTEGMA-*b*-P(DEGEA-*co*-AA) with a molar ratio of DEGEA to AA units of 100 : 5.2 at pH = 3.24 underwent multiple phase transitions upon heating, from a clear, free-flowing liquid (< 15 °C), to a clear, free-standing gel (15 to 46 °C), to a clear, free flowing hot liquid (47 to 56 °C), and a cloudy mixture (≥ 57 °C). With the increase of pH, the sol-to-gel transition temperature ($T_{\text{sol-gel}}$) shifted to higher values, while the gel-to-sol transition ($T_{\text{gel-sol}}$) and the clouding temperature (T_{clouding}) of the sample remained essentially the same. These transitions and the tunability of $T_{\text{sol-gel}}$ originated from the thermosensitive properties of two blocks of the diblock copolymer and the pH dependence of the LCST of P(DEGEA-*co*-AA), which were confirmed by dynamic light scattering and differential scanning calorimetry studies. Using the vial inversion test method, we mapped out the C-shaped sol-gel phase diagrams of the diblock copolymer in aqueous buffers in the moderate concentration range at three

different pH values (3.24, 5.58, and 5.82, all measured at ~ 0 °C). While the upper temperature boundaries overlapped, the lower temperature boundary shifted upward and the critical gelation concentration increased with the increase of pH. The AA content in PTEGMA-*b*-P(DEGEA-*co*-AA) was found to have a significant effect on the pH dependence of $T_{\text{sol-gel}}$. For PTEGMA-*b*-P(DEGEA-*co*-AA) with a molar ratio of DEGEA to AA units of 100 : 10, the $T_{\text{sol-gel}}$ of its 25 wt% aqueous solution increased faster with the increase of pH than that of PTEGMA-*b*-P(DEGEA-*co*-AA) with a DEGEA-to-AA molar ratio of 100 : 5.2.

3.1 Introduction

Aqueous micellar gels of stimuli-responsive block copolymers have received considerable attention for use in a wide variety of fields, particularly in biomedical applications such as sustained and triggered release of substances and tissue engineering.[1-4] Generally, these micellar hydrogels are formed by in situ gelation of free-flowing liquid precursors via application of external stimuli; the processes are usually reversible, allowing for, e.g., minimally invasive administration by injection via syringe and needle and easy removal of polymers by changing environmental conditions. A notable example of injectable drug delivery systems reported by Jeong et al. was based on aqueous solutions of poly(ethylene oxide) (PEO)-containing diblock copolymers that underwent sol-gel transitions upon temperature changes.[4] The polymer solutions were loaded with a model drug in the sol state at an elevated temperature. Upon subcutaneous injection and cooling to the body temperature, the polymer solutions turned into gels instantaneously that subsequently acted as matrices for sustained release of drug molecules.

Depending on the polymer architecture and the properties of component blocks, stimuli-responsive block copolymers can form two basic types of aqueous micellar gels:[2,3] (i) gels of discrete micelles, in which non-interconnected block copolymer micelles, often spherical, are packed into an ordered structure,[5,6] and (ii) 3-D network gels, in which one block, e.g., the central block of an ABA triblock copolymer, forms bridges among micellar cores.[7] Among numerous micellar gels of the first type,[1-6] aqueous gels of PEO-*b*-poly(propylene oxide)-*b*-PEO (PEO-*b*-PPO-*b*-PEO) triblock copolymers with various block lengths are undoubtedly the most intensively studied.

70

When the temperature is above the lower critical solution temperature (LCST) of PPO (~ 15 °C),[2,3,8] PEO-*b*-PPO-*b*-PEO molecules self-assemble into discrete micelles with the dehydrated PPO block forming the core and the PEO blocks constituting the corona. If the polymer concentration is above the critical gelation concentration (CGC), micelles are packed into an ordered structure and macroscopically, the aqueous solution turns into an immobile gel (a soft solid). Upon further increasing temperature, the PEO blocks undergo shrinking and the gel melts into a liquid.[2,3,5] More recently, Aoshima et al. synthesized a series of well-defined vinyl ether block copolymers composed of two or more thermosensitive blocks with different LCSTs by using living cationic polymerization and studied their solution behavior.[9] For 20 wt% aqueous solutions of diblock copolymers, multi-stage transitions from clear liquids to transparent gels, to hot clear liquids, and phase separated opaque mixtures were observed upon heating.[8d] The sol-to-gel and gel-to-sol transitions were closely related to the LCSTs of two thermosensitive blocks.

It should be noted here that the sol-gel phase diagrams of PEO-*b*-PPO-*b*-PEO and many other thermosensitive diblock copolymers at low/moderate concentrations are usually C-shaped curves.[2,3] The sol-to-gel transition, corresponding to the lower temperature boundary in the phase diagram, is driven by the enhancement of micellization and the ordering of micelles with the increase of temperature, while the gel-to-sol transition, corresponding to the upper boundary, is caused by the shrinking of the corona at elevated temperatures. For a diblock copolymer with a particular molecular weight and a specific composition, the sol-to-gel ($T_{\text{sol-gel}}$) and gel-to-sol transition temperature ($T_{\text{gel-sol}}$) at a certain concentration are fixed. The sol-gel phase diagram hence

is also fixed once the polymer is made. Note that the addition of salts can modify the transition temperatures and the phase diagram, but the changes are irreversible.[2,3]

Our lab has embarked on an effort to develop strategies to actively control unimer-micelle and sol-gel transitions of thermosensitive hydrophilic block copolymers in water,[10] especially in a reversible manner,[10c,11] and to tune the sol-gel phase diagrams.[11] The LCST of a thermosensitive water-soluble polymer that contains a small amount of a weak acid or base is known to depend on solution pH and can be varied reversibly.[10c,11,12] By incorporating a small amount of carboxylic acid groups into the higher LCST block of a doubly thermosensitive hydrophilic diblock copolymer, poly(methoxytri(ethylene glycol) acrylate-*co*-acrylic acid)-*b*-poly(ethoxydi(ethylene glycol) acrylate) (P(TEGMA-*co*-AA)-*b*-PDEGEA), we showed in Chapter 2 that the upper temperature boundary of the C-shaped sol-gel phase diagram of this diblock copolymer in water can be modified by changing solution pH while the lower temperature boundary remained the same.[11] Note that PTEGMA and PDEGEA are thermosensitive water-soluble polymers with LCSTs of 58 and 9 °C,[11,13] respectively, which belong to a new class of thermosensitive polymers with a short oligo(ethylene glycol) pendant from each repeat unit.[9,13,14]

In this work, we synthesized well-defined diblock copolymers, PTEGMA-*b*-P(DEGEA-*co*-AA), with the lower LCST block incorporated with a small amount of AA groups and studied their solution properties at various pH values. The block copolymers were prepared by reversible addition-fragmentation chain transfer polymerization (RAFT)[15] and post-polymerization modification (Scheme 3.1). We show that 25 wt% aqueous solutions of PTEGMA-*b*-P(DEGEA-*co*-AA) can undergo sol-gel-sol-cloudy transitions upon heating and the sol-to-gel transition can be continuously and reversibly

72
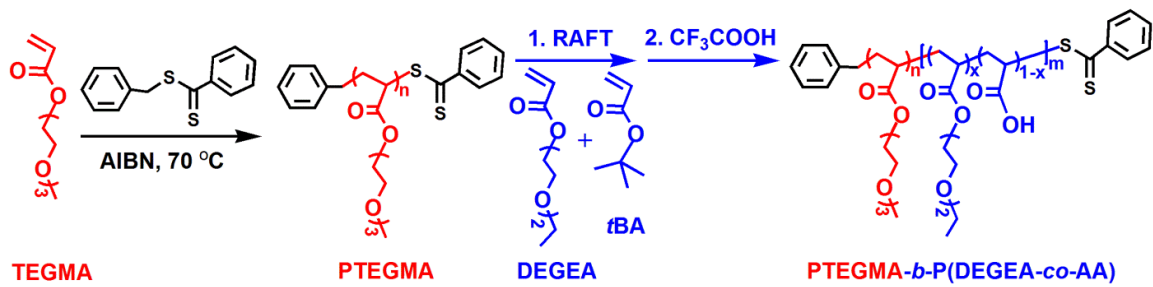
Scheme 3.1 Preparation of PTEGMA-*b*-P(DEGEA-*co*-AA) by Reversible Addition Fragmentation Chain Transfer Polymerization (RAFT) and Post-Polymerization Modification.

tuned by adjusting solution pH. We note here that there are many examples of thermo- and pH-sensitive block copolymer aqueous micellar gels reported in the literature.[16-19] The block copolymers used in those studies were usually prepared by either growing pH-sensitive blocks from or introducing pH-responsive groups onto the chain ends of a block copolymer that can form thermoreversible gels in water (e.g., PEO-*b*-PPO-*b*-PEO).[16-18] Other types of multiblock copolymers were also employed.[19] We emphasize here that our design of multi-responsive block copolymers, via the statistical incorporation of a small amount of pH-responsive groups into one block, is different, which allows the LCST to be readily tuned.

3.2 Experimental Part

3.2.1 Materials

Di(ethylene glycol) ethyl ether acrylate (or ethoxydi(ethylene glycol) acrylate, DEGEA, ≥ 90%, Aldrich) and *tert*-butyl acrylate (*t*BA, 99%, Fisher Scientific) were dried over calcium hydride overnight, distilled under reduced pressure, and stored in a refrigerator prior to use. Methoxytri(ethylene glycol) acrylate (TEGMA) was prepared using a procedure described in the literature.[13] Benzyl dithiobenzoate, a RAFT chain transfer agent (CTA), was synthesized according to a literature procedure[20] and the molecular structure was confirmed by ^{1}H and ^{13}C NMR spectroscopy. Anisole (99%, anhydrous, Acros) and trifluoroacetic acid (99%, Acros) were used as received. Hexanes, diethyl ether, 1.0 M KOH solution (volumetric standard solution), and 1.0 M HCl solution (volumetric standard solution) were purchased from Fisher Scientific. 2,2'-Azobis(2-methylpropionitrile) (AIBN, 98%, Aldrich) was recrystallized in ethanol twice

and dried under high vacuum at room temperature. A solution of the purified AIBN in

N,*N*-dimethylformamide (DMF, extra dry, Acros) with a concentration of 3.55 wt% was

made and used for RAFT polymerizations. Potassium hydrogen phthalate (KHP, 99.98%,

primary standard) was purchased from Fisher Scientific and used without further

purification. Aqueous KHP buffers with a salt concentration of 20 mM were made by

dissolving KHP in Milli-Q water and the pH values were adjusted by adding either a 1.0

M aqueous KOH or a 1.0 M aqueous HCl solution. All pH values were measured with a

pH meter (Accumet AB15 pH meter from Fisher Scientific, calibrated with pH = 4.01,

7.00, and 10.01 standard buffer solutions) in an ice/water bath (0 °C). All other solvents

and chemicals were purchased from either Aldrich or Fisher and used as received.

3.2.2 General Characterization

Size exclusion chromatography (SEC) was carried out at ambient temperature using

PL-GPC 50 Plus (an integrated GPC system from Polymer Laboratories, Inc) equipped

with a refractive index detector, one GRAL guard column (8 × 50 mm, 10 micron

particle), and two GRAL linear columns (each 8 × 300 mm, 10 micron particles,

molecular weight range from 500 to 1,000,000 according to Polymer Standards Service-

USA, Inc). *N*,*N*-Dimethylformamide was used as the carrier solvent at a flow rate of 1.0

mL/min. Polystyrene standards (Polymer Laboratories, Inc.) were used for calibration.

The data were processed using Cirrus^{TM} GPC/SEC software (Polymer Laboratories, Inc.).

The ^{1}H NMR (300 MHz) spectra were recorded on a Varian Mercury 300 NMR

spectrometer and the residual solvent proton signal was used as the internal standard.

3.2.3 Synthesis of Poly(methoxytri(ethylene glycol) acrylate) (PTEGMA) Macro-CTAs by RAFT

Described below is a typical procedure for the synthesis of PTEGMA macro-CTAs. Benzyl dithiobenzoate (32.4 mg, 0.133 mmol), 2,2'-azobis(2-methylpropionitrile) (AIBN, 59.0 mg of a solution of AIBN in DMF with a concentration of 3.55 wt%, 0.0128 mmol), TEGMA (14.011 g, 64.3 mmol), and anisole (14.45 g) were added into a 50 mL two-necked flask. The mixture was degassed by three freeze-pump-thaw cycles. After a small sample was taken for ^{1}H NMR spectroscopy analysis using a degassed syringe, the flask was immersed in a 70 °C oil bath. The polymerization was monitored by ^{1}H NMR spectroscopy. The flask was removed from the oil bath after 270 min and a sample was taken immediately for the determination of the monomer conversion by ^{1}H NMR spectroscopy. The reaction mixture was diluted with THF and precipitated in hexanes. The obtained polymer was further purified by three cycles of dissolution in THF (10 mL) and precipitation in a mixture of hexane and diethyl ether (v : v = 60 : 40, 150 mL). The polymer was then dried under high vacuum. SEC analysis results (polystyrene standards): $M_{n,SEC}$ = 37.8 kDa; polydispersity index (PDI) = 1.22. The degree of polymerization (DP) of the obtained PTEGMA macro-CTA was calculated from the monomer conversion and the monomer-to-CTA ratio. The peaks located in the range of 4.0 - 4.5 ppm, which were from -CH_2OOC- of monomer TEGMA and the polymer, were used as internal standard. The conversion was calculated from the integral values of the peaks from 5.7 to 5.9 ppm (CHH=CH- from TEGMA monomer) at t = 0 min and 270 min. The calculated DP was 170.

3.2.4 Synthesis of Doubly Thermosensitive Diblock Copolymers PTEGMA-*b*-poly(ethoxydi(ethylene glycol) acrylate-*co-tert*-butyl acrylate) (PTEGMA-*b*-P(DEGEA-*co-t*BA))

Below is a typical procedure for the synthesis of PTEGMA-*b*-P(DEGEA-*co-t*BA) from a PTEGMA macro-CTA by RAFT. PTEGMA macro-CTA ($M_{n,SEC}$ = 37.8 kDa, 3.750 g, 0.101 mmol), AIBN (46.7 mg of a solution of AIBN in DMF with a concentration of 3.55 wt%, 0.0101 mmol), DEGEA (9.513 g, 50.6 mmol), *t*BA (0.324 g, 2.53 mmol), and anisole (19.74 g) were added into a 50 mL two-necked flask. The mixture was stirred under a nitrogen atmosphere to dissolve the polymer; the solution was then degassed by three freeze-pump-thaw cycles. A zero-min sample was withdrawn for ^{1}H NMR spectroscopy analysis, and the flask was placed in a 70 °C oil bath. The polymerization was monitored by ^{1}H NMR spectroscopy. After the reaction proceeded for 250 min, the flask was removed from the oil bath and the mixture was diluted with THF. The polymer was precipitated in hexanes. The diblock copolymer was further purified by three cycles of dissolution in THF (15 mL) and precipitation in a mixture of hexane and diethyl ether (v : v = 60 : 40, 150 mL). The polymer was then dried under high vacuum and analyzed by ^{1}H NMR spectroscopy and SEC. SEC results (polystyrene standards): $M_{n,SEC}$ = 62.2 kDa; PDI = 1.24. From the ^{1}H NMR spectrum of the diblock copolymer, the numbers of DEGEA and *t*BA units were calculated to be 77 and 4, respectively.

3.2.5 Removal of *t*-Butyl Groups of PTEGMA-*b*-P(DEGEA-*co*-*t*BA) Using Trifluoroacetic Acid (TFA)

PTEGMA-*b*-P(DEGEA-*co*-*t*BA) ($M_{n,SEC}$ = 62.2 kDa and PDI = 1.24, 5.042 g) was dissolved in dry dichloromethane (10 mL) in a 25 mL flask. After the addition of trifluoroacetic acid (5.89 g), the reaction mixture was stirred at room temperature for 48 h. The volatiles were then evaporated via a rotary evaporator. The residue was then dissolved in 100 mL dichloromethane and the volatiles were evaporated again using a rotavapor. This process was repeated an additional two times to remove as much TFA as possible. The polymer was then dissolved in THF (15 mL) and precipitated in a mixture of hexane and diethyl ether (v/v = 60:40, 100 mL) three times. The polymer was dried under high vacuum (4.336 g, yield: 86%). The successful removal of *tert*-butyl group was confirmed by ^{1}H NMR spectroscopy analysis; the *tert*-butyl peak located at 1.4 ppm disappeared.

3.2.6 Preparation of 25 wt% Aqueous Solution of PTEGMA-*b*-P(DEGEA-*co*-AA)

Below is a typical procedure for the preparation of 25 wt% aqueous solutions of PTEGMA-*b*-P(DEGEA-*co*-AA). PTEGMA-*b*-P(DEGEA-*co*-AA), obtained from PTEGMA-*b*-P(DEGEA-*co*-*t*BA) with $M_{n,SEC}$ of 62.2 kDa and PDI of 1.24, was added into a pre-weighed vial (inner diameter: 20 mm). The vial was then placed in a larger flask and dried under high vacuum at 55 °C for 12 h. The mass of the dried polymer was 0.766 g. An aqueous KHP buffer (20 mM, 2.298 g) with a pH of 3.05 was added into the vial, and the mixture was sonicated in an ice/water ultrasonic bath (Fisher Scientific Model B200 Ultrasonic Cleaner) to dissolve the polymer. The vial was then stored in a refrigerator (~ 4 °C) overnight and a homogeneous solution was obtained.

3.2.7 Rheological Measurements

Rheological experiments were conducted on a TA Instruments rheometer (Model TA AR 2000ex). A cone-plate geometry with a cone diameter of 20 mm and an angle of 2° (truncation 52 μm) was used. The temperature was controlled by the bottom Peltier plate. In each rheological measurement, a sample (90 μL) was loaded onto the plate by a micropipette. The solvent trap was filled with water and a solvent trap cover was used to minimize water evaporation. The dynamic viscoelastic properties (dynamic storage modulus G' and loss modulus G'') of a polymer solution were measured by oscillatory shear experiments performed at a fixed frequency of 1 Hz in a heating ramp at a heating rate of 1 °C/min. The linear viscoelastic regime was determined by oscillatory strain sweep experiments from strain amplitude of 0.01% to 80% at frequencies of 0.5, 1.0, 2.5, and 5.0 Hz. A strain amplitude of $\gamma = 1.0$ %, which was within the linear viscoelastic regime, was used in all dynamic viscoelastic measurements. The apparent viscosity of a polymer solution versus temperature curve was obtained from a temperature ramp experiment performed at a heating rate of 3 °C/min and a shear rate of 10 s^{-1}.

3.2.8 Dynamic Light Scattering (DLS) Study of 0.02 wt% Solutions of PTEGMA-*b*-P(DEGEA-*co*-AA) in 20 mM Aqueous KHP Buffers at Various pH Values

DLS studies of thermo-induced micellization of PTEGMA-*b*-P(DEGEA-*co*-AA), obtained from PTEGMA-*b*-P(DEGEA-*co*-*t*BA) with $M_{n,SEC}$ of 62.2 kDa and PDI of 1.24, in 20 mM aqueous KHP buffers were conducted on a Brookhaven Instruments BI-200SM goniometer equipped with a PCI BI-9000AT digital correlator, a temperature controller, and a solid-state laser (model 25-LHP-928-249, $\lambda = 633$ nm) at a scattering angle of 90°. Four 0.02 wt% aqueous solutions of PTEGMA-*b*-P(DEGEA-*co*-AA) in 20 mM KHP

buffers with pH values of 3.24, 5.58, 5.82, and 6.52, respectively, were made. The polymer solutions were filtered through Millipore hydrophilic PTFE filters (0.2 μm pore size) into borosilicate glass tubes with an inner diameter of 7.5 mm and the tubes were sealed with PE stoppers. For each solution, the glass tube was placed in the cell holder of the light scattering instrument and gradually heated. At each temperature, the solution was equilibrated for 20 min prior to data recording. The time intensity-intensity correlation functions were analyzed with a Laplace inversion program (CONTIN).

3.2.9 Differential Scanning Calorimetry (DSC) Study of Thermo-Induced Transitions of 25 wt% Aqueous Solutions of PTEGMA-*b*-P(DEGEA-*co*-AA)

DSC analysis of polymer solutions was conducted on a TA Q-1000 DSC instrument, which was calibrated with sapphire disks. A 25 wt% polymer solution with a specific pH value (~14 mg) was loaded into a pre-weighed aluminum hermetic pan and sealed carefully. The DSC thermogram was recorded at a heating rate of 1 °C/min using an empty pan as reference.

3.2.10 Small-Angle X-Ray Scattering Experiments

Small-angle X-ray scattering experiments were conducted on a Bruker NanoStar equipped with a rotating anode X-ray generator and a Vantec 2000 area detector. Copper K_α radiation ($\lambda = 1.5418$ Å) was used. The 25 wt% aqueous solution of PTEGMA-*b*-P(DEGEA-*co*-AA) was loaded into a quartz capillary sample holder, which was then inserted into a cooling/heating stage. The temperature of the cooling/heating stage was controlled by a Materials Research Instruments TCPUP temperature controller. The calibration was performed using silver behenate as the standard sample.

3.2.11 Determination of Sol-Gel Phase Diagrams of Diblock Copolymers in Water by Vial Inversion Tests

A glass vial that contained an aqueous solution of a diblock copolymer in a 20 mM KHP buffer with a known concentration was placed in the water bath of a Fisher Scientific Isotemp refrigerated circulator. The inner diameter of the vial was 20 mm. The pH of the sample was measured with a pH meter in an ice/water bath. The temperature of the sample was increased in a stepwise fashion. At each temperature, the solution was equilibrated for 20 min before the vial was held in a tilted or inverted position for 5 s to visually examine if the solution was a mobile liquid or an immobile gel under its own weight. The temperature at which the solution changed from a mobile to an immobile state (or vice versus) was taken as $T_{\text{sol-gel}}$ (or $T_{\text{gel-sol}}$). The clouding temperature was determined by visual inspection. Polymer solutions with different concentrations were obtained by adding a predetermined amount of water into or evaporating water from the sample with a known concentration; their sol-to-gel and gel-to-sol transition temperatures as well as clouding temperatures were determined by vial inversion tests and visual examination as described above.

3.3 Results and Discussion

3.3.1 Synthesis of Multi-Responsive PTEGMA-*b*-P(DEGEA-*co*-AA)

The doubly thermosensitive hydrophilic diblock copolymers with the lower LCST block containing a small amount of carboxylic acid groups, PTEGMA-*b*-P(DEGEA-*co*-AA), were prepared by RAFT and post-polymerization modification according to the procedure illustrated in Scheme 3.1 The precursor diblock copolymers, PTEGMA-*b*-

P(DEGEA-*co*-*t*BA), were synthesized by a two-step RAFT polymerization process; the PTEGMA macro-CTAs were prepared using benzyl dithiobenzoate as CTA and AIBN as initiator, followed by the block copolymerization of a mixture of DEGEA and *t*BA with a molar ratio of either 100 : 5 or 100 : 10. Figure 3.1a shows the size exclusion chromatography traces of a PTEGMA macro-CTA (**H-1** in Table 3.1) and the corresponding diblock copolymer precursor **DB-1-P**. The $M_{n,SEC}$ and the polydispersity index (PDI) of **H-1** were 37.8 kDa and 1.22 (relative to polystyrene standards), respectively, and its degree of polymerization (DP) was 170, calculated from the monomer conversion and the monomer-to-CTA ratio. After the block copolymerization, the peak shifted to the high molecular weight side and remained relatively narrow (PDI = 1.24), indicating that the polymerization was controlled. The numbers of DEGEA and *t*BA units in **DB-1-P** were 77 and 4, respectively, which were calculated from the ^{1}H NMR spectrum of **DB-1-P** (Figure 3.1b) using the integral values of the peak at 4.4 − 4.0 ppm (-CH_2OOC- of TEGMA and DEGEA units), the peak at 2.5 − 2.1 ppm (-CH$_2$CH- of TEGMA, DEGEA and *t*BA units), and the peak at 1.3 − 1.1 ppm (-CH$_2$CH_3 of DEGEA units) along with the DP of PTEGMA (DP = 170). The molar ratio of DEGEA and *t*BA units in the copolymer was 100 : 5.2, essentially the same as the ratio of 100 : 5.0 for the two monomers in the feed. The *tert*-butyl groups in the precursor diblock copolymers were then removed using trifluoroacetic acid, yielding the targeted multi-responsive diblock copolymers, PTEGMA-*b*-P(DEGEA-*co*-AA). Figure 3.1c shows the ^{1}H NMR spectrum of **DB-1**, obtained from the precursor **DB-1-P**. The successful cleavage of *tert*-butyl groups was evidenced by the complete disappearance of the *tert*-butyl peak located at 1.4 ppm. Compared with **DB-1**, **DB-2** possessed a slightly higher AA content;[21] the
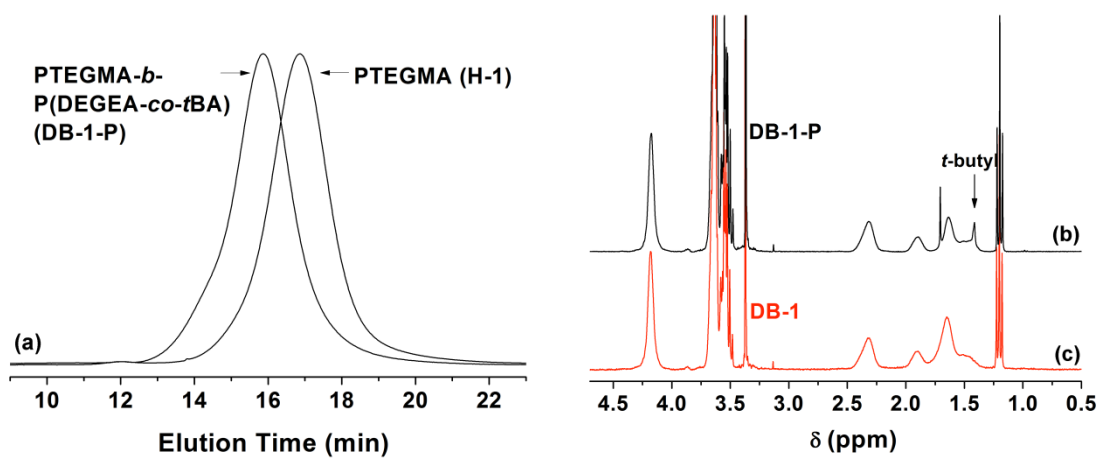
Figure 3.1 (a) Size exclusion chromatography traces of PTEGMA macro-CTA (**H-1**) and diblock copolymer PTEGMA-*b*-P(DEGEA-*co*-*t*BA) (**DB-1-P**), and ^{1}H NMR spectra of (b) PTEGMA-*b*-P(DEGEA-*co*-*t*BA) (**DB-1-P**) and (c) PTEGMA-*b*-P(DEGEA-*co*-AA) (**DB-1**). CDCl₃ was used as solvent in ^{1}H NMR spectroscopy analysis.

molar ratio of DEGEA to AA in the P(DEGEA-*co*-AA) block was 100 : 10, in contrast to 100 : 5.2 in **DB-1**. In addition, the block lengths were also slightly different. The characterization data of these polymers are summarized in Table 3.1.

3.3.2 Temperature-Induced Sol-Gel-Sol-Cloudy Transitions of 25 wt% Aqueous Solution of PTEGMA-*b*-P(DEGEA-*co*-AA) (DB-1) at pH = 3.24

We first studied the solution properties of **DB-1** in aqueous buffers under various conditions. To examine the thermally induced sol-gel-sol transitions, a 25 wt% aqueous solution of **DB-1** was prepared by dissolving the diblock copolymer in a 20 mM aqueous KHP buffer solution and the pH of the polymer solution was adjusted to 3.24 in an ice/water bath (~ 0 °C). The solution was gradually heated from 5 to 65 °C. At each selected temperature, the solution was equilibrated for 20 min before the vial was tilted or inverted to visually inspect whether the sample was a free-flowing liquid, or a free-standing gel, or a cloudy liquid. As shown in Figure 3.2a1, at 10 °C, the sample flowed freely when tilted. With the increase of temperature to 15 °C, the solution turned into a clear gel and stayed immobile even if the vial was inverted. The sample remained in the gel state in the temperature range of 15 to 46 °C (b1, c1, and d1 in Figure 3.2 show the sample at 20, 25, and 35 °C, respectively). At 47 °C, the gel melted into a liquid and flowed under its own weight upon tilting (Figure 3.2e1 shows the sample at 52 °C). The sample stayed clear until 57 °C, at which it became cloudy (Figure 3.2f1 shows the sample at 65 °C). This clouding temperature (57 °C) was almost the same as the cloud point of PTEGMA in water at a concentration of 0.5 wt% (58 °C) reported in the literature.[13] Thus, upon heating from 5 °C, the 25 wt% aqueous solution of PTEGMA-*b*-P(DEGEA-*co*-AA) (**DB-1**) with a pH of 3.24 underwent sol-to-gel, gel-to-sol, and clear

Table 3.1 Characterization Data for Two PTEGMA Macro-CTAs, Two PTEGMA-*b*-P(DEGEA-*co*-*t*BA) Diblock Copolymer Precursors, and Two PTEGMA-*b*-P(DEGEA-*co*-AA) Multi-Responsive Diblock Copolymers.

Sample	Polymer [a]	$M_{n,SEC}$ (kDa), PDI [b]	$n_{TEGMA} : n_{DEGEA} : n_{tBA\ (or\ AA)}$ [c]
H-1	PTEGMA	37.8, 1.22	170 : 0 : 0
DB-1-P	PTEGMA-*b*-P(DEGEA-*co*-*t*BA)	62.2, 1.24	170 : 77 : 4
DB-1	PTEGMA-*b*-P(DEGEA-*co*-AA)	NA	170 : 77 : 4
H-2	PTEGMA	29.9, 1.24	140 : 0 : 0
DB-2-P	PTEGMA-*b*-P(DEGEA-*co*-*t*BA)	53.4, 1.26	140 : 80 : 8
DB-2	PTEGMA-*b*-P(DEGEA-*co*-AA)	NA	140 : 80 :8

[a] PTEGMA macro-CTAs and PTEGMA-*b*-P(DEGEA-*co*-*t*BA)s were synthesized by RAFT; PTEGMA-*b*-P(DEGEA-*co*-AA) diblock copolymers were obtained from PTEGMA-*b*-P(DEGEA-*co*-*t*BA) precursors by the removal of *t*-butyl groups using trifluoroacetic acid. [b] The values of $M_{n,SEC}$ and PDI of diblock copolymer precursors were measured by SEC using polystyrene standards for calibration and DMF as solvent. [c] The degrees of polymerization (DPs) of PTEGMA macro-CTAs were calculated from the monomer conversion and the monomer-to-CTA ratio. The numbers of DEGEA and *t*BA (or AA) units in the diblock copolymers were determined from ^{1}H NMR spectra with the use of DPs of PTEGMA macro-CTAs.
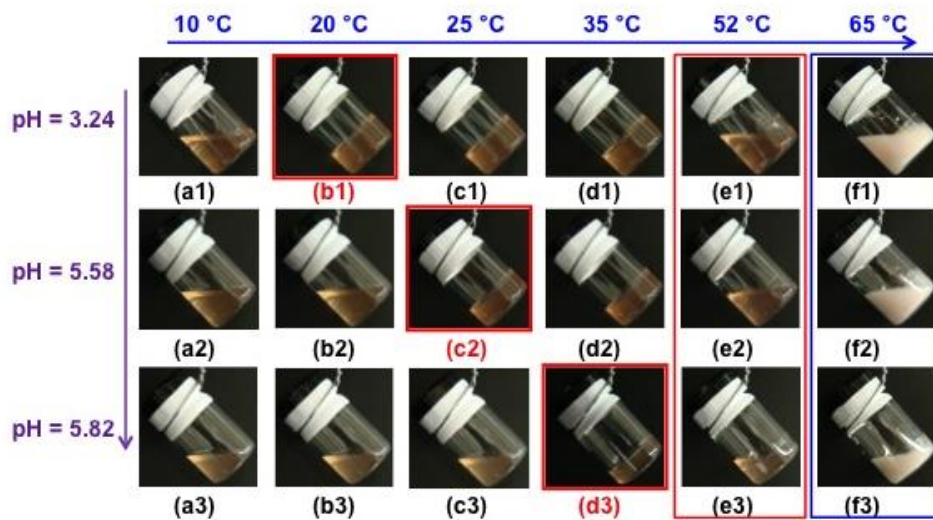
Figure 3.2 Digital optical pictures of 25 wt% aqueous solutions of PTEGMA-*b*-P(DEGEA-*co*-AA) (**DB-1**) at pH of 3.24 (1st row), 5.58 (2nd row), and 5.82 (3rd row) and temperature of 10 °C (1st column), 20 °C (2nd column), 25 °C (3rd column), 35 °C (4th column), 52 °C (5th column), and 65 °C (6th column).

sol-to-cloudy sol transitions at 15 °C ($T_{\text{sol-gel}}$), 47 °C ($T_{\text{gel-sol}}$), and 57 °C (T_{clouding}), respectively. Note that these thermo-induced sol-gel-sol-cloudy transitions were reversible.

3.3.3 Effect of Solution pH on Sol-Gel-Sol-Cloudy Transitions of 25 wt% Aqueous Solution of PTEGMA-*b*-P(DEGEA-*co*-AA) (DB-1)

To examine the effect of solution pH on thermally induced sol-gel-sol-cloudy transitions, we gradually raised the pH of a 25 wt% aqueous solution of **DB-1** from pH = 3.24 by adding a 1.0 M KOH solution via a microsyringe in a stepwise fashion in an ice/water bath. After each injection, the solution was stirred at the same temperature (~ 0 °C) to ensure that it was homogeneous before the pH value was measured. The solution was then gradually heated and the $T_{\text{sol-gel}}$, $T_{\text{gel-sol}}$, and T_{clouding} were determined by visual inspection. The results are summarized in Figure 3.3.

As expected, the $T_{\text{sol-gel}}$ increased with the increase of solution pH, from 15 °C at pH = 3.24 to 22 °C at pH = 5.58, to 29 °C at pH = 5.82, and to 39 °C at pH = 5.90. The change was 24 °C over a range of 2.66 pH units. Initially, the increase of $T_{\text{sol-gel}}$ was slow, only 2 °C when the pH was raised from 3.24 to 4.93. Above pH 5.30, the $T_{\text{sol-gel}}$ changed significantly faster; an increase of 20 °C was observed in only 0.55 pH units, from 19 °C at pH 5.35 to 39 °C at pH 5.90. This faster increase of $T_{\text{sol-gel}}$ at pH > 5.3 is believed to result from the increased degree of ionization of carboxylic acid groups in the P(DEGEA-*co*-AA) block. In contrast, the $T_{\text{gel-sol}}$ remained unchanged in the studied pH range except pH 5.87 and 5.90 at which the values of $T_{\text{gel-sol}}$ were found to be 46 °C, 1 °C lower than $T_{\text{gel-sol}}$ at other pH values. The T_{clouding} stayed at 57 °C throughout the studied pH range, which is understandable because the transition from a clear sol to a cloudy sol was
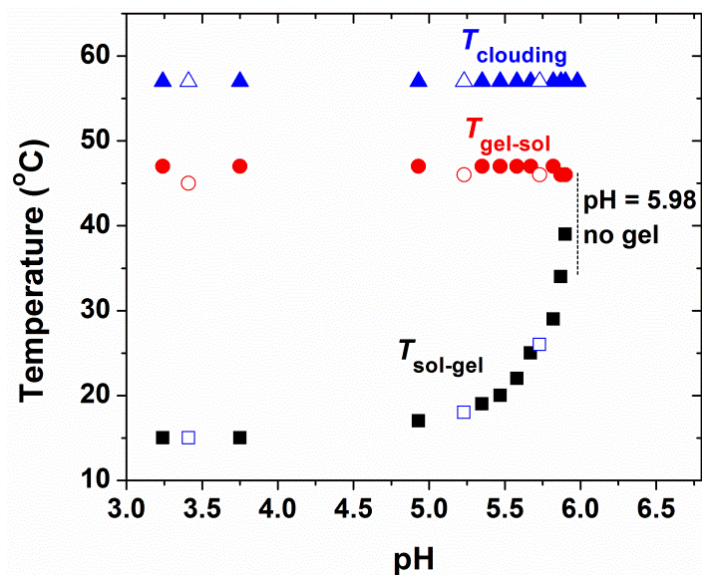
Figure 3.3 Sol-to-gel transition temperature ($T_{\text{sol-gel}}$), gel-to-sol transition temperature ($T_{\text{gel-sol}}$), and clouding temperature (T_{clouding}) of the 25 wt% aqueous solution of PTEGMA-*b*-P(DEGEA-*co*-AA) (**DB-1**) as a function of pH. The transition temperatures were determined by visual examination. Solid and unfilled symbols represent the data obtained from the processes of increasing and decreasing pH, respectively.

determined by the LCST behavior of the higher LCST block – the PTEGMA block, which did not contain any carboxylic acid groups. With further increasing the pH of the solution to 5.98, no gel was formed in the temperature range from 5 to 65 °C.

To test the reproducibility of $T_{\text{sol-gel}}$, $T_{\text{gel-sol}}$, and T_{clouding} at specific pH values, we then gradually lowered the solution pH by injecting a 1.0 M HCl aqueous solution in a stepwise fashion. As shown in Figure 3.3, upon decreasing the pH to 5.73, 5.23, and 3.41, all three values of $T_{\text{sol-gel}}$ were right on the curve, and the T_{clouding} remained at 57 °C, indicating an excellent reproducibility of these two transition temperatures. The $T_{\text{gel-sol}}$ was found to be 46 °C at pH of 5.73 and 5.23, and 45 °C at pH of 3.41, which were $1 - 2$ °C lower than those during the course of increasing the pH (47 °C). We speculate that the observed small differences in $T_{\text{gel-sol}}$ likely resulted from the small increase in the salt concentration due to the neutralization reaction; the gel-to-sol transition, which is governed by the change of volume fraction of micelles with temperature, is more sensitive to the small change in the salt concentration in the sample. Nevertheless, the results from both processes of increasing and decreasing pH demonstrated that the $T_{\text{sol-gel}}$ of the 25 wt% aqueous buffer solution of PTEGMA-*b*-P(DEGEA-*co*-AA) can be precisely tuned over a temperature range of 24 °C by changing the solution pH between 3.24 and 5.90 while the $T_{\text{gel-sol}}$ and T_{clouding} showed no or little change.

The effect of solution pH on sol-gel-sol-cloudy transitions of the 25 wt% aqueous solution of PTEGMA-*b*-P(DEGEA-*co*-AA) (**DB-1**) can be clearly seen from the pictures in Figure 3.2. At 20 °C, the sample was a free-standing clear gel when the pH was 3.24 (Figure 3.2b1) but became a free-flowing clear sol at pH = 5.58 (Figure 3.2b2). Similarly, at 25 °C, the sample was in the clear gel state at pH of 3.24 and 5.58, but changed to a

clear sol when the pH was raised to 5.82. Note that from the vial inversion tests, the $T_{\text{sol-}}$

$_{\text{gel}}$ of the sample was 15 °C at pH = 3.24, 22 °C at pH = 5.58, and 29 °C at pH = 5.82. The

pH variation had little or no effect on the gel-to-sol and clouding transitions, respectively;

the sample was a clear sol at 52 °C and a clouding sol at 65 °C, regardless of whether the

pH was 3.24, 5.58 or 5.82.

3.3.4 Rheological Properties of 25 wt% Aqueous Solutions of PTEGMA-*b*-P(DEGEA-*co*-AA) (DB-1) at Three Different pH Values (pH = 3.24, 5.58, and 5.82)

Rheological measurements were conducted to characterize the solution properties of

25 wt% aqueous solutions of **DB-1** with pH values of 3.24, 5.58, and 5.82. For each pH,

to ensure that the dynamic viscoelastic properties (dynamic storage modulus G' and

dynamic loss modulus G'') were measured in the linear viscoelastic regime, we first

carried out dynamic strain amplitude sweeps from 0.01 % to 80 % strain for the sample in

the gel state at four frequencies (f = 0.5, 1.0, 2.5, and 5.0 Hz). As can be seen from Figure

3.4, for all four frequencies, the gel at pH = 3.24 and T = 30 °C exhibited a linear

response up to 4 % strain, which is typical for diblock copolymer micellar gels[22] and is

significantly smaller than that of 3-D micellar network gels of ABA triblock copolymers

(up to ~ 15 % strain).[7f,22] This is because the gelation mechanism of moderately

concentrated aqueous solutions of AB diblock copolymers is the packing of spherical

micelles into an ordered structure. The lack of physical crosslinking of micelles makes

diblock copolymer micellar gels not as robust as interconnected micellar network gels.

Similar linear viscoelastic regimes were found for the samples with pH of 5.58 at 30 °C

and pH of 5.82 at 35 °C. In light of these observations, we used a strain amplitude of 1 %

for all dynamic tests.
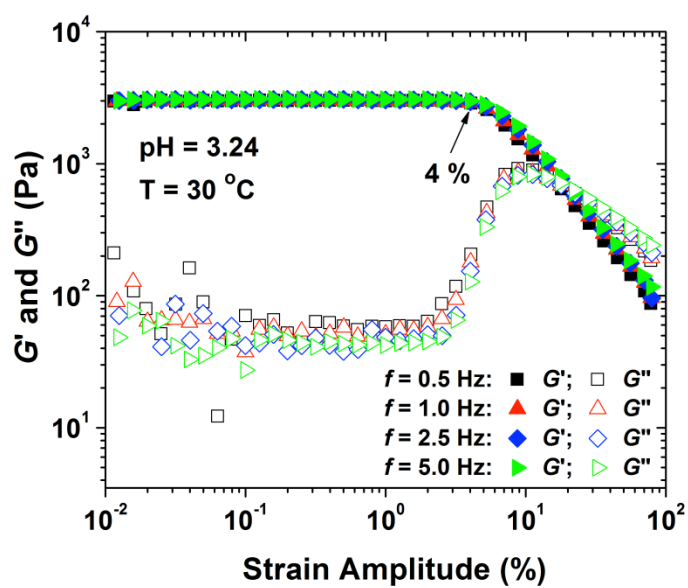
Figure 3.4 Dynamic strain amplitude sweeps at frequencies of 0.5, 1.0, 2.5, and 5.0 Hz for the 25 wt% aqueous solution of PTEGMA-*b*-P(DEGEA-*co*-AA) (**DB-1**) with pH of 3.24 at 30 °C

Figure 3.5a shows G' and G'' as a function of temperature for the 25 wt% aqueous solution of **DB-1** with pH of 3.24. The data were collected from an oscillatory shear experiment that was performed in a heating ramp using a strain amplitude of 1 %, a fixed frequency of 1 Hz, and a heating rate of 1 °C/min. Below 15 °C, both G' and G'' were small and $G'' > G'$, indicating that the sample was in a sol state. With the increase of temperature to above 15 °C, G' and G'' increased rapidly and at > 17 °C, G' became larger than G'', suggesting that the solution turned into a gel. Between 19 and 42 °C, G' was at least one order of magnitude greater than G''. Above 42 °C, G' and G'' began to decrease and G' became smaller than G'' at > 48.3 °C, indicating that the gel changed to a sol. The crossover points of G' and G'' curves are commonly used as indicators of sol-to-gel and gel-to-sol transitions.[2,3,22] Using this method, the $T_{\text{sol-gel}}$ and the $T_{\text{gel-sol}}$ were found to be 17.0 and 48.3 °C, respectively, which were close to those determined by the vial inversion method (15 and 47 °C, respectively). Upon increasing the pH to 5.58, the $T_{\text{sol-gel}}$ shifted to 24.0 °C (Figure 3.5b), which was 7 °C higher than that at pH 3.24, and the $T_{\text{gel-sol}}$ remained virtually the same (48.5 °C). Again, the two transition temperatures were close to those from the vial inversion test ($T_{\text{sol-gel}}$ = 22 °C and $T_{\text{gel-sol}}$ = 47 °C). Further increasing the pH to 5.82 raised the $T_{\text{sol-gel}}$ to 30.5 °C (Figure 3.5c, $T_{\text{sol-gel}}$ = 29 °C by vial inversion test); significantly, the $T_{\text{gel-sol}}$ again remained essentially unchanged (48.3 °C), consistent with the observation from visual inspection. By looking through the three plots in Figure 3.5, one can easily ascertain that the gel zone became narrower with the increase of pH. A close examination of G' values in the gel zone revealed that the maximum value of G' decreased with the increase of pH, from 2864 Pa at pH = 3.24, to 2458 Pa at pH = 5.58, and to 2075 Pa at pH = 5.82. Since the G' of a diblock copolymer
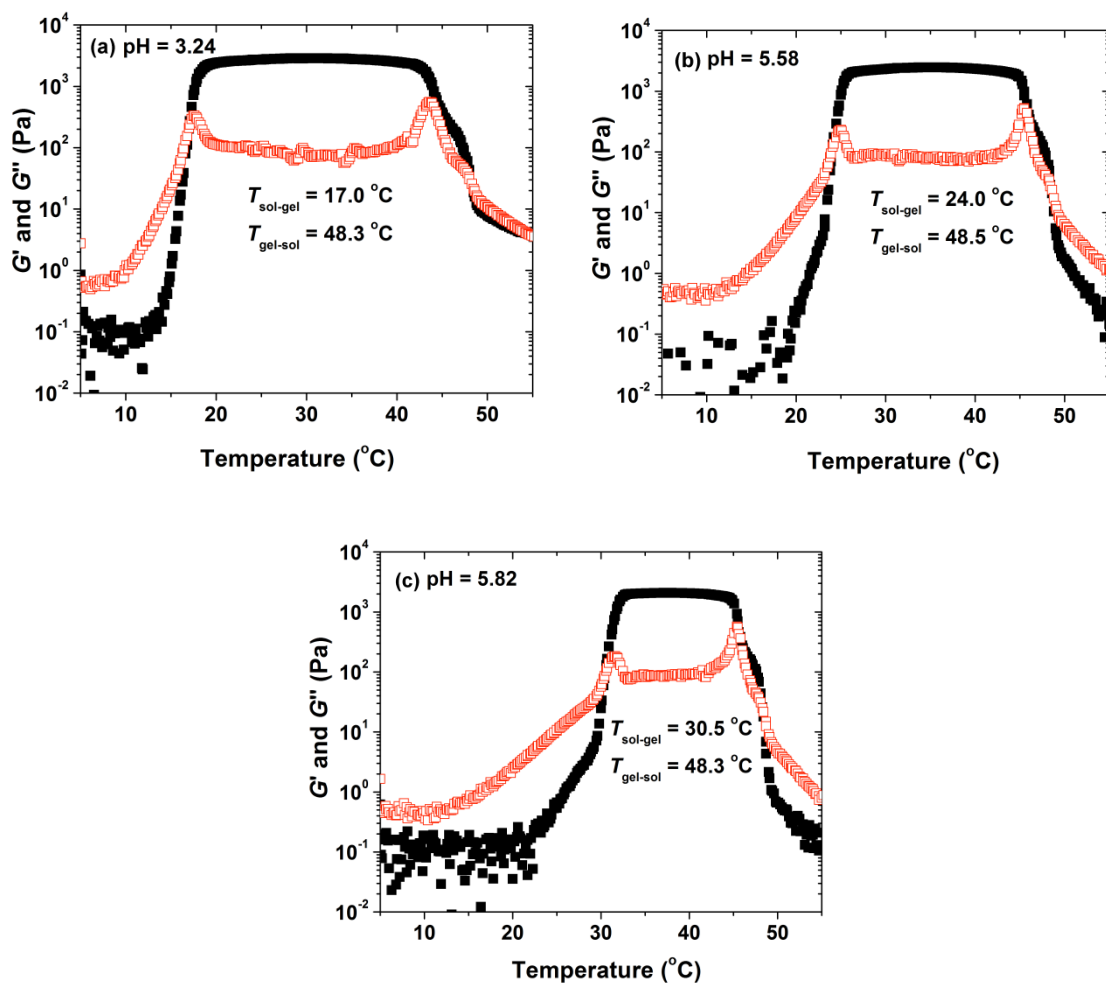
Figure 3.5 Dynamic storage modulus *G'* (solid black square) and loss modulus *G''* (red hollow square) of 25 wt% aqueous solution of **DB-1** at pH of (a) 3.24, (b) 5.58, and (c) 5.82 as a function of temperature. The data were collected from oscillatory shear experiments performed in a heating ramp using a heating rate of 1 °C/min, a strain amplitude of 1.0 %, and a frequency of 1 Hz.

micellar gel is related to the volume fraction of micelles in the gel, the slight decrease in

G' suggests that the volume fraction of micelles of **DB-1** in the 25 wt% aqueous solution

becomes smaller with the increase of solution pH, which presumably results from the

greater hydrophilicity of polymer chains at a higher degree of ionization of carboxylic

acid groups.

The effect of pH on solution property of **DB-1** also manifested in the temperature

dependence of apparent viscosity. Figure 3.6 shows the curves of apparent viscosity vs.

temperature for 25 wt% aqueous solutions of **DB-1** with pH values of 3.24, 5.58, and

5.82. The data were collected at a shear rate of 10 s^{-1} in a heating ramp with a heating rate

of 3 °C/min. For all three pH values, when the temperature was below a certain value, the

viscosity of the sample was low (on the order of tenths of 1 Pa•s or less), indicating that

the sample was in a sol state. When the temperature approached the $T_{\text{sol-gel}}$, the apparent

viscosity increased sharply. After reaching the highest point, it began to decrease and

eventually descended to a value less than 0.2 Pa•s. Clearly, with the increase of solution

pH, the first transition temperature, defined in Figure 3.6, shifted to the high temperature

side, from 14 °C at pH = 3.24, to 20 °C at pH = 5.58, and 25 °C at 5.82. These

temperatures correlated roughly with those determined by dynamic viscoelastic

measurements (17.0, 24.0, and 30.3 °C, respectively) and by the vial inversion method

(15, 22 °C, and 29 °C, respectively). In contrast, the transition temperature at the high

temperature side remained essentially the same (~ 50 °C). In addition, the maximum

apparent viscosity decreased with the increase of pH, from 16.36 Pa•s at pH = 3.24, to

11.86 Pa•s at pH 5.58, and 6.91 Pa•s at pH 5.82; this observation is in agreement with the

maximum G' values in Figure 3.5. It appeared that the micelles at higher pH values were
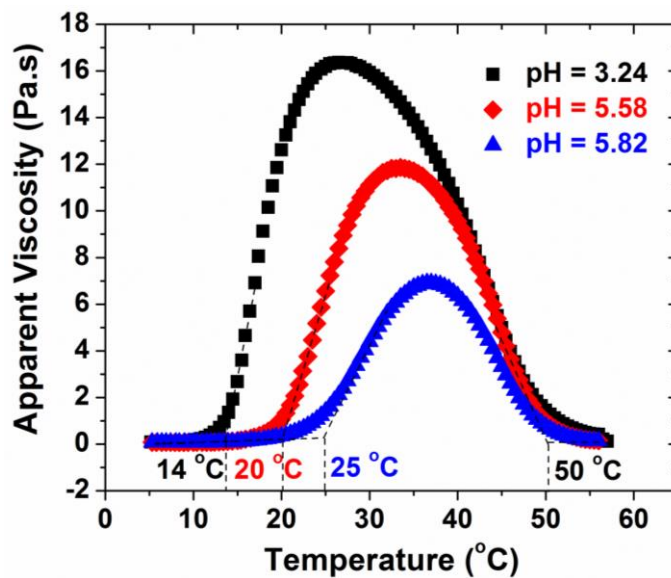
Figure 3.6 Apparent viscosity of the 25 wt% aqueous solution of PTEGMA-*b*-P(DEGEA-*co*-AA) (**DB-1**) as a function of temperature at pH of 3.24, 5.58, and 5.82. The data were collected in a heating ramp with a heating rate of 3 °C/min at a shear rate of 10 s^{-1}.

not packed as tightly as at pH 3.24. This study again showed that the $T_{\text{sol-gel}}$ of the 25 wt%

aqueous solution of **DB-1** can be tuned by changing the solution pH, while the $T_{\text{gel-sol}}$

remains the same.

3.3.5 Dynamic Light Scattering Study of Thermo-Induced Micellization of PTEGMA-*b*-P(DEGEA-*co*-AA) (DB-1) at the Concentration of 0.02 wt% in Aqueous Buffers at Various pH values

The observed solution behavior of the 25 wt% aqueous solution of **DB-1** originated

from the thermosensitive properties of the two blocks and the pH dependence of the

LCST of P(DEGEA-*co*-AA). Below the LCST of P(DEGEA-*co*-AA) at a particular pH,

the block copolymer dissolved molecularly in water. Above the LCST, the polymer

molecules self-assembled into micelles with the collapsed P(DEGEA-*co*-AA) block

forming the core and the PTEGMA block forming the corona. With the increase of

temperature, more polymer molecules are transferred into the micelles. When the

effective volume of micelles exceeded a critical value, the solution turned into a free-

standing gel. Further increasing temperature resulted in shrinking of PTEGMA corona,

which is typical for PEO-based thermosensitive water-soluble polymers.[2,3,23] When the

volume fraction of micelles dropped below the critical value, the clear gel melted into a

clear sol. With further raising the temperature to the LCST of PTEGMA, the PTEGMA

blocks in the corona collapsed and macroscopically, the clear sol turned into a cloudy

mixture (57 °C in the case of **DB-1**). The pH dependence of $T_{\text{sol-gel}}$ of the 25 wt% aqueous

solution of PTEGMA-*b*-P(DEGEA-*co*-AA) originated from the small amount of

carboxylic acid groups in the P(DEGEA-*co*-AA) block. At low pH values, the carboxylic

acid groups were in the unionized neutral form. As the pH increased, the carboxylic acid

96

groups began to ionize. Consequently, the polymer chains became more hydrophilic and the LCST transition of the P(DEGEA-*co*-AA) block occurred at higher temperatures. Since there were no pH-responsive groups in the PTEGMA block, the LCST of PTEGMA was not affected and the $T_{\text{gel-sol}}$ and T_{clouding} exhibited little or no change with pH.

To investigate the effects of pH on thermo-induced micellization of PTEGMA-*b*-P(DEGEA-*co*-AA) and aggregation of block copolymer micelles, we conducted dynamic light scattering (DLS) studies of **DB-1** in dilute aqueous buffers at a concentration of 0.02 wt%. Figure 3.7 shows the DLS results for 0.02 wt% aqueous solutions of **DB-1** at four different pH values (3.24, 5.58, 5.82, and 6.52). These solutions were made by using a 20 mM KHP aqueous buffer and the pH values were adjusted by adding either a 1.0 M KOH solution or a 1.0 M HCl solution. For the solution with pH of 3.24, when the temperature was below 10 °C, the scattering intensity was low and the apparent hydrodynamic diameter (D_{h}) was < 10 nm, indicating that the block copolymer was molecularly dissolved in the buffer (i.e., in the unimer state). When the solution was heated to 13 °C, the scattering intensity began to increase and a mixture of unimers and micelles was observed. The critical micellization temperature (CMT), determined from the scattering intensity versus temperature curve (Figure 3.7a), was 13 °C. In the temperature range of 15 °C to 55 °C, the scattering intensity increased initially and then leveled off; at each temperature, only one size distribution with an apparent average D_{h} of ~ 53 nm was observed. When the temperature reached 58 °C, the scattering intensity increased dramatically and aggregates with an apparent D_{h} of > 1000 nm were formed; by visual

97
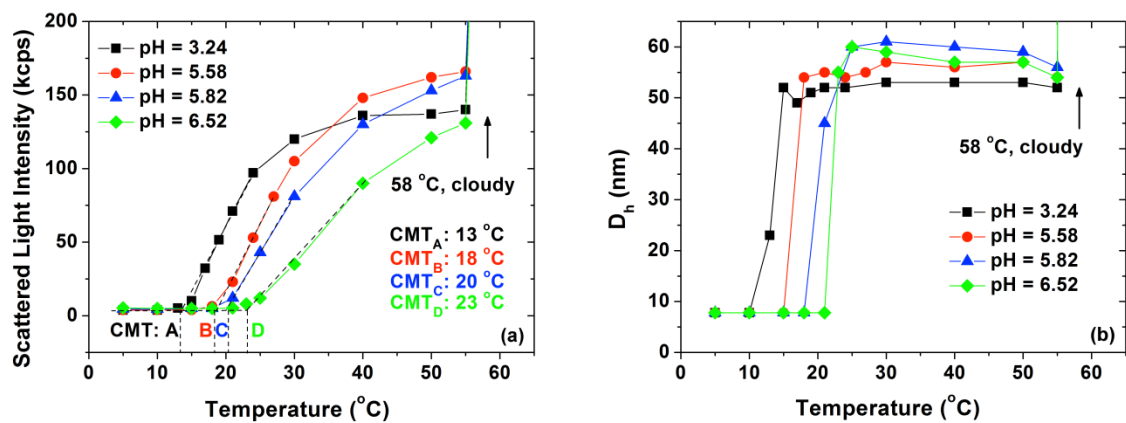
Figure 3.7 (a) Scattered light intensity at scattering angle of 90° and (b) apparent hydrodynamic size D_h, obtained from CONTIN analysis, as a function of temperature in a dynamic light scattering study of 0.02 wt% solutions of PTEGMA-*b*-P(DEGEA-*co*-AA) (**DB-1**) in 20 mM aqueous KHP buffer with pH = 3.24, 5.58, 5.82, and 6.52.

inspection, the solution turned cloudy. The clouding temperature is essentially the same as the reported cloud point of PTEGMA in water.[13]

With the increase of pH, the CMT shifted to higher temperatures, from 13 °C at pH = 3.24 to 18 °C at pH = 5.58, 20 °C at pH 5.82, and 23 °C at pH 6.52. Apparently, this is caused by the increased degree of ionization of carboxylic acid groups in the lower LCST block. In contrast to the CMT, the clouding temperature, the temperature at which the solution turned cloudy due to the LCST behavior of the PTEGMA block, remained unchanged (58 °C for all four pH values) as expected. Although the DLS results were consistent with the effects of pH on $T_{\text{sol-gel}}$, $T_{\text{gel-sol}}$, and T_{clouding}, the CMT did not increase with pH at the same pace as $T_{\text{sol-gel}}$. This could be due to the difference in the nature of sol-gel transition and micellization. The former reflects the change of volume fraction of micelles with temperature, which is presumably more sensitive to pH changes enabling $T_{\text{sol-gel}}$ to be tuned over a wider temperature range, while the latter reflects the thermo-induced self-association of block copolymer molecules.

3.3.6 Differential Scanning Calorimetry (DSC) Study of 25 wt% Aqueous Solutions of PTEGMA-*b*-P(DEGEA-*co*-AA) (DB-1) with pH of 3.24, 5.58 and 5.82

We further studied the LCST transitions of PTEGMA-*b*-P(DEGEA-*co*-AA) in water using differential scanning calorimetry (DSC). Figure 3.8 shows the DSC thermograms of 25 wt% aqueous solutions of **DB-1** with pH of 3.24, 5.58, and 5.82. Clearly, there were two endothermic peaks in each thermogram, which demonstrated that the transitions were entropically driven, consistent with the commonly accepted mechanism for the LCST behavior of thermosensitive hydrophilic polymers in water.[24] For pH 3.24, the peak positions of the LCST transitions of P(DEGEA-*co*-AA) and PTEGMA blocks were
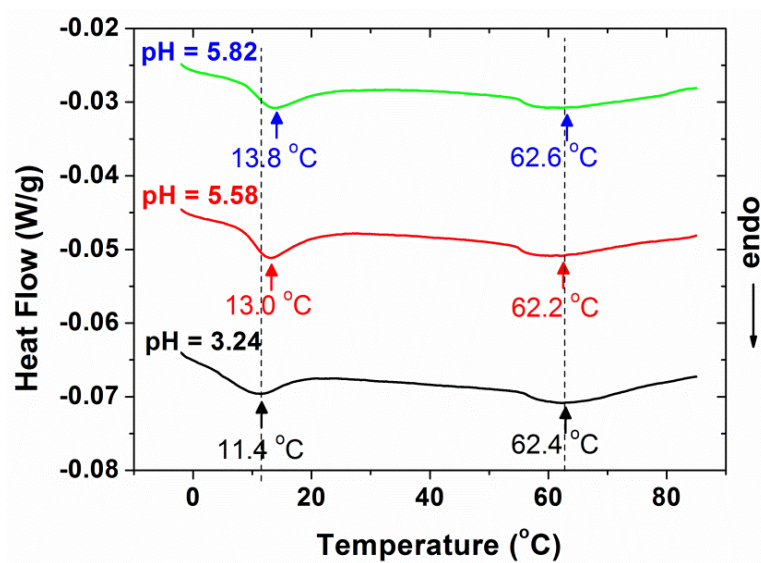
Figure 3.8 Differential scanning calorimetry thermograms of 25 wt% aqueous solutions of PTEGMA-*b*-P(DEGEA-*co*-AA) (**DB-1**) with pH values of 3.24, 5.58, and 5.82. The heating rate was 1 °C/min. For the sake of clarity, the thermograms were shifted vertically.

located at 11.4 and 62.4 °C, respectively. For pH 5.58 and 5.82, the P(DEGEA-*co*-AA) peak shifted to 13.0 and 13.8 °C, respectively. The changes were small but discernible. Differently, the peak position for the PTEGMA block remained at ~ 62.4 °C. In addition, the onset temperature of the LCST transition of PTEGMA at three pH values stayed at ~55 °C, which was close to the clouding temperature in Figure 3.3 by visual inspection (57 °C) and that in Figure 3.7 by DLS (58 °C). These results are consistent with the observations in Figures 3.2 and 3.5 that with the increase of pH the $T_{\text{sol-gel}}$ shifted to higher temperatures while the $T_{\text{gel-sol}}$ and T_{clouding} remained essentially the same. Note that compared with the changes of $T_{\text{sol-gel}}$ of the 25 wt% aqueous solution of **DB-1** and CMT of **DB-1** in the 0.02 wt% aqueous solution with the increase of pH from 3.24 to 5.58 and 5.82, the shifts of the endothermic peak of P(DEGEA-*co*-AA) in the DSC thermograms were smaller. These differences could be due to the distinct mechanisms underlying the sol-gel transition, micellization, and the LCST transition. While DSC measures the heat associated with the dehydration of segments in the thermosensitive blocks, i.e., the LCST transition, DLS characterizes the CMT, the temperature at which block copolymer molecules begin to self-assemble into micelles, which describes the cooperative behavior of multiple block copolymer chains. On the other hand, the $T_{\text{sol-gel}}$, determined by rheological measurements, is related to the rheological/mechanical property of a macroscopic sample and is determined by how the volume fraction of micelles in a moderately concentrated aqueous solution changes with temperature. This temperature indicates the packing of micelles into an ordered structure. It appears that the small changes in LCST transition of the thermosensitive blocks caused by pH variations are amplified in the effects of pH on CMT and $T_{\text{sol-gel}}$.

101

3.3.7 Sol-Gel Phase Diagrams of PTEGMA-*b*-P(DEGEA-*co*-AA) (DB-1) in KHP Aqueous Buffers with pH of 3.24, 5.58, and 5.82

The sol-gel phase diagrams of moderately concentrated aqueous solutions of **DB-1** with three different pH values (3.24, 5.58, and 5.82) were mapped out by the vial inversion method and are displayed in Figure 3.9.[25] All three diagrams are C-shaped curves, the characteristic shape of sol-gel phase diagrams of thermosensitive AB diblock copolymers in water. A striking feature of Figure 3.9 is that the upper temperature boundaries for three pH values overlapped while the lower temperature boundary shifted upward with the increase of pH from 3.24, to 5.58, and 5.82. The gap between any two curves appeared to be either essentially independent of concentration or increase slightly with the decrease of polymer concentration. Note that the clouding temperature was 57 °C, regardless of polymer concentration and solution pH. The fact that there was a difference between clouding temperature and $T_{\text{gel-sol}}$ suggests that the gel-to-sol transition was not entirely and directly governed by but related to the LCST transition of the PTEGMA block.

A second salient feature of Figure 3.9 is that with the increase of pH the critical gelation concentration (CGC) increased. The CGC was ~ 19 wt% at pH = 3.24, ~ 21 wt% at 5.58, and ~ 22 wt% at pH of 5.82. The CGC is the minimum concentration at which the volume fraction of block copolymer micelles in water reaches the critical value for gelation and is in some sense controlled by the balance between the thermo-enhanced micellization of the block copolymer and the thermo-induced shrinking of the corona. Apparently, the change of solution pH greatly affected the volume fraction of block copolymer micelles and its temperature dependence. We speculate that there are two
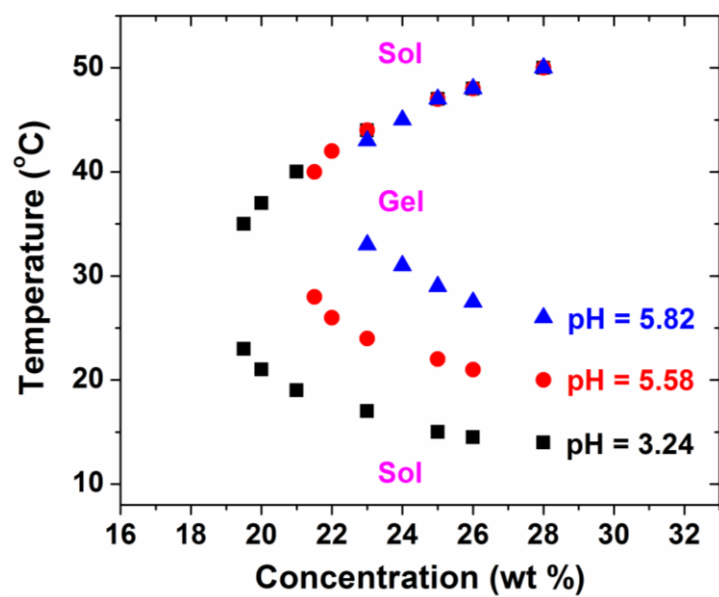
Figure 3.9 Sol-gel phase diagrams of moderately concentrated aqueous solutions of PTEGMA-*b*-P(DEGEA-*co*-AA) (**DB-1**) in KHP buffers with pH of 3.24, 5.58, and 5.82.

possible reasons for this observation. (i) With the increase of pH, the degree of ionization of carboxylic acid groups increased and the polymer chain became more hydrophilic. As a result, there were more block copolymer molecules staying in water instead of entering micelles at temperatures above the CMT. (ii) When the solution pH is increased, the thermo-induced micellization occurs at a higher temperature, and thus the PTEGMA block would shrink to a greater extent. Both factors could cause the decrease of the total volume of micelles in water (i.e., the increase in CGC) at higher pH values. This is supported by the observation that although the 25 wt% aqueous solution of **DB-1** with pH of 5.98 did not form a gel in the temperature range of 5 – 65 °C as mentioned earlier, an increase of the polymer concentration to 29 wt% at the same pH resulted in a gel with the $T_{sol\text{-}gel}$ of 35 °C and the $T_{gel\text{-}sol}$ of 50 °C.

3.3.8 Small-Angle X-Ray Scattering Study of Micellar Gels at pH of 3.24, 5.58, and 5.82

To confirm that the gels are formed by packing of spherical micelles of PTEGMA-*b*-P(DEGEA-*co*-AA), we conducted small-angle X-ray scattering (SAXS) experiments for three 25 wt% aqueous solutions of **DB-1** in 20 mM KHP buffers with pH of 3.24, 5.58, and 5.82, respectively. Figure 3.10 shows the two-dimensional SAXS patterns recorded at 35 °C at which all samples were in the gel state as well as one-dimensional curves obtained by integrating the corresponding 2D scattering patterns. Evidently, the micelles in all three gels were arranged in a crystalline order, as testified by the appearance of diffraction spots instead of diffuse scattering halos. For the samples with pH of 5.58 and 5.82, in addition to the strongest diffractions at $q \approx 0.19$ nm^{-1}, weaker diffractions can also be seen at larger q values. The q values of these observed diffractions (1:$\sqrt{2}$:$\sqrt{3}$) are
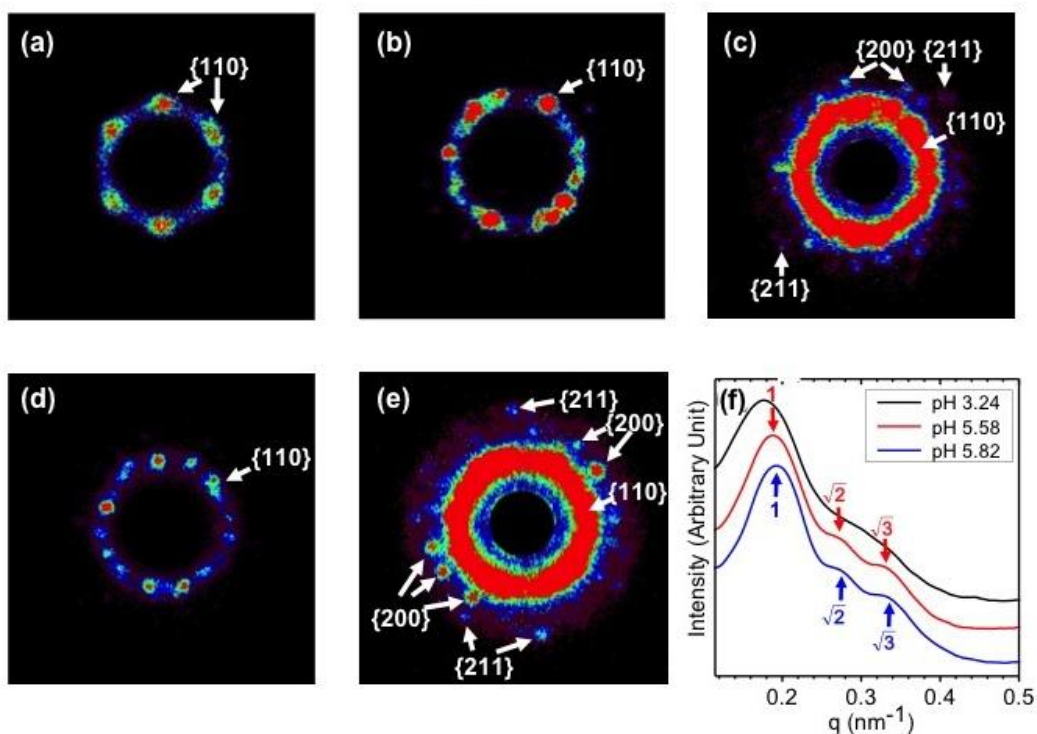
Figure 3.10 SAXS patterns of 25 wt% aqueous solutions of PTEGMA-*b*-P(DEGEA-*co*-AA) (**DB-1**) in KHP buffers with pH of 3.24, 5.58, and 5.82 at 35 °C. (a) Two-dimensional (2-D) scattering pattern of **DB-1** at pH 3.24; (b) 2-D scattering pattern of **DB-1** at pH 5.58 with the contrast adjusted to show strong {110} diffractions; (c) 2D scattering pattern of **DB-1** at pH 5.58 with the contrast adjusted to show weaker diffractions; (d) 2D scattering pattern of **DB-1** at pH 5.82 with the contrast adjusted to show strong {110} diffractions; (e) 2D scattering pattern of **DB-1** at pH 5.82 with the contrast adjusted to show weaker diffractions; (f) One-dimensional curves generated by integrating corresponding 2D scattering patterns. Black: pH 3.24; Red: pH 5.58; Blue: pH 5.82. The intensity is in logarithmic scale.

fully consistent with spherical micelles packed into a bcc crystalline lattice (Figure 3.10f).[2,26] The strongest diffractions at the smallest q values were indexed as {110} diffractions. Note that {110} diffractions are indeed the strongest low-index diffractions given by hard spheres packed in a bcc lattice. The diffractions with larger q values were indexed as {200} and {211} diffractions accordingly as shown in Figure 3.10. The center-to-center distance (D) of adjacent micelles can be calculated by using Equation 2.1, where a is the cell edge length, and was 40.9 and 39.9 nm for the gels with pH of 5.58 and 5.82, respectively.

$$D = \frac{\sqrt{3}}{2}a \text{ for a bcc lattice} \qquad \text{(Equation 2.1)}$$

The lattice for the gel at pH 3.24 cannot be determined on the basis of q value ratios, since only one set of diffraction spots at $q \approx 0.18$ nm^{-1} is clearly resolved. However, as the diffraction pattern is obviously of a single crystal type, the packing lattice of micelles can still be deduced. The most typical packing schemes of spherical particles are face-centered cubic (fcc), hexagonal closed-packing (hcp), and bcc. With the polarized light microscopy results showing that the gel was optically isotropic, the hcp lattice can be ruled out. Note that the six diffraction spots in Figure 3.10a are of the same q value and distributed symmetrically with six fold symmetry. To produce such a diffraction pattern from a fcc single crystal, it would be a <111> zone diffraction and {220} diffractions will be the ones with the smallest q value. It is simply not possible to generate six {111} diffractions, the strongest diffractions of a fcc lattice, by a fcc single crystal. On the other hand, if the diffraction spots shown in Figure 3.10a are from {220} diffractions of a fcc lattice, the center-to-center distance (D) of adjacent micelles, calculated by using Equation 2.2, would be unreasonably large (70.9 nm).

$$D = \frac{\sqrt{2}}{2}a \text{ for a fcc lattice} \qquad \text{(Equation 2.2)}$$

where a is the cell edge length. In contrast, the <111> zone diffraction of a bcc single crystal features six {110} diffraction spots, the strongest low index diffractions, in the exactly same fashion as shown in Figure 3.10a. Therefore, the most probable packing scheme of micelles in the gel at pH of 3.24 is also a bcc lattice, just like the gels at other two pH values.

The center-to-center distance of adjacent micelles in the gel with pH of 3.24 calculated by using Equation 2.1 was 43.4 nm, slightly larger than those in the gels at pH of 5.58 and 5.82 (40.9 and 39.9 nm, respectively). These D values were slightly smaller than the apparent hydrodynamic sizes of **DB-1** at three pH values in dilute aqueous buffers with a concentration of 0.02 wt%, which were in the range of $50 - 60$ nm (Figure 3.7). Note that we use the term of "center-to-center distance of adjacent micelles" instead of the micelle size because the micelles could be deformed when the volume fraction of micelles exceeds the critical value for the physical jamming.

3.3.9 Thermo-Induced Sol-Gel-Sol-Cloudy Transitions of Moderately Concentrated Aqueous Solutions of DB-2

DB-2 had a slightly higher AA content than that of **DB-1**; the molar ratio of DEGEA to AA units in the P(DEGEA-*co*-AA) block was 100 : 10, in contrast to 100 : 5.2 in **DB-1**. The characterization data for this diblock copolymer can be found in Table 3.1 and in Appendix B. For comparison with **DB-1**, we made a 25 wt% aqueous solution of **DB-2** using a 20 mM aqueous KHP buffer and adjusted its pH value by adding either a 1.0 M NaOH or a 1.0 M HCl standard solution. The $T_{\text{sol-gel}}$, $T_{\text{gel-sol}}$, and T_{clouding} at each pH were determined by vial inversion tests. Figure 3.11a shows the transition temperatures as the
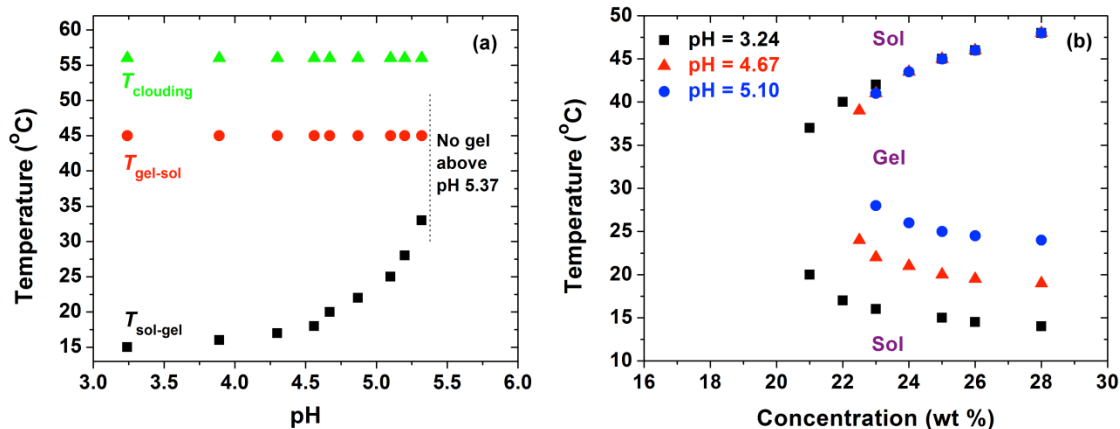
Figure 3.11 (a) Sol-to-gel transition temperature ($T_{\text{sol-gel}}$), gel-to-sol transition temperature ($T_{\text{gel-sol}}$), and clouding temperature (T_{clouding}) of a 25 wt% aqueous solution of PTEGMA-*b*-P(DEGEA-*co*-AA) (**DB-2**) as a function of pH, and (b) sol-gel phase diagrams of **DB-2** at three different pH values (3.24, 4.67, and 5.10). The transition temperatures were determined by vial inversion tests through visual examination.

function of solution pH. Similar to the 25 wt% aqueous solution of **DB-1**, the $T_{\text{gel-sol}}$ and

T_{clouding} were not affected by the pH changes and remained at 45 and 56 °C, respectively,

in the pH range of 3.24 – 5.37, while the $T_{\text{sol-gel}}$ increased with the increase of solution pH

but at a faster pace than that of **DB-1**. For example, from pH 3.24 to 5.32, the $T_{\text{sol-gel}}$ of

the 25 wt% aqueous solution of **DB-2** increased by 18 °C and above pH 5.37 no gelation

was observed in the studied temperature (up to 60 °C). In contrast, for **DB-1**, the increase

was only 4 °C from pH 3.24 to 5.35. This is presumably due to the greater content of

carboxylic acid groups in the lower LCST block of **DB-2**. It is clear that the solution

property of PTEGMA-*b*-P(DEGEA-*co*-AA) is sensitive to the AA content in the lower

LCST block. This exemplifies an additional means to tune the solution properties of

PTEGMA-*b*-P(DEGEA-*co*-AA) via the control of the AA content. Figure 3.11b shows

the sol-gel phase diagrams of **DB-2** in aqueous KHP buffers in the moderate

concentration range at three pH values (pH = 3.24, 4.67, and 5.10). Similar to the

diagrams of **DB-1** shown in Figure 3.9, the upper temperature boundaries overlapped for

the three pH values, while the lower temperature boundary shifted upward with the

increase of solution pH from 3.24 to 4.67 and 5.10. In addition, the CGC increased with

the increase of pH, from 20.5 wt% at pH = 3.24 to 22.0 wt% at pH = 4.67, and 22.5 wt%

at pH = 5.10. By comparing the sol-gel phase diagrams of **DB-1** and **-2**, again, one can

easily find out that the change of $T_{\text{sol-gel}}$ with pH for **DB-2** is significantly faster than

those for **DB-1**.

3.4 Conclusions

Well-defined doubly thermosensitive hydrophilic diblock copolymers, PTEGMA-*b*-P(DEGEA-*co*-AA), with different AA contents in the lower LCST block were prepared by RAFT and post-polymerization modification.[27] A 25 wt% aqueous solution of PTEGMA-*b*-P(DEGEA-*co*-AA) with a DEGEA-to-AA molar ratio of 100 : 5.2 (**DB-1**) underwent multiple phase transitions, from a clear, free-flowing liquid (< 15 °C), to a clear gel (15 to 46 °C), to a clear liquid (47 to 56 °C), and a cloudy sol (≥ 57 °C). We showed that the $T_{\text{sol-gel}}$ can be tuned over a temperature of > 20 °C, while the $T_{\text{gel-sol}}$ and the T_{clouding} remained virtually the same in the studied pH range. DLS studies demonstrated that the CMT of **DB-1** increased with the increase of pH. From DSC analysis, two endothermic peaks were observed for 25 wt% aqueous solutions of **DB-1**, which corresponded to the LCST transitions of two thermosensitive blocks, and the peak of the P(DEGEA-*co*-AA) block shifted to higher temperatures with the increase of solution pH. Using the vial inversion test method, we mapped out the sol-gel phase diagrams of moderately concentrated aqueous solutions of **DB-1** at pH values of 3.24, 5.58, and 5.82. While the upper temperature boundaries overlapped, the lower temperature boundary shifted upward and the critical gelation concentration increased with the increase of pH. The robustness of the method for tuning $T_{\text{sol-gel}}$ was further confirmed by the study of solution properties of **DB-2**, which had a higher AA content in the lower LCST block. The $T_{\text{sol-gel}}$ of a 25 wt% aqueous solution of **DB-2** was found to increase with the increase of pH at a faster pace, and the sol-gel phase diagrams of **DB-2** exhibited the same characteristic features as those of **DB-1**. This work demonstrated that the $T_{\text{sol-gel}}$ of moderately concentrated aqueous solutions of doubly thermosensitive

hydrophilic diblock copolymers can be tuned by incorporating a small amount of stimuli-responsive groups into the lower LCST block and applying a 2nd external stimulus, providing a simple yet robust strategy for the design of multi-responsive injectable gels for potential applications.

References

1. (a) Park, M. H.; Joo, M. K.; Choi, B. G.; Jeong, B. *Acc. Chem. Res.* **2012**, *45*, 424-433. (b) Madsen, J.; Armes, S. P. *Soft Matter* **2012**, *8*, 592-605. (c) He, C. L.; Kim, S. W.; Lee, D. S. *J. Controlled Release* **2008**, *127*, 189-207. (d) Gil, E. S.; Hudson, S. M. *Prog. Polym. Sci.* **2004**, *29*, 1173-1222.

2. (a) Hamley, I. W. *Block Copolymers in Solution: Fundamentals and Applications*; John Wiley & Sons: Chichester, U.K., 2005. (b) Hamley, I. W. *The Physics of Block Copolymers*; Oxford University Press: Oxford, U.K., 1998.

3. Hamley, I. W. *Philos. Trans. R. Soc. London A* **2001**, *359*, 1017-1044.

4. Jeong, B. M.; Bae, Y. H.; Lee, D. S.; Kim, S. W. *Nature* **1997**, *388*, 860-862.

5. (a) Hvidt, S.; Jørgensen, E. B.; Schillén, K.; Brown, W. *J. Phys. Chem.* **1994**, *98*, 12320-12328. (b) Mortensen, K.; Brown, W.; Norden, B. *Phys. Rev. Lett.* **1992**, *68*, 2340-2343. (c) Alexandridis, P.; Hatton, T. A. *Colloids and Surfaces A: Physicochem. Eng. Aspects* **1995**, *96*, 1-46. (d) Wanka, G.; Hoffmann, H.; Ulbricht, W. *Macromolecules* **1994**, *27*, 4145-4159. (f) Zhou, Z; Chu, B. *Macromolecules* **1994**, *27*, 2025-2033. (g) Mortensen, K.; Brown, W.; Jørgensen, E. *Macromolecules* **1994**, *27*, 5654-5666.

6. (a) Li, H.; Yu, G.-E.; Price, C.; Booth, C.; Hecht, E.; Hoffmann, H. *Macromolecules* **1997**, *30*, 1347-1354. (b) Alexandridis, P.; Olsson, U.; Kindman, B. *Langmuir* **1997**, *12*, 23-34. (c) Hamley, I. W.; Pople, J. A.; Fairclough, J. P. A.; Ryan, A. J.; Booth, C.; Yang, Y.-W. *Macromolecules* **1998**, *31*, 3906-3911.

7. (a) Li, C.; Tang, Y.; Armes, S. P.; Morris, C. J.; Rose, S. F.; Lloyd, A. W.; Lewis, A. L. *Biomacromolecules* **2005**, *6*, 994-999. (b) Madsen, J. ; Armes, S. P.; Lewis, A. L.

Macromolecules **2006**, *39*, 7455-7457. (c) Kirkland, S. E.; Hensarling, R. M.; McConaught, S. D.; Guo, Y.; Jarrett, W. L.; McCormick, C. L. *Biomacromolecules* **2008**, *9*, 481-486. (d) Fechler, N.; Badi, N.; Schade, K.; Pfeifer, S.; Lutz, J.-F. *Macromolecules* **2009**, *42*, 33-36. (e) O'Lenick, T. G.; Jiang X. G.; Zhao, B. *Langmuir* **2010**, *26*, 8787–8796. (f) O'Lenick, T. G.; Jin, N. X.; Woodcock, J. W.; Zhao, B. *J. Phys. Chem. B.* **2011**, *115*, 2870-2881. (g) Woodcock, J. W.; Wright, R. A. E.; Jiang, X. G.; O'Lenick, T. G.; Zhao, B. *Soft Matter*, **2010**, *6*, 3325-3336. (f) Woodcock, J. W.; Jiang, X. G.; Wright, R. A. E.; Zhao, B. *Macromolecules* **2011**, *44*, 5764-5775.

8. Liu, S.; Billingham, N. C.; Armes, S. P. *Angew. Chem. Int. Ed.* **2001**, *40*, 2328-2331.

9. (a) Aoshima, S.; Kanaoka, S. *Adv. Polym. Sci.* **2008**, *210*, 169-208. (b) Aoshima, S.; Sugihara, S. *J. Polym. Sci. Part A: Polym. Chem.* **2000**, *38*, 3962-3965. (c) Sugihara, S. Kanaoka, S.; Aoshima, S. *J. Polym. Sci. Part A: Polym. Chem.* **2004**, *42*, 2601-2611. (d) Sugihara, S.; Kanaoka, S.; Aoshima, S. *Macromolecules* **2005**, *38*, 1919-1927.

10. (a) Jiang, X. G.; Lavender, C. A.; Woodcock, J. W.; Zhao, B. *Macromolecules* **2008**, *41*, 2632-2643. (b) Jiang, X. G.; Jin, S; Zhong, Q. X.; Dadmun, M. D.; Zhao, B. *Macromolecules* **2009**, *42*, 8468-8476. (c) Jiang X. G.; Zhao, B. *Macromolecules* **2008**, *41*, 9366-9375.

11. Jin, N. X.; Woodcock, J. W.; Xue. C. M.; O'Lenick, T. G.; Jiang, X. G.; Jin, S.; Dadmun, M. D.; Zhao, B. *Macromolecules* **2011**, *44*, 3556-3566.

12. (a) Yin, X.; Hoffman, A. S.; Stayton, P. S. *Biomacromolecules* **2006**, *7*, 1381-1385. (b) Feil, H.; Bae, Y. H.; Feijen, J.; Kim, S. W. *Macromolecules* **1993**, *26*, 2496-2500.

(c) Bulmus, V.; Ding, Z.; Long, C. J.; Stayton, P. S.; Hoffman, A. S. *Bioconjugate Chem.* **2000**, *11*, 78-83. (d) Lokitz, B. S.; York, A. W.; Stempka, J. E.; Treat, N. D.; Li, Y.; Jarrett, W. L.; McCormick, C. L. *Macromolecules* **2007**, *40*, 6473-6480. (e) Yamamoto, S.-I.; Pietrasik, J.; Matyjaszewski, K. *Macromolecules* **2008**, *41*, 7013-7020. (f) Luo, C. H.; Liu, Y.; Li, Z. B. *Macromolecules* **2010**, *43*, 8101-8108. (g) Tsitsilianis, C.; Gotzamanis, G.; Iatridi, Z. *Euro. Polym. J.* **2011**, *47*, 497-510. (h) Iatridi, Z.; Mattheolabakis, G.; Avgoustakis, K.; Tsitsilianis, C. *Soft Matter* **2011**, *7*, 11160-11168. (i) Horton, J. M.; Bao, C. H.; Bai, Z. F.; Lodge, T. P.; Zhao, B. *Langmuir* **2011**, *27*, 13324-13334.

13. Hua, F. J.; Jiang, X. G.; Li, D. J.; Zhao, B. *J. Polym. Sci. Part A: Polym. Chem.* **2006**, *44*, 2454-2467.

14. (a) Han, S.; Hagiwara, M.; Ishizone, T. *Macromolecules* **2003**, *36*, 8312-8319. (b) Lutz, J.-F.; Hoth, A. *Macromolecules* **2006**, *39*, 893-896. (c) Zhao, B.; Li, D. J.; Hua, F. J.; Green, D. R. *Macromolecules* **2005**, *38*, 9509-9517. (d) Jiang, X. G.; Zhao, B. *J. Polym. Sci. Part A: Polym. Chem.* **2007**, *45*, 3707-3721. (e) Jiang, X. W.; Smith, M. R.; Baker, G. L. *Macromolecules* **2008**, *41*, 318-324. (f) Horton, J. M.; Bai, Z. F.; Lodge, T. P.; Zhao, B. *Langmuir* **2011**, *27*, 2019-2027.

15. Chiefari, J.; Chong, Y. K.; Ercole, F.; Krstina, J.; Jeffery, J.; Le, T. P. T.; Mayadunne, R. T. A.; Meijs, G. F.; Moad, C. L.; Moad, G.; Rizzardo, E.; Thang, S. H. *Macromolecules* **1998**, *31*, 5559-5562.

16. (a) Determan, M. D.; Cox, J. P.; Seifert, S.; Thiyagarajan, P.; Mallapragada, S. K. *Polymer* **2005**, *46*, 6933-6946. (b) Determan, M. D.; Guo, L.; Thiyagarajan, P.; Mallapragada, S. K. *Langmuir* **2006**, *22*, 1469-1473.

17. (a) Shim, W. S.; Yoo, J. S.; Bae, Y. H.; Lee, D. S. *Biomacromolecules* **2005**, *6*, 2930-2934. (b) Shim, W. S.; Kim, S. W.; Lee, D. S. *Biomacromolecules* **2006**, *7*, 1935-1941.

18. (a) Park, S. Y.; Lee, Y.; Bae, K. H.; Ahn, C. H.; Park, T. G. *Macromol. Rapid Commun.* **2007**, *28*, 1172-1176. (b) Suh, J. M.; Bae, S. J.; Jeong, B. *Adv. Mater.* **2005**, *17*, 118-120. (c) Joo, M. K.; Park, M. H.; Choi, B. G.; Jeong, B. *J. Mater. Chem.* **2009**, *19*, 5891-5905.

19. (a) Shim, W.S.; Kim, J. H.; Park, H.; Kim, K.; Kwon, I. C.; Lee, D. S. *Biomaterials* **2006**, *27*, 5178-5185. (b) Dayananda, K.; He, C. L.; Park, D. K.; Park, T. G.; Lee, D. S. *Polymer* **2008**, *49*, 4968-4973. (c) Huynh, D. P.; Nguyen, M. K.; Kim, B. S.; Lee, D. S. *Polymer* **2009**, *50*, 2565-2571.

20. Chong, Y. K.; Krstina, J.; Le, T. P. T.; Moad, G.; Postma, A.; Rizzardo, E.; Thang, S. H. *Macromolecules* **2003**, *36*, 2256-2272.

21. The SEC traces of **H-2** and **DB-2-P** and ^{1}H NMR spectra of **DB-2-P** and **DB-2** can be found in Appendix B.

22. Noro, A.; Matshushita, Y.; Lodge, T. P. *Macromolecules* **2009**, *42*, 5802-5810.

23. Bai, Z. F.; Lodge, T. P. *J. Phys. Chem. B* **2009**, 113, 14151-14157.

24. (a) Schild , H. G. *Prog. Polym. Sci.* **1992**, *17*, 163-249. (b) Urry, D. W. *J. Phys. Chem. B* **1997**, *101*, 11007-11028.

25. The pH variations with the changes of polymer concentration and temperature were negligible or very small. See the data in Appendix B.

26. (a) Hamley, I. W.; Daniel, C.; Mingvanish, W.; Mai, S.-M.; Booth, C.; Messe, L.; Ryan, A. J. *Langmuir* **2000**, *16*, 2508-2514. (b) Torija, M. A.; Choi, S.-H.; Lodge, T. P.; Bates, F. S. *J. Phys. Chem. B.* **2011**, *115*, 5840-5848.

27. The work presented in this Chapter has been published in *the Journal of Physical Chemistry B* as an article (*J. Phys. Chem. B.* **2012***, 116,* 3125-3137). http://pubs.acs.org/doi/abs/10.1021/jp300298a

Appendix B

for

Chapter 3. Tuning Thermally Induced Sol-to-Gel Transitions of Aqueous Solutions of Doubly Thermosensitive Diblock Copolymers Poly(methoxytri(ethylene glycol) acrylate)-*b*-poly(ethoxydi(ethylene glycol) acrylate-*co*-acrylic acid)
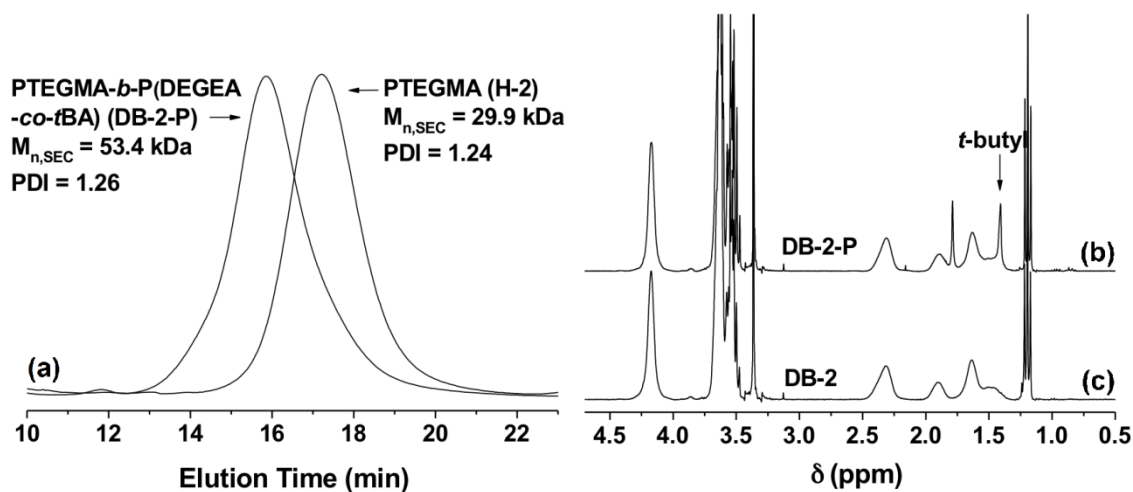
Figure B1. (a) Size exclusion chromatography traces of PTEGMA macro-CTA (**H-2**) and diblock copolymer PTEGMA-*b*-P(DEGEA-*co-t*BA) (**DB-2-P**), and ^{1}H NMR spectra of (b) PTEGMA-*b*-P(DEGEA-*co-t*BA) (**DB-2-P**) and (c) PTEGMA-*b*-P(DEGEA-*co*-AA) (**DB-2**). CDCl$_3$ was used as solvent in ^{1}H NMR spectroscopy analysis.
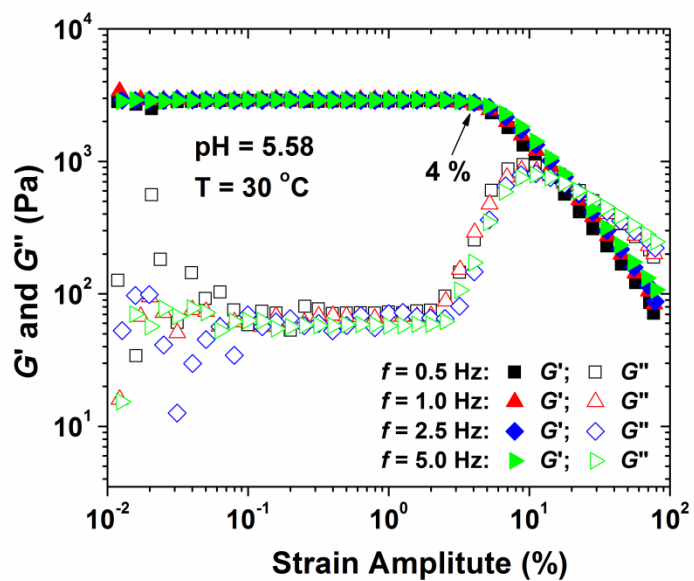
Figure B2. Dynamic strain amplitude sweeps at frequencies of 0.5, 1.0, 2.5, and 5.0 Hz for the 25 wt% aqueous solution of PTEGMA-*b*-P(DEGEA-*co*-AA) (**DB-1**) with pH of 5.58 at 30 °C.

119
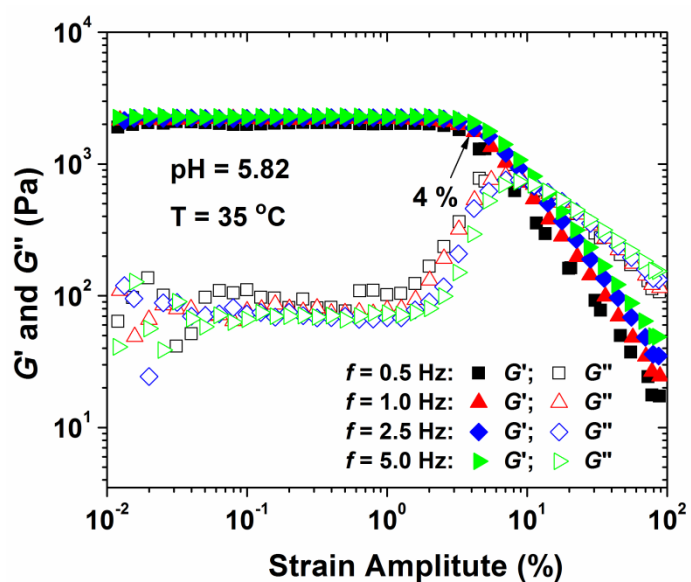
Figure B3. Dynamic strain amplitude sweeps at frequencies of 0.5, 1.0, 2.5, and 5.0 Hz for the 25 wt% aqueous solution of PTEGMA-*b*-P(DEGEA-*co*-AA) (**DB-1**) with pH of 5.82 at 35 °C.

B1. pH Variations with the Changes of Block Copolymer Concentration at a Specific Temperature

The pH value of a 25 wt% aqueous solution of **DB-1** in a KHP buffer with pH of 3.24 was determined in an ice/water bath with a pH meter (calibrated at 0 °C using pH = 4.01, 7.00, and 10.01 standard buffer solutions). The sample was diluted to 19.5 wt% and the pH was found to be 3.22, measured at 0 °C. We then concentrated the solution to 28 wt% by evaporating a calculated amount of water. After the solution was sonicated in an ice/water bath to ensure that it was homogenous, the pH was measured and was 3.24. These observations demonstrated that the pH variations with the change of polymer concentration in the determination of the sol-gel phase diagrams were negligible.

B2. pH Variations with the Changes of Temperature at Specific Polymer Concentrations

We also investigated how the pH values of moderately concentrated aqueous solutions of PTEGMA-*b*-P(DEGEA-*co*-AA) in KHP buffers were affected by temperature changes. The pH values of moderately concentrated aqueous solutions of **DB-1** and **DB-2** in KHP buffers at 0, 25, and 55 °C were measured. For each diblock copolymer, two solutions were investigated, one at a lower pH (< 3.5) and on at higher pH value (> 4.5). The polymer concentration in each sample was slightly below the critical gelation concentration so that the sample did not form a gel in the studied temperature range. The pH meter was calibrated at corresponding temperatures (0, 25, and 55 °C) by using pH = 4.01, 7.00, and 10.01 standard buffer solutions. The data are summarized in Table B1. For both **DB-1** and **DB-2**, when the pH values of the solutions were < 3.5, the pH variations of the solutions in the range of 0 to 55 °C were small (≤

0.10 pH units). The pH changes for the two samples with higher pH values were slightly larger (0.25 and 0.21 pH units for **DB-1** and **DB-2**, respectively). These changes were comparable to those of 20 mM aqueous KHP buffers with similar pH values (Table B2).

Table B1. The Effect of Temperature on pH Values of Moderately Concentrated Aqueous Solutions of **DB-1** and **DB-2**

Sample	0 °C	25 °C	55 °C	Δ pH
18 wt% solution of **DB-1**	3.37	3.40	3.45	0.08
20 wt% solution of **DB-1**	5.65	5.70	5.90	0.25
20 wt% solution of **DB-2**	3.38	3.39	3.48	0.10
21 wt% solution of **DB-2**	4.71	4.77	4.92	0.21

Table B2. The Effect of Temperature on pH Values of Aqueous KHP Buffers

Buffer	0 °C	25 °C	45 °C	65 °C	Δ pH
20 mM Aqueous KHP Buffer	3.32	3.30	3.34	3.38	0.08
20 mM Aqueous KHP Buffer	4.49	4.45	4.49	4.60	0.15
20 mM Aqueous KHP Buffer	5.32	5.40	5.43	5.47	0.15

Chapter 4. Shifting Sol-Gel Phase Diagram of A Doubly Thermosensitive Hydrophilic Diblock Copolymer Poly(methoxytri(ethylene glycol) acrylate-*co*-acrylic acid)-*b*-poly(ethoxydi(ethylene glycol) acrylate-*co*-acrylic acid) in Aqueous Solution

Abstract

    This Chapter shows that the C-shaped sol-gel phase diagram of a doubly thermosensitive hydrophilic diblock copolymer with each block containing a small amount of weak acid groups in aqueous solution in the moderate concentration range can be readily and reversibly shifted by changing the solution pH. The diblock copolymer, poly(methoxytri(ethylene glycol) acrylate-*co*-acrylic acid)-*b*-poly(ethoxydi(ethylene glycol) acrylate-*co*-acrylic acid) (P(TEGMA-*co*-AA)-*b*-P(DEGEA-*co*-AA)), was synthesized by reversible addition-fragmentation chain transfer polymerization and post-polymerization modification. A 20 wt% aqueous solution of P(TEGMA-*co*-AA)-*b*-P(DEGEA-*co*-AA) with pH of 3.29 underwent sol-to-gel, gel-to-sol, and clear sol-to-cloudy sol transitions at 17 °C ($T_{\text{sol-gel}}$), 38 °C ($T_{\text{gel-sol}}$), and 55 °C (T_{clouding}), respectively, upon heating. With the increase of pH, all transition temperatures shifted to high values; for instance, the $T_{\text{sol-gel}}$, $T_{\text{gel-sol}}$, and T_{clouding} were 20, 45, and 63 °C, respectively, at pH = 5.10, and 28, 52, and 77 °C, respectively, at pH = 5.79. Using vial inversion tests, we mapped out sol-gel phase diagrams of the diblock copolymer in aqueous solutions at three pH values (3.29, 5.10, and 5.79, measured at ~ 0 °C); the whole sol-gel phase diagram shifted upward with the increase of pH. When the pH was lowered from 5.79 to 5.10, the diagram shifted back, though there was a 1 °C difference at each selected concentration, compared with the original curve of pH = 5.10. The tunability of sol-gel-sol-clouding transitions stemmed from the pH dependences of thermosensitive properties of two blocks, which were confirmed by a dynamic light scattering study. The results from small-angle X-ray scattering experiments indicated that spherical micelles of P(TEGMA-*co*-AA)-*b*-P(DEGEA-*co*-AA) in 20 wt% aqueous solutions at selected pH

and temperatures were packed into crystalline structures, either body-centered cubic or face-centered cubic, in the gel states.

4.1 Introduction

Thermosensitive hydrophilic block copolymers that contain one or more thermosensitive blocks can self-assemble into micelles with the collapsed thermosensitive block forming the core and the more hydrophilic block constituting the corona when the temperature is above the lower critical solution temperature (LCST) of the thermosensitive block (or of the lower LCST block).[1-4] If the polymer concentration is sufficiently high, i.e., above the critical gelation concentration (CGC), aqueous solutions of such block copolymers can undergo thermally induced reversible transitions between free-flowing liquids and free-standing gels. These injectable block copolymer micellar gels have received growing interest due to their potential applications in a variety of areas, including controlled and triggered release of substances and tissue engineering.[2,3]

Generally, there are two types of thermosensitive block copolymer micellar gels:[1] (i) gels of discrete micelles, in which non-interconnected micelles, often spherical, are packed into an ordered structure;[5,6] (ii) three-dimensional micellar network gels, in which one block of multiblock copolymers forms bridges among micellar cores.[7] The CGC for the first type of micelle gels is relatively high, typically ~ 20 wt%, while for the network gels, the CGC can be significantly lower, e.g., $3 - 4$ wt%.[7e] Representative examples of the former include aqueous gels of poly(ethylene oxide)-*b*-poly(propylene oxide)-*b*-poly(ethylene oxide) (PEO-*b*-PPO-*b*-PEO) triblock copolymers, which have been intensively studied in the past decades.[5] More recently, Aoshima et al. reported that 20 wt% aqueous solutions of thermosensitive diblock copolymers composed of different thermosensitive poly(vinyl ether)s underwent multi-stage transitions, from clear liquids to transparent gels, to hot clear liquids, and phase separated opaque mixtures upon heating.[8]

The sol-gel phase diagrams of PEO-*b*-PPO-*b*-PEO and thermosensitive hydrophilic diblock copolymers in water in the moderate concentration range are usually C-shaped curves.[1] The sol-to-gel transition, corresponding to the lower temperature boundary, occurs when the volume fraction of micelles exceeds a critical value and is driven by the enhancement of micellization and the ordering of micelles with the increase of temperature. The most common lattices by which micelles pack are body-centered cubic (bcc) and face-centered cubic (fcc) structures.[1a] The gel-to-sol transition, corresponding to the upper temperature boundary, is caused by the thermally induced shrinking of the corona, which decreases the volume fraction of micelles, at elevated temperatures.[1] It should be emphasized here that for a thermosensitive hydrophilic diblock copolymer composed of either one thermosensitive block and one hydrophilic block or two thermosensitive blocks with a particular molecular weight and composition, the sol-to-gel ($T_{\text{sol-gel}}$) and gel-to-sol transition temperature ($T_{\text{gel-sol}}$) at a specific concentration are fixed. The sol-gel phase diagram in the moderate concentration range hence is also fixed. Although one can add salts to modify the transition temperatures and the phase diagram, the changes are irreversible.[1,8b]

Our lab has been interested in developing strategies to control and tune self-assembly of thermosensitive hydrophilic block copolymers in water.[7c-e,9,10] Through the introduction of a small amount of stimuli-responsive groups into the thermosensitive block of a block copolymer, our lab previously demonstrated that the LCST of the thermosensitive block can be modified and as such the block copolymer can undergo multiple micellization and dissociation transition in water in response to the combination of two external stimuli.[9] In particular, by statistically incorporating a small amount of

carboxylic acid groups into one block of doubly thermosensitive hydrophilic diblock copolymers of poly(methoxytri(ethylene glycol) acrylate) (PTEGMA) and poly(ethoxydi(ethylene glycol) acrylate) (PDEGEA), we showed that one boundary, either the upper or lower, of the C-shaped sol-gel phase diagram of the diblock copolymer in water can be shifted independently by changing the solution pH (Scheme 4.1a and 4.1b).[10] PTEGMA and PDEGEA are thermosensitive water-soluble polymers with LCSTs of 58 and 9 °C, respectively.[10,11] The underlying principle is that the LCST of a thermosensitive hydrophilic polymer that contains a small amount of a weak acid or base depends on the solution pH and can be tuned continuously and reversibly.[10,12]

In this work, we show that both the upper and lower temperature boundaries of the C-shaped sol-gel phase diagram of a doubly thermosensitive hydrophilic diblock copolymer, P(TEGMA-*co*-AA)-*b*-P(DEGEA-*co*-AA) with each block containing ~ 5 % of carboxylic acid groups, in water can be shifted simultaneously and reversibly by varying the solution pH (Scheme 4.1c). The diblock copolymer was synthesized by reversible addition fragmentation chain transfer (RAFT) polymerization[13] and post-polymerization modification (Scheme 4.2). Note that there are a number of reports on thermo- and pH-sensitive block copolymer aqueous micellar gels in the literature.[14,15] The block copolymers used in those studies were usually prepared by either growing pH-sensitive blocks from or introducing pH-responsive groups at the chain ends of a block copolymer that can form thermoreversible gels in water (e.g., PEO-*b*-PPO-*b*-PEO).[14] Other types of multiblock copolymers were also employed.[15] We stress here that our design of thermo- and pH-sensitive P(TEGMA-*co*-AA)-*b*-P(DEGEA-*co*-AA), via the statistical incorporation of a small amount of weak acid groups into both blocks, is
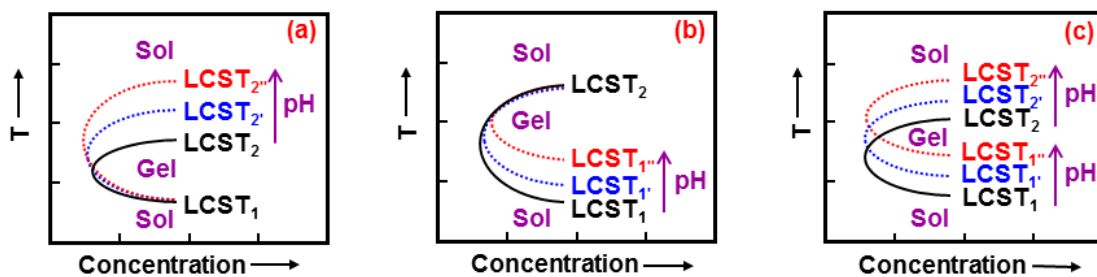
Scheme 4.1 pH-Induced Shifting of (a) Upper Temperature Boundary, (b) Lower Temperature Boundary, and (c) Both Upper and Lower Temperature Boundaries of Sol-Gel Phase Diagrams of Doubly Thermosensitive Hydrophilic Diblock Copolymers in Water.
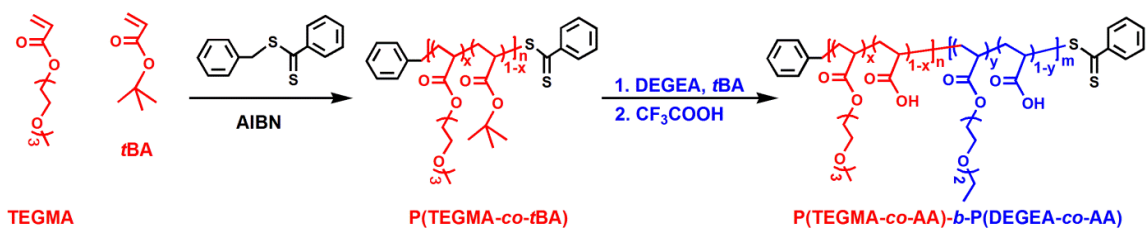
Scheme 4.2 Synthesis of Doubly Thermosensitive Hydrophilic Diblock Copolymer P(TEGMA-*co*-AA)-*b*-P(DEGEA-*co*-AA) with Each Block Containing a Small Amount of Carboxylic Acid Groups.

different, which enables the LCSTs of the entire blocks to be readily tuned.

4.2 Experimental Section

4.2.1 Materials

Hexanes, diethyl ether, 1.0 M KOH solution (volumetric standard solution), and 1.0 M HCl solution (volumetric standard solution) were obtained from Fisher Scientific. Anisole (99%, anhydrous) and trifluoroacetic acid (99%) were purchased from Acros and used as received. 2,2′-Azobis(2-methylpropionitrile) (AIBN, 98%, Aldrich) was recrystallized in ethanol twice and then dried under high vacuum at room temperature. The purified AIBN was then dissolved in *N,N*-dimethylformamide (DMF, extra dry, Acros) to make a solution with a concentration of 3.52 wt% for RAFT polymerizations. Ethoxydi(ethylene glycol) acrylate (or di(ethylene glycol) ethyl ether acrylate, DEGEA, ≥ 90%, Aldrich) and *tert*-butyl acrylate (*t*BA, 99%, Fisher Scientific) were dried with calcium hydride overnight, distilled under reduced pressure, and stored in a refrigerator prior to use. Methoxytri(ethylene glycol) acrylate (TEGMA) was synthesized according to the procedure described in the literature.[10,11] Benzyl dithiobenzoate was synthesized according to a procedure reported in the literature[16] and the molecular structure was confirmed by ^{1}H and ^{13}C NMR spectroscopy. 30 mM aqueous potassium hydrogen phthalate (KHP) buffers were made by dissolving KHP in Milli-Q water and the pH values were adjusted by adding either a 1.0 M KOH solution of a 1.0 M HCl solution. All pH values in this work were measured with a pH meter (Accumet AB15 pH meter from Fisher Scientific, calibrated with pH = 4.01, 7.00, and 10.01 standard buffer solutions) in

an ice/water bath (0 °C). All other solvents and chemicals were used without any further treatment.

4.2.2 General Characterization

Size exclusion chromatography (SEC) was carried out at room temperature using PL-GPC 20 (an integrated GPC system from Polymer Laboratories, Inc) with a refractive index detector, one PLgel 5 μm guard column (50 × 7.5 mm), and two PLgel 5 μm mixed-C columns (each 300 × 7.5 mm, linear range of molecular weight from 200 to 2,000,000 Da according to Polymer Laboratories). The data were processed using Cirrus GPC/SEC software (Polymer Laboratories). Tetrahydrofuran was used as the carrier solvent at a flow rate of 1.0 mL/min. Polystyrene standards (Polymer Laboratories, Inc.) were used for calibration. The ^{1}H NMR (300 MHz) spectra were recorded on a Varian Mercury 300 NMR spectrometer.

4.2.3 Synthesis of Poly(methoxytri(ethylene glycol) acrylate-*co-tert*-butyl acrylate) (P(TEGMA-*co-t*BA) Macro-CTA by RAFT

2,2′-Azobis(2-methylpropionitrile) (AIBN, 59.0 mg of a solution of AIBN in DMF with a concentration of 3.52 wt%, 0.0127 mmol), benzyl dithiobenzoate (31.6 mg, 0.130 mmol), *tert*-butyl acrylate (0.412 g, 3.22 mmol), methoxytri(ethylene glycol) acrylate (13.998 g, 64.2 mmol), and anisole (15.83 g) were added into a 50 mL two-necked flask. The mixture was stirred under a nitrogen atmosphere and degassed by three freeze-pump-thaw cycles. A sample was withdrawn from the polymerization mixture for ^{1}H NMR spectroscopy analysis, and then the flask was placed in a 70 °C oil bath. The reaction was monitored by ^{1}H NMR spectroscopy. After the polymerization proceeded for 200 min, the flask was removed from the oil bath and a sample was taken immediately for the

134

determination of the monomer conversion by ^{1}H NMR spectroscopy. The polymerization mixture was diluted with THF and precipitated in hexanes. The polymer was then dissolved in THF (10 mL) and precipitated in a mixture of hexane and diethyl ether (v : v = 60 : 40, 200 mL). This process was repeated an additional two times. The polymer was then dried in vacuum. SEC analysis results (polystyrene standards): $M_{n,SEC}$ = 22.6 kDa; polydispersity index (PDI) = 1.17. The DP of the polymer was calculated from the monomer conversion and the monomer-to-CTA ratio. The peaks located in the range of 4.0 – 4.5 ppm, which were from -CH_2OOC- of monomer TEGMA and the TEGMA units in the copolymer, were used as internal standard. The conversion was calculated from the integral values of the peaks from 5.7 to 5.9 ppm (CHH=CH- from TEGMA and tBA) at t = 0 and 200 min. The calculated DP was 158. The composition of the copolymer was determined from the ^{1}H NMR spectrum of the purified polymer. The numbers of TEGMA and tBA units were 150 and 8, respectively.

4.2.4 Synthesis of Poly(methoxytri(ethylene glycol) acrylate-*co-tert*-butyl acrylate)-*b*-poly(ethoxydi(ethylene glycol) acrylate-*co-tert*-butyl acrylate) (P(TEGMA-*co-t*BA)-*b*-P(DEGEA-*co-t*BA)) by RAFT

P(TEGMA-*co-t*BA) macro-CTA ($M_{n,SEC}$ = 22.6 kDa, PDI = 1.17, 3.728 g, 0.111 mmol), AIBN (41.2 mg of a solution of AIBN in DMF with a concentration of 3.52 wt%, 0.0088 mmol), DEGEA (10.394 g, 55.3 mmol), tBA (0.359 g, 2.80 mmol), and anisole (18.19 g) were added into a 50 mL two-necked flask. The mixture was stirred under nitrogen and then degassed by three freeze-pump-thaw cycles. After a sample was taken for ^{1}H NMR spectroscopy analysis, the flask was placed in a 70 °C oil bath. ^{1}H NMR spectroscopy was used to monitor the reaction progress. After the polymerization

proceeded for 204 min, the polymerization was stopped by removing the flask from the oil bath and diluting the mixture with THF. The polymer solution was precipitated in hexanes. The polymer was then dissolved in THF (15 mL) and precipitated in a mixture of hexane and diethyl ether (v : v = 60 : 40, 200 mL). This process was repeated an additional two times. The block copolymer was then dried in vacuum and analyzed by ^{1}H NMR spectroscopy and SEC. SEC results (polystyrene standards): $M_{n,SEC}$ = 36.0 kDa; PDI = 1.20.

4.2.5 Synthesis of P(TEGMA-*co*-acrylic acid)-*b*-P(DEGEA-*co*-acrylic acid) (P(TEGMA-*co*-AA)-*b*-P(DEGEA-*co*-AA)) from P(TEGMA-*co*-tBA)-*b*-P(DEGEA-*co*-tBA) by Removal of *t*-Butyl Groups Using Trifluoroacetic Acid

P(TEGMA-*co*-tBA)-*b*-P(DEGEA-*co*-tBA) ($M_{n,SEC}$ = 36.0 kDa, PDI = 1.20, 4.910 g) was dissolved in dry dichloromethane (10 mL) in a 25 mL flask, followed by the addition of trifluoroacetic acid (9.71 g). After stirring at room temperature for 48 h, the mixture was transferred into a 500 mL round-bottom flask and was diluted with 150 mL dichloromethane. The volatiles were removed by the use of a rotary evaporator. This process was repeated an additional two times to remove as much trifluoroacetic acid as possible. The polymer was then dissolved in THF (15 mL) and precipitated in a mixture of hexane and diethyl ether (v/v = 60:40, 100 mL) three times. After drying in vacuum, the polymer was obtained as a pink viscous liquid (4.490 g, yield: 91%). The removal of *tert*-butyl group was evidenced by the disappearance of the *tert*-butyl peak located at 1.4 ppm in the ^{1}H NMR spectrum.

4.2.6 Preparation of 20 wt% Aqueous Solution of P(TEGMA-*co*-AA)-*b*-P(DEGEA-*co*-AA)

The following is a typical procedure for the preparation of a 20 wt% aqueous solution of P(TEGMA-*co*-AA)-*b*-P(DEGEA-*co*-AA). P(TEGMA-*co*-AA)-*b*-P(DEGEA-*co*-AA) was added into a pre-weighed vial (inner diameter: 20 mm). The vial was then placed in a larger flask and dried under high vacuum at 55 °C overnight. The mass of the dried polymer inside the vial was 0.684 g. A 30 mM aqueous KHP buffer with pH of 3.05 (2.736 g) was added into the vial. The mixture was then sonicated in an ice/water ultrasonic bath (Fisher Scientific Model B200 Ultrasonic Cleaner) to dissolve the polymer. The vial was then stored in a refrigerator (~ 4 °C) overnight and a homogeneous clear solution was obtained.

4.2.7 Rheological Measurements

Rheological experiments were conducted using a rheometer from TA Instruments (Model TA AR 2000ex). A cone-plate geometry with a cone diameter of 20 mm and an angle of 2 ° (truncation 52 μm) was used. The temperature was controlled by the bottom Peltier plate. In each measurement, 85 μL of a polymer solution was loaded onto the plate by a micropipet. The solvent trap was filled with water and a solvent trap cover was used to minimize water evaporation. The linear viscoelastic regime for a polymer gel sample at a specific temperature was determined by dynamic strain amplitude sweep experiments from strain amplitude of 0.01 % to 80 % at frequencies of 0.5, 1, 2.5, and 5 Hz, respectively. Dynamic viscoelastic properties (dynamic storage modulus G' and loss modulus G'') of a polymer solution sample were measured by oscillatory shear experiments performed at a fixed frequency of 1 Hz in a heating ramp at a heating rate of

1 °C/min. A strain amplitude of $\gamma = 1.0$ %, which was within the linear viscoelastic regime, was used in all dynamic viscoelastic measurements. The flow properties (shear stress-shear rate curves) of a polymer solution sample at selected temperatures were measured by a shear rate ramp from 0 to 600 s^{-1} for duration of 6 min.

4.2.8 Small-Angle X-Ray Scattering Experiments

Small-angle X-ray scattering experiments were conducted on a Bruker NanoStar equipped with a rotating anode X-ray generator and a Vantec 2000 area detector. Copper K_α radiation ($\lambda = 1.5418$ Å) was used. The 20 wt% aqueous solution of P(TEGMA-*co*-AA)-*b*-P(DEGEA-*co*-AA) was loaded into a quartz capillary sample holder, which was then inserted into a cooling/heating stage. The temperature of the cooling/heating stage was controlled by a Materials Research Instruments TCPUP temperature controller. The calibration was performed using silver behenate as the standard sample.

4.2.9 Dynamic Light Scattering Study of Thermally Induced Micellization of P(TEGMA-*co*-AA)-*b*-P(DEGEA-*co*-AA) in Dilute Aqueous Solution at Various pH values

Dynamic light scattering (DLS) studies of aqueous solutions of P(TEGMA-*co*-AA)-*b*-P(DEGEA-*co*-AA) were conducted with a Brookhaven Instruments BI-200SM goniometer equipped with a PCI BI-9000AT digital correlator, a temperature controller, and a solid-state laser (model 25-LHP-928-249, $\lambda = 633$ nm) at a scattering angle of 90°. Four 0.02 wt% solutions of P(TEGMA-*co*-AA)-*b*-P(DEGEA-*co*-AA) in 20 mM KHP aqueous buffers with pH values of 3.29, 5.10, 5.79, and 6.50, respectively, were prepared. The solutions were filtered into borosilicate glass tubes with an inner diameter of 7.5 mm using Millipore hydrophilic PTFE filters (0.2 μm pore size) and the tubes were sealed

with PE stoppers. The glass tube was placed in the cell holder of the light scattering instrument and gradually heated. At each selected temperature, the solution was equilibrated for 20 min prior to data recording. The time intensity-intensity correlation functions were analyzed with a Laplace inversion program (CONTIN).

4.2.10 Determination of Sol-Gel Phase Diagrams of P(TEGMA-*co*-AA)-*b*-P(DEGEA-*co*-AA) in Aqueous Solutions by Vial Inversion Tests

A glass vial that contained an aqueous solution of P(TEGMA-*co*-AA)-*b*-P(DEGEA-*co*-AA) with a known concentration was placed in the water bath of a Fisher Scientific Isotemp refrigerated circulator. The inner diameter of the vial was 20 mm. The temperature was gradually increased. At each selected temperature, the solution was equilibrated for 20 min before the vial was tilted or inverted for 5 s to visually examine if the solution was a mobile liquid or an immobile gel under its own weight. The temperature at which the solution changed from a mobile to an immobile state (or vice versus) was taken as the sol-to-gel (or gel-to-sol) transition temperature. The clouding temperature was determined by visual examination. Polymer solutions with different concentrations were obtained by adding a predetermined amount of water into the vial or evaporating water from the solution. Their sol-to-gel/gel-to-sol transition temperatures and clouding temperatures were determined by visual inspection.

4.3 Results and Discussion

4.3.1 Synthesis of P(TEGMA-*co*-AA)-*b*-P(DEGEA-*co*-AA)

P(TEGMA-*co*-AA)-*b*-P(DEGEA-*co*-AA), a doubly thermosensitive hydrophilic diblock copolymer with both blocks containing a small amount of carboxylic acid groups,

was made from P(TEGMA-*co*-*t*BA)-*b*-P(DEGEA-*co*-*t*BA) by the removal of *t*-butyl groups using trifluoroacetic acid (Scheme 4.2). The precursor P(TEGMA-*co*-*t*BA)-*b*-P(DEGEA-*co*-*t*BA) was prepared by a two-step RAFT process. P(TEGMA-*co*-*t*BA) was synthesized first by RAFT polymerization of a mixture of TEGMA and *t*BA with a molar ratio of 100 : 5.0 at 70 °C using AIBN as initiator and benzyl dithiobenzoate as chain transfer agent. The polymerization was stopped after 200 min. SEC analysis showed that the $M_{n,SEC}$ was 22.6 kDa and the polydispersity index (PDI) was 1.17 (Figure 4.1a). The degree of polymerization was 158, which was calculated from the monomer conversion and the monomer-to-CTA ratio; the molar ratio of TEGMA to *t*BA units, determined from the ^{1}H NMR spectrum, was 100 : 5.1, essentially the same as the feed ratio. P(TEGMA-*co*-*t*BA) was then used as macro-CTA for RAFT polymerization of DEGEA and *t*BA with a molar ratio of 5.1. From SEC analysis, the peak shifted to the high molecular side and remained narrow (PDI = 1.20), indicating that the block copolymerization was also controlled. The numbers of DEGEA and *t*BA units in the P(DEGEA-*co*-*t*BA) block were 70 and 4, respectively. These were calculated from the ^{1}H NMR spectrum of P(TEGMA-*co*-*t*BA)-*b*-P(DEGEA-*co*-*t*BA) (Figure 4.1b) using the integral values of the peak at 4.4 − 4.0 ppm (-CH_2OOC- of TEGMA and DEGEA units), the peak at 2.5 to 2.1 ppm (-CH$_2$CH- of TEGMA, DEGEA and *t*BA units), and the peaks from 1.3 to 1.1 ppm (-CH$_2$CH_3 of DEGEA units) along with the numbers of PTEGMA and *t*BA units in the P(TEGMA-*co*-*t*BA) block. The molar ratio of DEGEA to *t*BA units in the P(DEGEA-*co*-*t*BA) block was 100 : 5.7, very close to the feed ratio. Thus, the molecular formula of the diblock copolymer is P(TEGMA$_{150}$-*co*-*t*BA$_8$)-*b*-P(DEGEA$_{70}$-*co*-*t*BA$_4$), where the subscripts denote the numbers of monomer units. The *t*-butyl groups

140
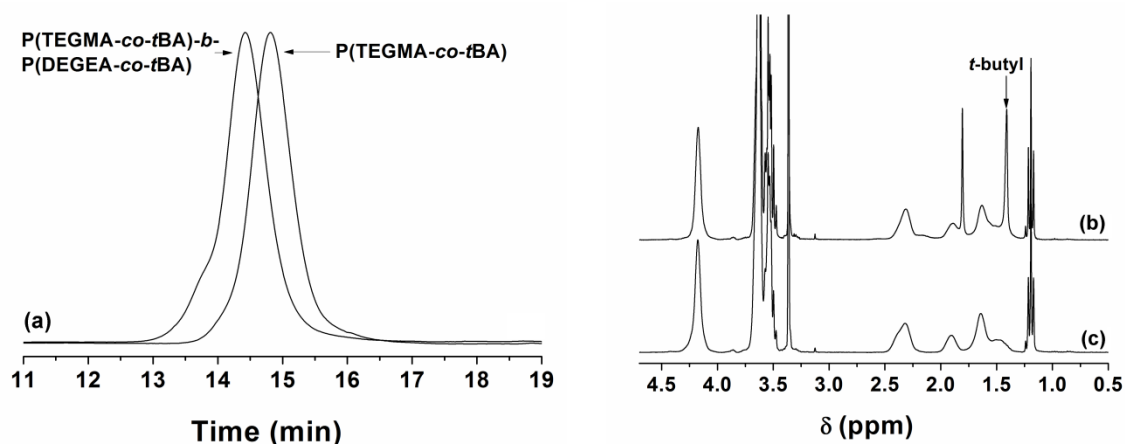
Figure 4.1 (a) Size exclusion chromatography traces of P(TEGMA-*co-t*BA) macro-CTA and diblock copolymer P(TEGMA-*co-t*BA)-*b*-P(DEGEA-*co-t*BA), and (b) ^{1}H NMR spectra of P(TEGMA-*co-t*BA)-*b*-P(DEGEA-*co-t*BA) and (c) P(TEGMA-*co*-AA)-*b*-P(DEGEA-*co*-AA). CDCl$_3$ was used as solvent in ^{1}H NMR spectroscopy analysis.

in the diblock copolymer were then removed using trifluoroacetic acid. The successful

cleavage of *t*-butyl groups can be seen from Figure 4.1c in which the *t*-butyl peak located

at 1.4 ppm disappeared.

4.3.2 Thermally Induced Sol-Gel-Sol-Cloudy Transitions of 20 wt% Aqueous

Solution of P(TEGMA-*co*-AA)-*b*-P(DEGEA-*co*-AA) with pH of 3.29

To study the thermally induced sol-gel-sol-cloudy transitions, a 20 wt% aqueous

solution of P(TEGMA-*co*-AA)-*b*-P(DEGEA-*co*-AA) was made by dissolving the diblock

copolymer in a 30 mM potassium hydrogen phthalate (KHP) buffer solution and the

solution pH was adjusted to 3.29 (measured in an ice/water bath). The sample was

gradually heated to examine the temperature-induced phase transitions. As shown in

Figure 4.2a1, the solution at 10 °C was a clear free-flowing liquid with a very small

viscosity. Upon increasing the temperature to 17 °C, the sample turned into a clear, free-

standing gel, which remained immobile under its own weight when tilted or inverted. The

sample remained in the gel state in the temperature range of 17 – 37 °C. Figure 4.2b1 to

3.2d1 shows the gel at 18, 25, and 30 °C, respectively. At 38 °C, it began to flow under

its own weight when tilted but remained clear. When the temperature was raised to 55 °C,

the clear sol turned cloudy. These transitions can be clearly seen from Figure 4.2e1 to

3.2j1. Thus, upon heating, the 20 wt% aqueous solution of P(TEGMA-*co*-AA)-*b*-

P(DEGEA-*co*-AA) with pH of 3.29 underwent sol-to-gel, gel-to-sol, and clear sol-to-

cloudy sol transitions at 17 °C ($T_{\text{sol-gel}}$), 38 °C ($T_{\text{gel-sol}}$), and 55 °C (T_{clouding}), respectively.

It should be noted here that these thermally induced sol-gel-sol-cloudy transitions were

sharp (within 1 °C) and reversible.
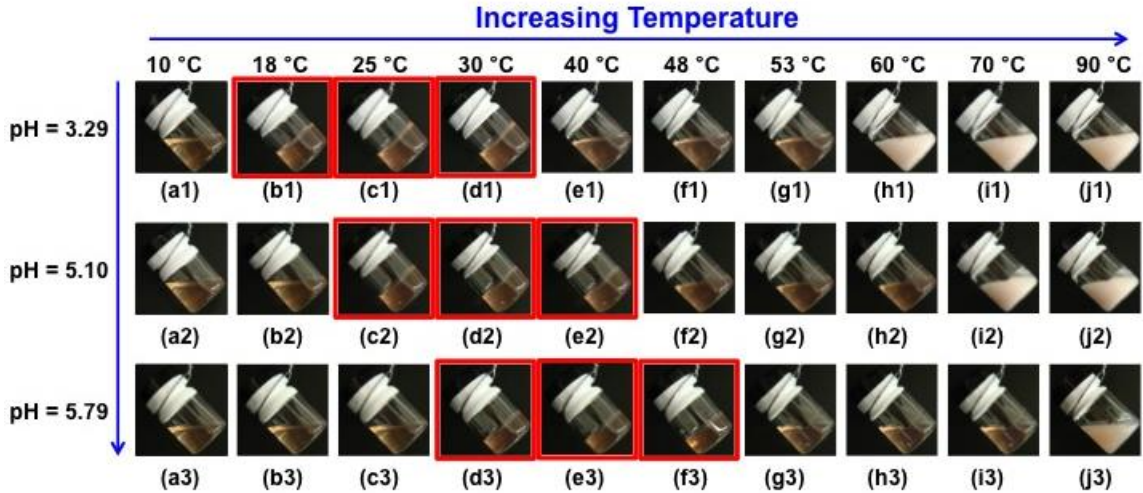
Figure 4.2 Digital optical pictures of 20 wt% aqueous solutions of P(TEGMA-*co*-AA)-*b*-P(DEGEA-*co*-AA) at pH of 3.29 (the 1st row), 5.10 (the 2nd row), and 5.79 (the 3rd row) and temperature of 10 °C (1st column), 18 °C (2nd column), 25 °C (3rd column), 30 °C (4th column), 40 °C (5th column), 48 °C (6th column), 53 °C (7th column), 60 °C (8th column), 70 °C (9th column), and 90 °C (10th column).
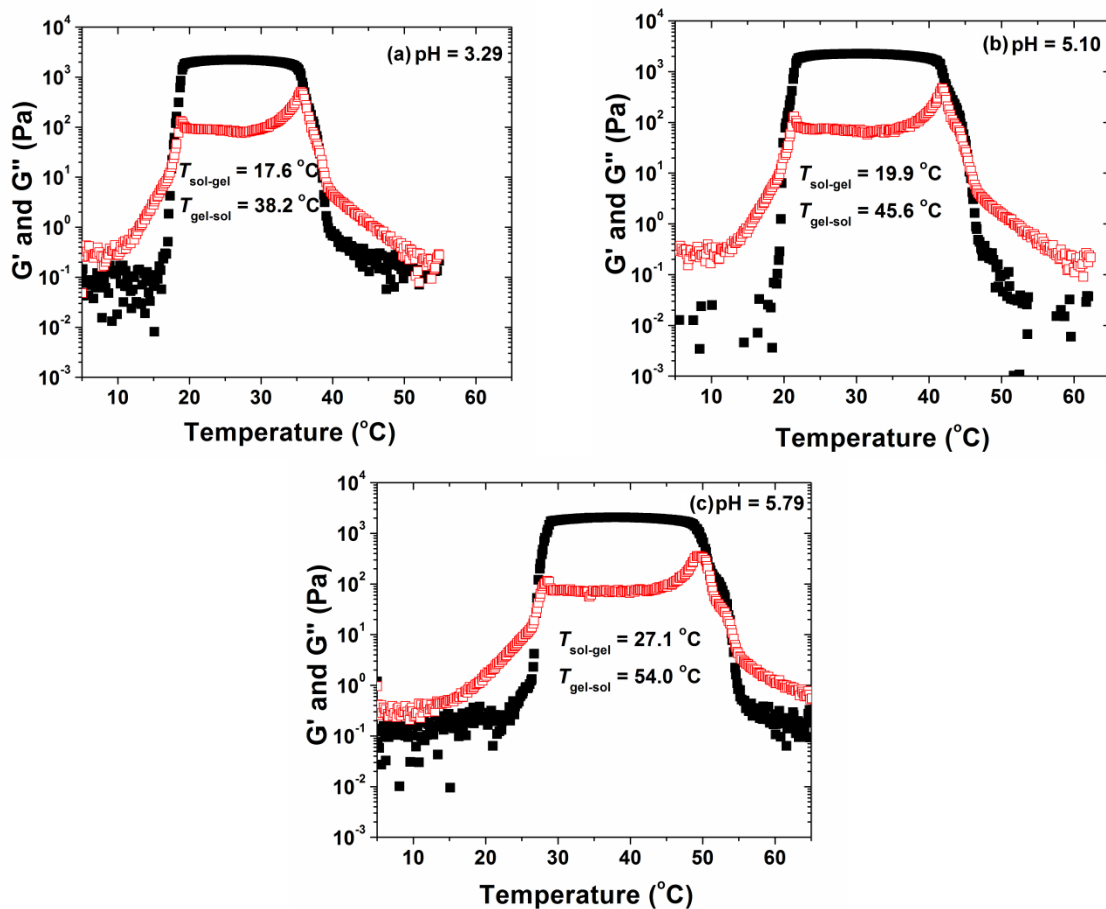
Figure 4.3 Dynamic storage modulus *G'* (solid black square) and dynamic loss modulus *G''* (red hollow square) of 20 wt% aqueous solution of P(TEGMA-*co*-AA)-*b*-P(DEGEA-*co*-AA) at pH of (a) 3.29, (b) 5.10, and (c) 5.79 as a function of temperature. The data were collected from oscillatory shear experiments performed in a heating ramp using a heating rate of 1 °C/min, a strain amplitude of 1.0 %, and a frequency of 1 Hz.

The $T_{sol\text{-}gel}$ and $T_{gel\text{-}sol}$ determined by visual inspection as discussed above are in good agreement with the results from rheological measurements. Figure 4.3a shows the data collected from an oscillatory shear experiment, which was performed in a heating ramp using a strain amplitude of 1 %, a fixed frequency of 1 Hz, and a heating rate of 1 °C/min for the 20 wt% aqueous solution of P(TEGMA-*co*-AA)-*b*-P(DEGEA-*co*-AA) with pH of 3.29. We confirmed from a dynamic strain amplitude sweep that the strain amplitude of 1 % was within the linear viscoelastic regime.[17] It can be seen from Figure 4.3a that when temperature was below 12 °C, both dynamic storage modulus G' and dynamic loss modulus G'' were small. Above 13 °C, G' and G'' increased rapidly with the increase of temperature and at ~ 17 °C, G' overcame G'', suggesting that the solution had turned into a gel. In the temperature range of 18 to 35 °C, G' was at least one order of magnitude greater than G''. Above 35 °C, G' and G'' began to decrease and G' became smaller than G'' at ~ 38 °C, indicating that the gel melted into a sol. The crossover points of G' and G'' curves are commonly used as indicators of sol-to-gel and gel-to-sol transitions.[1,18] Using this method, the $T_{sol\text{-}gel}$ and the $T_{gel\text{-}sol}$ were 17.6 and 38.2 °C, respectively, virtually the same as those determined by the vial inversion method (17 and 38 °C, respectively).

4.3.3 pH Dependences of $T_{sol\text{-}gel}$, $T_{gel\text{-}sol}$, and $T_{clouding}$ of 20 wt% Aqueous Solution of P(TEGMA-*co*-AA)-*b*-P(DEGEA-*co*-AA)

The incorporation of a small amount of weak acid groups into both thermosensitive blocks of a doubly thermosensitive diblock copolymer allows their LCSTs to be tuned continuously and reversibly by changing the solution pH, making it possible to shift both temperature boundaries of the sol-gel phase diagram of the diblock copolymer in aqueous solution. To study the pH dependences of $T_{sol\text{-}gel}$, $T_{gel\text{-}sol}$, and $T_{clouding}$ of the 20 wt%

aqueous solution of P(TEGMA-*co*-AA)-*b*-P(DEGEA-*co*-AA), we gradually increased the pH by injecting a small amount of a 1.0 M KOH aqueous solution using a microsyringe in a stepwise manner in an ice/water bath. After each injection, the sample was sonicated in an ice/water bath before the pH value was recorded at ~ 0 °C using a pH meter. The solution was then gradually heated and the $T_{\text{sol-gel}}$, $T_{\text{gel-sol}}$, and T_{clouding} were determined by visual inspection as for the sample with pH of 3.29. The results are summarized in Figure 4.4.

As shown in Figure 4.4a, $T_{\text{sol-gel}}$ and T_{clouding} increased monotonically with the increase of pH, while $T_{\text{gel-sol}}$ increased initially with pH up to 5.79 and then leveled off at pH = 5.90 and decreased slightly at pH 6.00. At and above pH = 6.10, no transition from a clear sol to a clear gel was observed in the studied temperature range. Interestingly, the changes of $T_{\text{sol-gel}}$, $T_{\text{gel-sol}}$, and T_{clouding} with the increase of pH occurred at different paces, which can be seen from Figure 4.4b where three curves were vertically shifted for comparison. Initially, the increases of all three transition temperatures were small when the pH was raised from 3.29 to 4.64. Above pH = 5.10, the changes of $T_{\text{gel-sol}}$ and T_{clouding} became faster, but $T_{\text{sol-gel}}$ still increased slowly until pH reached 5.46. Over the pH range of 3.29 to 5.90, the change was 30 °C for T_{clouding}, but only 15 and 14 °C for $T_{\text{sol-gel}}$ and $T_{\text{gel-sol}}$, respectively. Since $T_{\text{sol-gel}}$ and T_{clouding} are directly governed by the LCSTs of the two blocks in P(TEGMA-*co*-AA)-*b*-P(DEGEA-*co*-AA), the data in Figure 4.4 suggests that the pH dependences of LCSTs of P(TEGMA-*co*-AA) and P(DEGEA-*co*-AA) are slightly different, despite the fact that the AA content in the two blocks are essentially identical. This is presumably due to the different hydrophobicity of PTEGMA and PDEGEA. In contrast, $T_{\text{gel-sol}}$ is determined by how the volume fraction of block
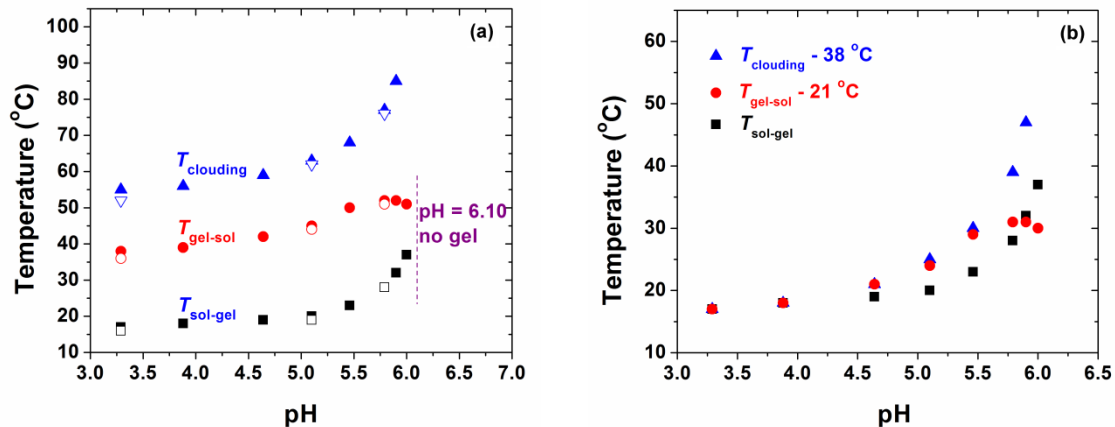
Figure 4.4 (a) Sol-to-gel transition temperature ($T_{sol-gel}$, square), gel-to-sol transition temperature ($T_{gel-sol}$, circle), and clouding temperature ($T_{clouding}$, triangle) of the 20 wt% aqueous solution of P(TEGMA-*co*-AA)-*b*-P(DEGEA-*co*-AA) in 30 mM aqueous KHP buffer as a function of pH. Solid and hollow symbols represent the data obtained from the processes of increasing and decreasing pH, respectively. (b) Plots of ($T_{clouding}$ − 38 °C), ($T_{gel-sol}$ − 21 °C), and $T_{sol-gel}$ versus pH for comparing the changes of $T_{clouding}$, $T_{gel-sol}$, and $T_{sol-gel}$ with the increase of pH.

copolymer micelles changes with temperature. Although the LCST transition of P(TEGMA-*co*-AA) block plays an important role in the gel to sol transition, the $T_{\text{gel-sol}}$ is not directly determined by it. Like other PEO-based thermosensitive polymers,[19] the P(TEGMA-*co*-AA) block gradually shrank upon heating. At certain point, the volume fraction of micelles dropped to below a critical value and a gel-to-sol transition occurred. In addition, at higher pH values, both blocks became more hydrophilic, which may result in more block copolymer molecules staying in water as unimers. Thus, the change of $T_{\text{gel-sol}}$ with pH is more complicated. Nevertheless, we showed that all three transitions can be tuned by adjusting the solution pH.

We then studied the reproducibility of $T_{\text{sol-gel}}$, $T_{\text{gel-sol}}$, and T_{clouding} at specific pH values by gradually lowering the solution pH from 6.10. A 1.0 M HCl aqueous solution was injected via a microsyringe in a stepwise fashion. As shown in Figure 4.4a, upon decreasing the pH to 5.79, 5.10, and 3.29, all values of three transition temperatures were either right on the curve ($T_{\text{sol-gel}}$ at 5.79) or $1 - 3$ °C lower than those obtained from the process of increasing pH. We speculate that the observed small differences might result from the small increase in the salt concentration due to the neutralization reaction; it is known that the addition of K$^+$, a salting out cation, typically suppresses the LCST transition and thus also reduces slightly the volume of micelles. Nevertheless, the results from both processes of increasing and decreasing pH demonstrated that the $T_{\text{sol-gel}}$, $T_{\text{gel-sol}}$, and T_{clouding} of the 20 wt% aqueous buffer solution of P(TEGMA-*co*-AA)-*b*-P(DEGEA-*co*-AA) can be tuned reversibly, though not entirely, by varying the solution pH.

148

The effect of pH on sol-gel-sol-cloudy transitions can be easily appreciated from Figure 4.2. At 18 °C, the sample was a clear free-standing gel at pH 3.29 but became a clear sol when the pH was changed to 5.10 and 5.79 (Figure 4.2b2 and b3). At 40 °C, the sample was a clear sol at pH 3.29 but a clear gel at pH 5.10 and 5.79 (Figure 4.2e1, e2, and e3). While the sample was a cloudy liquid at pH 3.29 and T = 60 °C (Figure 4.2h1), it was a clear sol at the same temperature when the pH was changed to 5.10 and 5.79 (Figure 4.2 h2 and h3).

Figure 4.3b and c shows the data from the temperature ramp experiments for the samples with pH of 5.10 and 5.79, respectively. The $T_{sol-gel}$ and $T_{gel-sol}$ were 19.9 and 45.6 °C, respectively, for pH 5.10, and 27.1 and 54.0 °C, respectively, for pH 5.79. These values are in good agreement with those determined by vial inversion tests (20 and 45 °C for pH 5.10 and 28 and 52 °C for pH = 5.79). In addition, we found that the maximum value of G' increased slightly from 2212 Pa to 2251 Pa with the increase of pH from 3.29 to 5.10, then decreased to 2061 Pa when the pH was further increased to 5.79. Since the values of G' are determined by the volume fraction of micelles in the sample, this observation suggests that the volume fraction of micelles changes with pH in a quite complex manner. We speculate that the increased hydrophilicity of both blocks of P(TEGMA-*co*-AA)-*b*-P(DEGEA-*co*-AA) at higher pH values should be responsible for this observation. With the increase of pH, the degrees of ionization of carboxylic acid groups in both blocks became greater. For the P(TEGMA-*co*-AA) block, the increased hydrophilicity means that the corona occupies a greater volume, resulting in a higher volume fraction of micelles. On the other hand, we previously observed that the maximum value of G' of 25 wt% aqueous solution of P(DEGEA-*co*-AA)-*b*-PTEGMA

decreased with the increase of pH, presumably because the increased hydrophilicity of the P(DEGEA-*co*-AA) block results in more block copolymer molecules staying in the unimer state. The two effects were against each other. Thus, it is not surprising that the maximum value of *G'* increased initially and then decreased with the increase of pH.

4.3.4 Shear Stress-Shear Rate Curves of 20 wt% Solutions of P(TEGMA-*co*-AA)-*b*-P(DEGEA-*co*-AA) in 30 mM Aqueous KHP Buffer at pH of 3.29, 5.10, and 5.79

Figure 4.5 shows the shear stress-shear rate curves (flow curves) of three 20 wt% solutions of P(TEGMA-*co*-AA)-*b*-P(DEGEA-*co*-AA) in 30 mM aqueous KHP buffers with pH of 3.29, 5.10, and 5.79. At 10 °C, all three samples were Newtonian liquids as the shear stress increased linearly with shear rate. Similarly, the solutions with pH of 3.29 and 5.10 at 54 °C and the sample with pH of 5.79 at 60 °C were Newtonian liquids. Very differently, at 30 and 35 °C, all three samples exhibited shear stress-shear rate curves that had a characteristic of Bingham-Newtonian liquids, i.e., the shear stress increased proportionately with shear rate after the initial resistance was overcome. At 15 °C, while the sample with pH of 3.29 exhibited an intermediate behavior, the samples with pH of 5.10 and 5.79 were clearly Newtonian liquids. From Figure 4.5, one can also easily tell that the sample with pH of 3.29 was a gel at 18 °C, but a Newtonian liquid at 48 °C. In contrast, the 20 wt% solution with pH of 5.79 was a Newtonian liquid at 18 °C, but a gel at 48 °C. Thus, the effect of pH was also manifested in the flow properties of 20 wt% aqueous solutions of P(TEGMA-*co*-AA)-*b*-P(DEGEA-*co*-AA).
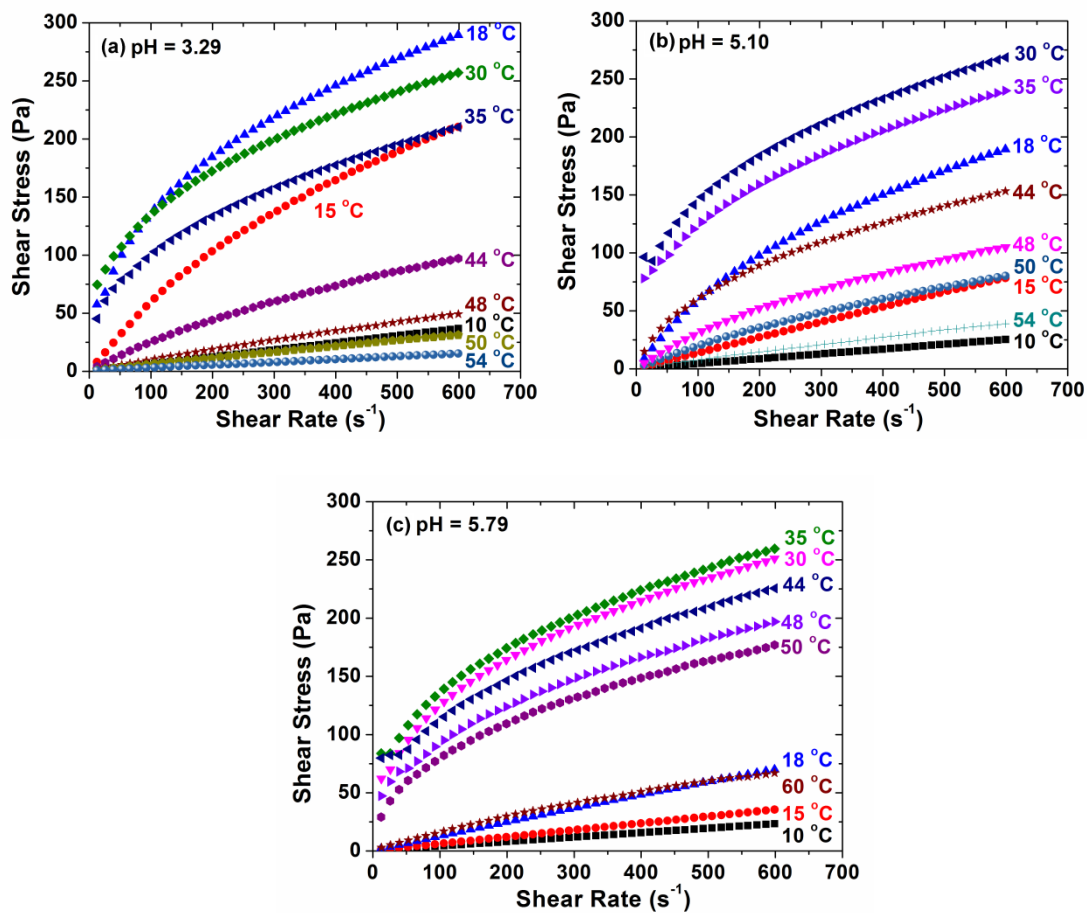
Figure 4.5 Shear stress-shear rate curves (flow curves) of 20 wt% aqueous solutions of P(TEGMA-*co*-AA)-*b*-P(DEGEA-*co*-AA) with pH of (a) 3.29, (b) 5.10, and (c) 5.79 at various temperatures.

4.3.5 Dynamic Light Scattering Study of Thermosensitive Properties of P(TEGMA-*co*-AA)-*b*-P(DEGEA-*co*-AA) in Aqueous KHP Buffer at a Concentration of 0.02 wt% at Various pH Values

The thermally induced sol-gel-sol-cloudy transitions of the 20 wt% aqueous solution of P(TEGMA-*co*-AA)-*b*-P(DEGEA-*co*-AA) stemmed from the thermosensitive properties of P(TEGMA-*co*-AA) and P(DEGEA-*co*-AA) blocks in water. At a particular pH, when the temperature is below the LCST of P(DEGEA-*co*-AA) block (LCST$_1$), the block copolymer was molecularly dissolved in water, i.e., in the unimer state (Scheme 4.3a). Above the LCST$_1$, the block copolymer self-assembled into micelles with the P(DEGEA-*co*-AA) block forming the core and the P(TEGMA-*co*-AA) block constituting the corona (Scheme 4.3b). When the effective volume fraction of micelles in the solution reaches a critical value, the micelles are packed into an ordered structure and the free-flowing liquid turned into a free-standing micellar gel (Scheme 4.3c). Like other PEO-based thermosensitive polymers,[19] with the increase of temperature, water becomes an increasingly poor solvent for P(TEGMA-*co*-AA), despite that the temperature is below the LCST. At certain temperature, the volume fraction of micelles becomes smaller than the critical value, i.e., the micelles are no longer constrained but can move around. Consequently, the clear gel is transformed into a sol (Scheme 4.3d). Upon further heating the solution to the LCST of P(TEGMA-*co*-AA) (LCST$_2$), the P(TEGMA-*co*-AA) blocks in the coronal layer undergo a LCST transition and macroscopically the clear sol turned into a cloudy mixture (Scheme 4.3e). The pH dependences of $T_{\text{sol-gel}}$, $T_{\text{gel-sol}}$, and T_{clouding} are a result of the statistical incorporation of a small amount of carboxylic acid groups into both thermosensitive blocks of the diblock copolymer. At low pH values, few
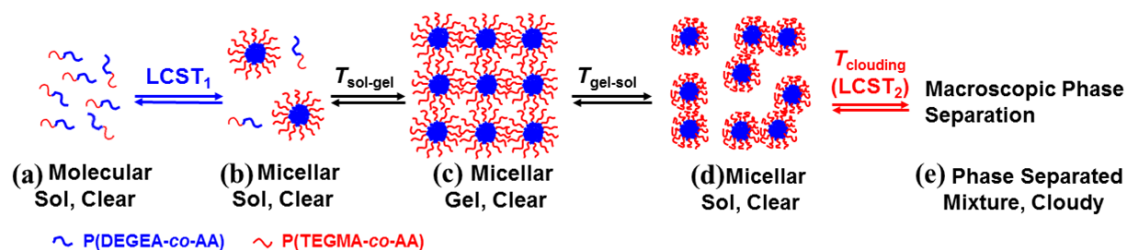
Scheme 4.3 Schematic Illustration of Transitions of 20 wt% Aqueous Solution of Multi-Responsive Diblock Copolymer P(TEGMA-*co*-AA)-*b*-P(DEGEA-*co*-AA) from (a) Clear Molecular Sol to (b) Clear Micellar Sol, to (c) Clear Micellar Gel, to (d) Clear Micellar Sol, and (e) Cloudy Mixture upon Increasing Temperature.

carboxylic acid groups are ionized. With the increase of pH, the degree of ionization of -COOH increases, causing the polymer to become more hydrophilic.[12] Consequently, the LCST transitions of both blocks occur at higher temperatures and so do $T_{sol\text{-}gel}$ and $T_{clouding}$. As discussed previously, the $T_{gel\text{-}sol}$ changes with pH in a more complex manner as this transition is not directly governed by the LCST transitions of the two blocks.

Dynamic light scattering was employed to study the effects of pH on thermo-induced micellization of P(TEGMA-*co*-AA)-*b*-P(DEGEA-*co*-AA) and aggregation of block copolymer micelles in dilute aqueous buffers with four different pH values at a concentration of 0.02 wt%. Figure 4.6 shows the DLS data collected from four 0.02 wt% solutions of P(TEGMA-*co*-AA)-*b*-P(DEGEA-*co*-AA) in 20 mM aqueous KHP buffers with pH values of 3.29, 5.10, 5.79, and 6.50. For the solution with pH of 3.29, below 13 °C, the scattering intensity was low, and the apparent hydrodynamic size (D_h) from CONTIN analysis was < 10 nm, indicating that the block copolymer was in the unimer state. When the temperature reached 13 °C, the scattering intensity collected at scattering angle of 90 ° began to increase and a mixture of unimers and micelles was observed. Thus, the critical micellization temperature (CMT) of P(TEGMA-*co*-AA)-*b*-P(DEGEA-*co*-AA) at this pH was 13 °C as shown in Figure 4.6a. With further raising the temperature, the scattering intensity continued to increase, but the apparent D_h of micelles stayed at ~ 53 nm until 57 °C, at which the scattering intensity jumped to 300 kcps and aggregates with a size of > 2000 nm were observed. Macroscopically, the solution turned cloudy. Apparently, this clouding temperature is the LCST transition of the P(TEGMA-*co*-AA) block, which is very close to the reported cloud point of PTEGMA (58 °C) in the literature.[11]
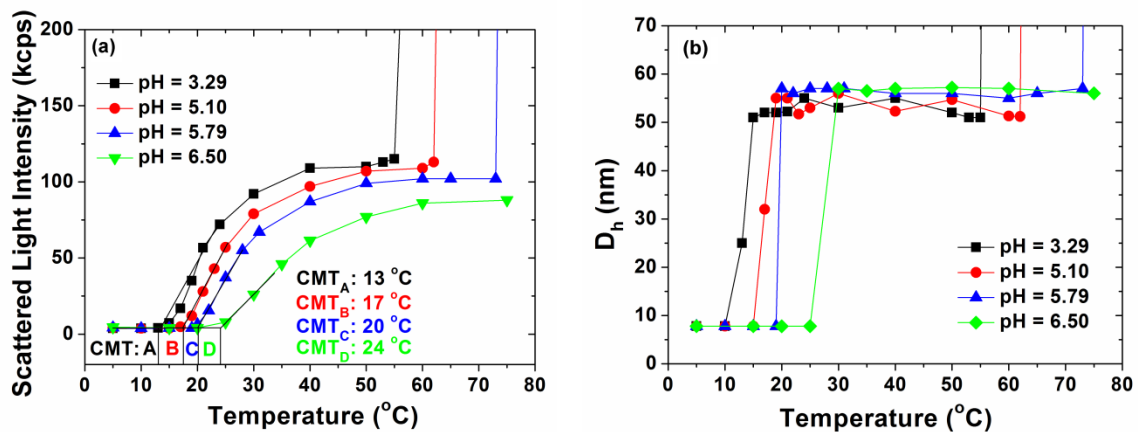
Figure 4.6 (a) Scattered light intensity at scattering angle of 90 ° and (b) apparent hydrodynamic size D_h, obtained from CONTIN analysis, as a function of temperature in a dynamic light scattering study of a 0.02 wt% solution of P(TEGMA-*co*-AA)-*b*-P(DEGEA-*co*-AA) in a 20 mM aqueous KHP buffer with pH = 3.29, 5.10, 5.79, and 6.50.

With the increase of pH, the CMT shifted to higher temperatures, from 13 °C at pH = 3.29 to 17 °C at pH = 5.10, 20 °C at pH 5.79, and 24 °C at pH 6.50. The clouding temperature also shifted upward, from 57 °C at pH = 3.29 to 64 °C at pH = 5.10, 75 °C at pH 5.79, and > 75 °C at pH 6.50. The solution with pH of 6.50 remained clear even at 97 °C. The clouding temperatures at pH of 3.29, 5.10, and 5.79 from DLS were close to those of 20 wt% aqueous solutions of P(TEGMA-co-AA)-b-P(DEGEA-co-AA) at the same pH values (55, 63, and 77 °C), respectively. Although the results from the DLS study are generally in agreement with the observed pH effects on $T_{\text{sol-gel}}$, $T_{\text{gel-sol}}$ (up to pH 5.79), and T_{clouding} of the 20 wt% solution, by comparing Figures 4.4 and 4.6, one can find that the CMT did not increase with pH at the same pace as $T_{\text{sol-gel}}$. The $T_{\text{sol-gel}}$ was 17 °C at pH = 3.29, 20 °C at pH = 5.10, and 28 °C at pH = 5.79, and no gel was observed at pH 6.10. This could be due to the difference in the underlying principles of thermo-induced micellization and sol-gel transition. The CMT determined by DLS is the temperature at which block copolymer molecules begin to self-organize into micelles, while $T_{\text{sol-gel}}$ is related to the rheological/mechanical property of a macroscopic sample and is determined by how the volume fraction of micelles in a moderately concentrated aqueous solution changes with temperature. It appears that the pH-induced small changes in the CMT of the diblock copolymer are amplified in the effects of pH on sol-gel transition. In summary, the DLS results confirmed that the tunability of $T_{\text{sol-gel}}$, $T_{\text{gel-sol}}$, and T_{clouding} originated from the pH dependences of the LCSTs of the two thermosensitive blocks.
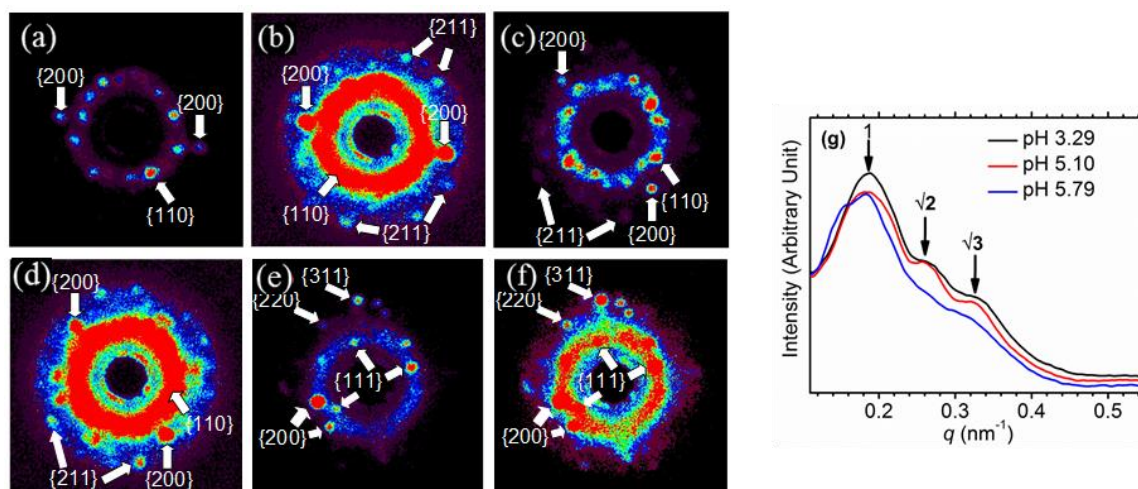
Figure 4.7 SAXS patterns of 20 wt% aqueous solutions of P(TEGMA-*co*-AA)-*b*-P(DEGEA-*co*-AA) in 30 mM KHP buffers with pH of 3.29, 5.10, and 5.79 at 27, 31, and 35 °C, respectively. (a) and (b) Two-dimensional (2-D) scattering pattern of the 20 wt% aqueous solution of P(TEGMA-*co*-AA)-*b*-P(DEGEA-*co*-AA) at pH = 3.29 and T = 27 °C; (c) and (d) 2-D scattering pattern of the micellar gel at pH = 5.10 and T = 31 °C; (e) and (f) 2-D scattering pattern of the micellar gel with pH of 5.79 at 35 °C. In (a), (c), and (e), the contrast was adjusted to show strong {110} diffractions; in (b), (d), and (f), the contrast was adjusted to show weaker diffractions; (g) One-dimensional curves generated by integrating corresponding 2D scattering patterns. Black: pH 3.29; Red: pH 5.10; Blue: pH 5.79. The intensity is in logarithmic scale.

4.3.6 Small-Angle X-Ray Scattering Study of Micellar Gels at pH 3.29, 5.10, and 5.79

Small-angle X-ray scattering (SAXS) was conducted to determine the structures of micellar gels formed from 20 wt% aqueous solutions of P(TEGMA-*co*-AA)-*b*-P(DEGEA-*co*-AA) with pH of 3.29, 5.10, and 5.79. Figure 4.7 shows the two-dimensional SAXS patterns of micellar gels at pH = 3.29 and T = 27 °C (a and b), pH = 5.10 and T = 31 °C (c and d), and pH = 5.79 and T = 35 °C (e and f), respectively, as well as one-dimensional curves obtained by integrating the corresponding 2D scattering patterns (G). Clearly, all 2-D SAXS patterns contain multiple diffraction spots, indicating that the micelles in all three gels self-assembled into an ordered crystalline structure. Besides the strongest diffraction spots at $q \approx 0.19$ nm^{-1}, weaker diffractions can also be seen at larger q values (and at slightly smaller q values in Figure 4.7e and f). For gels at pH 3.29 and 5.10, the ratios of the q values of the observed diffractions are 1 : $\sqrt{2}$: $\sqrt{3}$ (Figure 4.7g), suggesting that the spherical block copolymer micelles are packed into body-centered cubic (bcc) structures.[10b,20] The strongest diffractions at the smallest q values were indexed as {110} diffractions. Note that {110} diffractions are indeed the strongest low-index diffractions given by hard spheres packed in a bcc lattice. The diffractions with larger q values in these gels were indexed as {200} and {211} diffractions accordingly as shown in Figure 4.7a-d. Interestingly, the gel at pH 5.79 and 35 °C features a face-centered cubic (fcc) structure, which can be identified by the ratios of q values of 1: $\sqrt{(4/3)}$: $\sqrt{(8/3)}$: $\sqrt{(11/3)}$ (Figure 4.7g). The diffraction spots at the smallest q values were indexed as {111} diffraction, while wider angle diffractions were indexed as {200}, {220} and {311} diffractions as shown in Figure 4.7e and f. We

speculate that the higher degree of ionization of carboxyl groups at pH = 5.79 might have caused micelles to pack more like hard spheres due to the increased electrostatic repulsive interaction between negatively charged micelles. It is known that fcc is the most favored structure for the close packing of hard spheres.[1a]

The center-to-center distance (*D*) of adjacent micelles can be calculated by using Equations 3.1 and 3.2, where *a* is the cell edge length, and was 41.4, 42.4, and 46.0 nm for the gels with pH of 3.29, 5.10, and 5.79, respectively. We use the term of "center-to-center distance (D) of adjacent micelles" instead of micelle size because the micelles are very likely deformed in the gel state, particularly when the volume fraction of micelles is significantly greater than the critical value for the formation of gels. The center-to-center distances of adjacent micelles are noticeably smaller than the micelle sizes measured by DLS (51 − 57 nm in Figure 4.6). It should be noted here that in the DLS experiments, 0.02 wt% aqueous solutions of P(TEGMA-*co*-AA)-*b*-P(DEGEA-*co*-AA) were used while SAXS studies were conducted on 20 wt% aqueous solutions. The self-assembly behavior of the diblock copolymer in dilute and concentrated aqueous solutions may not be exactly the same. In addition, the hydrodynamic sizes of micelles obtained from DLS measurements are apparent hydrodynamic diameters because scattering data were collected at only one scattering angle (90 °). Thus, it is understandable that there is a difference between the results from DLS and SAXS.

$$D = \frac{\sqrt{3}}{2} a \text{ for a bcc lattice} \qquad \text{(Equation 3.1)}$$

$$D = \frac{1}{\sqrt{2}} a \text{ for a fcc lattice} \qquad \text{(Equation 3.2)}$$

4.3.7 Sol-Gel Phase Diagrams of P(TEGMA-*co*-AA)-*b*-P(DEGEA-*co*-AA) in Aqueous KHP Buffers with pH of 3.29, 5.10, and 5.79

We further determined the sol-gel phase diagrams of moderately concentrated aqueous solutions of P(TEGMA-*co*-AA)-*b*-P(DEGEA-*co*-AA) in KHP buffers at three different pH values, 3.29, 5.10, and 5.79 (all measured at ~ 0 °C), by vial inversion tests. Note that the pH variations within the studied concentration (17 − 25 wt%) and temperature range (0 − 55 °C) were small (see Appendix B).[17] As shown in Figure 4.8, all three sol-gel phase diagrams are C-shaped curves, characteristic of sol-gel phase diagrams of thermosensitive diblock copolymers in water. Clearly, with the increase of pH from 3.29 to 5.10 and 5.79, the whole sol-gel phase diagram, i.e., both lower and upper temperature boundaries, shifted upward, though the changes for the two boundaries are not the same. In particular, for the two curves at pH 3.29 and 5.10, the shift of the lower boundary was smaller than that of the upper boundary, while for the curves of pH 5.10 and 5.79, the changes of two boundaries appeared to be comparable. This is consistent with the observations on pH dependences of $T_{sol-gel}$, $T_{gel-sol}$, and $T_{clouding}$ of 20 wt% aqueous buffer solution of the diblock copolymer presented in Figure 4.4 and from the DLS study (Figure 4.6).

Interestingly, with the increase of pH, the critical gelation concentration (CGC) changed from ~ 17 wt% at pH = 3.29 to ~ 16.5 wt% at pH = 5.10, and then back to ~ 17 wt% at pH = 5.79 (Figure 4.8). Note that the CGC is the minimum concentration at which the volume fraction of block copolymer micelles in water reaches the critical value for gelation and is in some sense controlled by the balance between the thermo-enhanced micellization of the block copolymer and the thermo-induced shrinking of the corona.
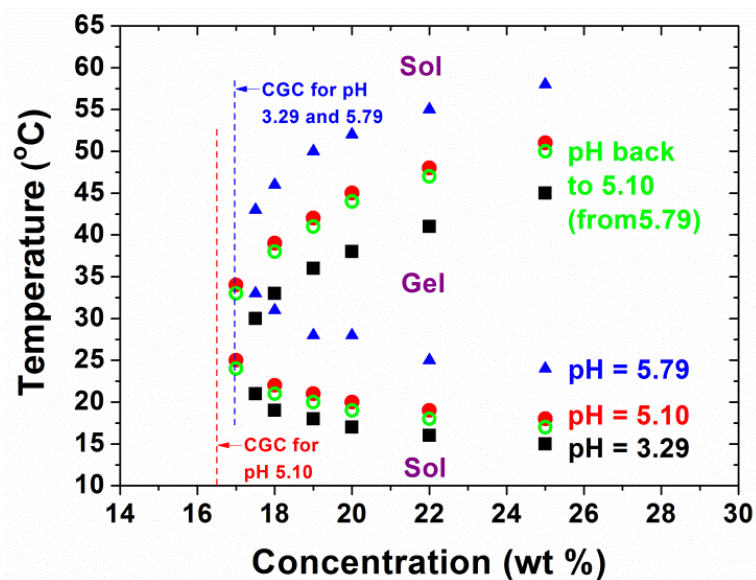
Figure 4.8 Sol-gel phase diagrams determined by the vial inversion method for P(TEGMA-*co*-AA)-*b*-P(DEGEA-*co*-AA) in 30 mM KHP buffer at pH of 3.29 (solid square), 5.10 (solid circle), and 5.79 (solid triangle). The green hollow circles shows the phase diagram at pH = 5.10 obtained by decreasing the pH from 5.79.

The lowest CGC at pH = 5.10 means the highest volume fraction of micelles at the same concentration. This is consistent with the results from temperature ramp experiments (Figure 4.3), where the highest maximum G' was observed at pH = 5.10. Apparently, the change of the solution pH affected the volume fraction of block copolymer micelles and its temperature dependence in a complex manner. With the increase of pH, the degrees of ionization of carboxylic acid in both blocks increased. Thus, the P(TEGMA-*co*-AA) block in the corona layer became more hydrophilic and occupied more volume, which would cause an increase in the volume fraction of micelles. This is supported by the results presented in Chapter 2 that the CGC of P(TEGMA-*co*-AA)-*b*-PDEGEA in water decreased with the increased of pH.[10a] On the other hand, the LCST transition of the P(DEGEA-*co*-AA) block occurred at a higher temperature, which means that the P(TEGMA-*co*-AA) blocks in the corona would shrink to a slightly greater extent at the sol-gel transition. In addition, the greater hydrophilicity of polymer chains at higher pH values would result in more block copolymer molecules staying in water as unimers instead of entering micelles at temperatures above the LCST. Consequently, the volume fraction of micelles would become smaller. It was shown in Chapter 3 that the CGC of PTEGMA-*b*-P(DEGEA-*co*-AA) in aqueous solution increased with the increase of pH.[10b] Apparently, for P(TEGMA-*co*-AA)-*b*-P(DEGEA-*co*-AA), the effects of pH on two blocks are against each other. As shown in Figures 4.4 and 4.6, the clouding temperature went up faster with pH than $T_{sol-gel}$ and CMT. Therefore, it is reasonable that the CGC of P(TEGMA-*co*-AA)-*b*-P(DEGEA-*co*-AA) increased when the pH was changed from 3.29 to 5.10 and then decreased with further raising pH to 5.79.

To investigate the reversibility of shifting of sol-gel phase diagram, we lowered the pH back to 5.10 from 5.79 and mapped out the sol-gel phase diagram by vial inversion tests. As shown in Figure 4.8, the new C-shaped curve almost overlapped with the original curve of pH = 5.10. However, all points were 1 °C lower than the original points at the same concentrations. This is likely due to the small increase in the salt concentration from the neutralization reaction.

4.4 Conclusions

A well-defined doubly thermosensitive hydrophilic diblock copolymer with both blocks containing a small amount of carboxylic acid groups, P(TEGMA-*co*-AA)-*b*-P(DEGEA-*co*-AA), was synthesized by RAFT and post-polymerization modification.[21] A 20 wt% solution of this diblock copolymer in a 30 mM aqueous KHP buffer with pH of 3.29 underwent clear sol-to-clear gel, clear gel-to-clear sol, clear sol-to cloudy sol transitions at 17, 38, and 55 °C, respectively, upon heating. Raising the pH of the 20 wt% solution shifted $T_{\text{sol-gel}}$ and T_{clouding} to higher temperatures in the studied pH range of 3.29 to 6.00, while $T_{\text{gel-sol}}$ increase initially with pH and then leveled off/decreased when the pH was $\geq$ 5.90. No gel was observed at pH $\geq$ 6.10. The data collected from rheological measurements are in good agreement with the results from the vial inversion tests and visual inspection. The observed thermally induced sol-gel-sol-cloudy transitions and the tunability of $T_{\text{sol-gel}}$, $T_{\text{gel-sol}}$, and T_{clouding} stemmed from the thermosensitive properties of and the pH dependences of the LCSTs of the two blocks, which were confirmed by dynamical light scattering studies. SAXS studies showed that the micelles were packed into bcc structures at pH = 3.29 and T = 27 °C as well as at pH = 5.10 and T = 31 °C.

Differently, the gel structure at pH = 5.79 and T = 35 °C was a fcc lattice. We further determined the sol-gel phase diagrams of the diblock copolymer in the moderate concentration range at pH of 3.29, 5.10, and 5.79; both the lower and upper temperature boundaries shifted upward by increasing the pH from 3.29, to 5.10, and 5.79. Lowering the pH back to 5.10 from 5.79 moved the diagram back, though all points were 1 °C lower than the original curve at pH = 5.10. This work demonstrated that the C-shaped sol-gel phase diagram of a doubly thermosensitive diblock copolymer in water in the moderate concentration range can be shifted continuously and reversibly by incorporating a small amount of weak acid groups into both blocks and adjusting the solution pH, providing a convenient means to manipulate the solution properties of thermosensitive hydrophilic blocks in water for potential applications.

References

1. (a) Hamley, I. W. *Block Copolymers in Solution: Fundamentals and Applications*; John Wiley & Sons: Chichester, U.K., 2005. (b) Hamley, I. W. *The Physics of Block Copolymers*; Oxford University Press: Oxford, U.K., 1998. (c) Hamley, I. W. *Philos. Trans. R. Soc. London A* **2001**, *359*, 1017-1044.

2. (a) Gil, E. S.; Hudson, S. M. *Prog. Polym. Sci.* **2004**, *29*, 1173-1222. (b) Dimitrov, I.; Trzebicka, B.; Müller, A. H. E.; Dworak, A.; Tsvetanov, C. B. *Prog. Polym. Sci.* **2007**, *32*, 1275-1343. (c) Madsen, J.; Armes, S. P. *Soft Matter* **2012**, *8*, 592-605.

3. (a) Jeong, B. M.; Bae, Y. H.; Lee, D. S.; Kim, S. W. *Nature* **1997**, *388*, 860-862. (b) He, C. L.; Kim, S. W.; Lee, D. S. *J. Controlled Release* **2008**, *127*, 189-207. (c) Park, M. H.; Joo, M. K.; Choi, B. G.; Jeong, B. *Acc. Chem. Res.* **2012**, *45*, 424-433. (d) Kirkland, S. E.; Hensarling, R. M.; McConaught, S. D.; Guo, Y.; Jarrett, W. L.; McCormick, C. L. *Biomacromolecules* **2008**, *9*, 481-486.

4. (a) Skrabania, K. ; Kristen, J. ; Laschewsky, A. ; Akdemir, O. ; Hoth, A. ; Lutz, J. F. *Langmuir* **2007**, *23*, 84-93. (b) Xie, D. H. ; Ye, X. D. ; Ding, Y. W. ; Zhang, G. Z. ; Zhao, N. ; Wu, K. ; Cao. Y. ; Zhu, X. X. *Macromolecules* **2009**, *42*, 2715-2720. (c) Woodcock, J. W., Jiang, X. G.; Wright, R. A. E.; Zhao, B. *Macromolecules* **2011**, *44*, 5764-5775. (d) O'Lenick, T. G.; Jiang X. M.; Zhao, B. *Polymer* **2009**, *50*, 4363-4371.

5. (a) Mortensen, K.; Brown, W.; Norden, B. *Phys. Rev. Lett.* **1992**, *68*, 2340-2343. (b) Hvidt, S.; Jørgensen, E. B.; Schillén, K.; Brown, W. *J. Phys. Chem.* **1994**, *98*, 12320-12328. (c) Wanka, G.; Hoffmann, H.; Ulbricht, W. *Macromolecules* **1994**, *27*, 4145-4159. (d) Zhou, Z; Chu, B. *Macromolecules* **1994**, *27*, 2025-2033. (e) Alexandridis, P.; Hatton, T. A. *Colloids and Surfaces A: Physicochem. Eng. Aspects* **1995**, *96*, 1-46.

6. (a) Li, H.; Yu, G.-E.; Price, C.; Booth, C.; Hecht, E.; Hoffmann, H. *Macromolecules* **1997**, *30*, 1347-1354. (b) Alexandridis, P.; Olsson, U.; Kindman, B. *Langmuir* **1997**, *12*, 23-34. (c) Hamley, I. W.; Pople, J. A.; Fairclough, J. P. A.; Ryan, A. J.; Booth, C.; Yang, Y.-W. *Macromolecules* **1998**, *31*, 3906-3911.

7. (a) Li, C.; Tang, Y.; Armes, S. P.; Morris, C. J.; Rose, S. F.; Lloyd, A. W.; Lewis, A. L. *Biomacromolecules* **2005**, *6*, 994-999. (b) Fechler, N.; Badi, N.; Schade, K.; Pfeifer, S.; Lutz, J.-F. *Macromolecules* **2009**, *42*, 33-36. (c) O'Lenick, T. G.; Jiang X. G.; Zhao, B. *Langmuir* **2010**, *26*, 8787–8796. (d) O'Lenick, T. G.; Jin, N. X.; Woodcock, J. W.; Zhao, B. *J. Phys. Chem. B.* **2011**, *115*, 2870-2881. (e) Woodcock, J. W.; Wright, R. A. E.; Jiang, X. G.; O'Lenick, T. G.; Zhao, B. *Soft Matter*, **2010**, *6*, 3325-3336.

8. (a) Aoshima, S.; Kanaoka, S. *Adv. Polym. Sci.* **2008**, *210*, 169-208. (b) Sugihara, S.; Kanaoka, S.; Aoshima, S. *Macromolecules* **2005**, *38*, 1919-1927.

9. (a) Jiang, X. G.; Lavender, C. A.; Woodcock, J. W.; Zhao, B. *Macromolecules* **2008**, *41*, 2632-2643. (b) Jiang, X. G.; Jin, S; Zhong, Q. X.; Dadmun, M. D.; Zhao, B. *Macromolecules* **2009**, *42*, 8468-8476. (c) Jiang X. G.; Zhao, B. *Macromolecules* **2008**, *41*, 9366-9375.

10. (a) Jin, N. X.; Woodcock, J. W.; Xue. C. M.; O'Lenick, T. G.; Jiang, X. G.; Jin, S.; Dadmun, M. D.; Zhao, B. *Macromolecules* **2011**, *44*, 3556-3566. (b) Jin, N. X.; Zhang, H.; Jin, S.; Dadmun, M. D.; Zhao, B. *J. Phys. Chem. B* **2012**, *116*, 3125-3137.

11. Hua, F. J.; Jiang, X. G.; Li, D. J.; Zhao, B. *J. Polym. Sci. Part A: Polym. Chem.* **2006**, *44*, 2454-2467.

12. (a) Feil, H.; Bae, Y. H.; Feijen, J.; Kim, S. W. *Macromolecules* **1993**, *26*, 2496-2500.

(b) Yin, X.; Hoffman, A. S.; Stayton, P. S. *Biomacromolecules* **2006**, *7*, 1381-1385.

(c) Lokitz, B. S.; York, A. W.; Stempka, J. E.; Treat, N. D.; Li, Y.; Jarrett, W. L.; McCormick, C. L. *Macromolecules* **2007**, *40*, 6473-6480. (d) Luo, C. H.; Liu, Y.; Li, Z. B. *Macromolecules* **2010**, *43*, 8101-8108. (e) Tsitsilianis, C.; Gotzamanis, G.; Iatridi, Z. *Euro. Polym. J.* **2011**, *47*, 497-510. (f) Horton, J. M.; Bao, C. H.; Bai, Z. F.; Lodge, T. P.; Zhao, B. *Langmuir* **2011**, *27*, 13324-13334. (g) Urry, D. W. *J. Phys. Chem. B* **1997**, *101*, 11007-11028.

13. Chiefari, J.; Chong, Y. K.; Ercole, F.; Krstina, J.; Jeffery, J.; Le, T. P. T.; Mayadunne, R. T. A.; Meijs, G. F.; Moad, C. L.; Moad, G.; Rizzardo, E.; Thang, S. H. *Macromolecules* **1998**, *31*, 5559-5562.

14. (a) Determan, M. D.; Cox, J. P.; Seifert, S.; Thiyagarajan, P.; Mallapragada, S. K. *Polymer* **2005**, *46*, 6933-6946. (b) Determan, M. D.; Guo, L.; Thiyagarajan, P.; Mallapragada, S. K. *Langmuir* **2006**, *22*, 1469-1473. (c) Shim, W. S.; Yoo, J. S.; Bae, Y. H.; Lee, D. S. *Biomacromolecules* **2005**, *6*, 2930-2934. (d) Park, S. Y.; Lee, Y.; Bae, K. H.; Ahn, C. H.; Park, T. G. *Macromol. Rapid Commun.* **2007**, *28*, 1172-1176. (e) Suh, J. M.; Bae, S. J.; Jeong, B. *Adv. Mater.* **2005**, *17*, 118-120. (f) Joo, M. K.; Park, M. H.; Choi, B. G.; Jeong, B. *J. Mater. Chem.* **2009**, *19*, 5891-5905.

15. (a) Shim, W.S.; Kim, J. H.; Park, H.; Kim, K.; Kwon, I. C.; Lee, D. S. *Biomaterials* **2006**, *27*, 5178-5185. (b) Dayananda, K.; He, C. L.; Park, D. K.; Park, T. G.; Lee, D. S. *Polymer* **2008**, *49*, 4968-4973. (c) Huynh, D. P.; Nguyen, M. K.; Kim, B. S.; Lee, D. S. *Polymer* **2009**, *50*, 2565-2571.

16. Chong, Y. K.; Krstina, J.; Le, T. P. T.; Moad, G.; Postma, A.; Rizzardo, E.; Thang, S. H. *Macromolecules* **2003**, *36*, 2256-2272.

17. See the data included in the Appendix C.

18. Noro, A.; Matshushita, Y.; Lodge, T. P. *Macromolecules* **2009**, *42*, 5802-5810.

19. (a) Bai, Z. F.; Lodge, T. P. *J. Phys. Chem. B* **2009**, 113, 14151-14157. (b) Horton, J. M.; Bai, Z. F.; Lodge, T. P.; Zhao, B. *Langmuir* **2011**, *27*, 2019-2027.

20. (a) Hamley, I. W.; Daniel, C.; Mingvanish, W.; Mai, S.-M.; Booth, C.; Messe, L.; Ryan, A. J. *Langmuir* **2000**, *16*, 2508-2514. (b) Torija, M. A.; Choi, S.-H.; Lodge, T. P.; Bates, F. S. *J. Phys. Chem. B.* **2011**, *115*, 5840-5848.

21. The work presented in this Chapter has been published in *Macromolecules* as an article (*Macromolecules* **2012**, *45*, 4790-4800).

    http://pubs.acs.org/doi/abs/10.1021/ma300791y

Appendix C

for

Chapter 4. Shifting Sol-Gel Phase Diagram of A Doubly Thermosensitive Hydrophilic Diblock Copolymer Poly(methoxytri(ethylene glycol) acrylate-*co*-acrylic acid)-*b*-poly(ethoxydi(ethylene glycol) acrylate-*co*-acrylic acid) in Aqueous Solution
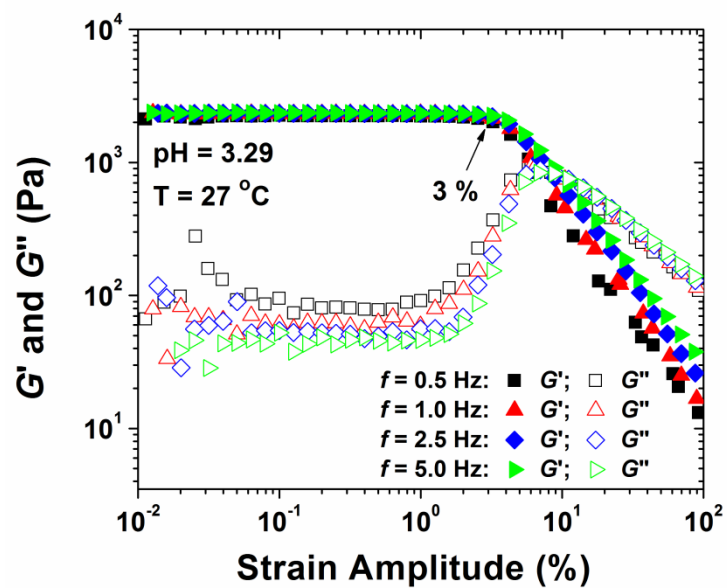
Figure C1. Dynamic strain amplitude sweeps at frequencies of 0.5 Hz, 1.0 Hz, 2.5 Hz, and 5.0 Hz for the 20 wt% aqueous solution of P(TEGMA-*co*-AA)-*b*-P(DEGEA-*co*-AA) with pH of 3.29 at 27 °C.
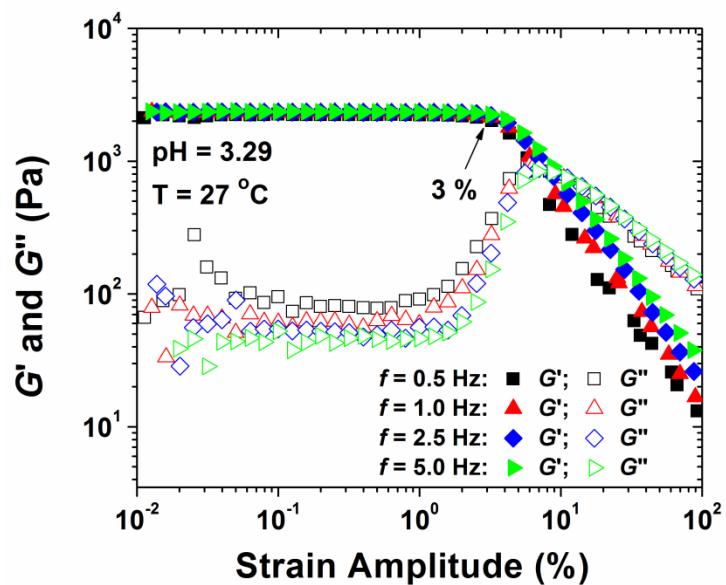
Figure C2. Dynamic strain amplitude sweeps at frequencies of 0.5, 1.0, 2.5, and 5.0 Hz for the 20 % aqueous solution of P(TEGMA-*co*-AA)-b-P(DEGEA-*co*-AA) with pH of 5.10 at 31 °C.
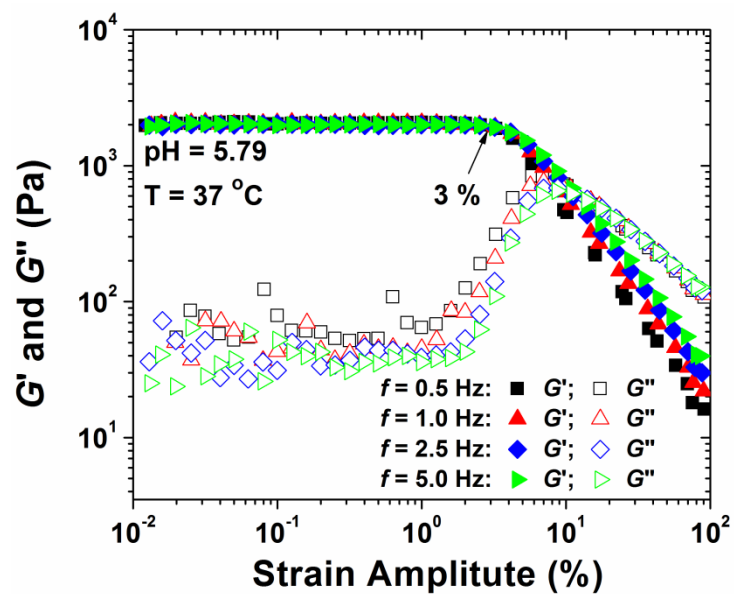
Figure C3. Dynamic strain amplitude sweeps at frequencies of 0.5, 1.0, 2.5, and 5.0 Hz for the 20 % aqueous solution of P(TEGMA-*co*-AA)-b-P(DEGEA-*co*-AA) with pH of 5.79 at 37 °C.

C.1 pH Variations with the Change of Block Copolymer Concentration at a Specific Temperature

The pH value of a 20 wt% aqueous solution of P(TEGMA-*co*-AA)-*b*-P(DEGEA-*co*-AA) in a 30 mM KHP buffer was first measured in an ice/water bath with a pH meter (calibrated at 0 °C using pH = 4.01, 7.00, and 10.01 standard buffer solutions). The obtained pH value was 3.29. The sample was then diluted to 16 wt% and the pH was found to be 3.26. We then concentrated the solution to 25 wt% by evaporating a calculated amount of water. After the solution was sonicated in an ice/water bath to ensure that it was homogenous, the pH was measured to be 3.30. The change of the pH was only 0.04 units, which made us believe that the pH variations with the change of polymer concentration in the determination of the sol-gel phase diagrams were negligible.

C.2 pH Variations with the Change of Temperature at a Specific Polymer Concentration

We also investigated the effect of temperature on the pH values of 16 wt% solutions of P(TEGMA-*co*-AA)-*b*-P(DEGEA-*co*-AA) in 30 mM KHP buffers. A 16 wt% polymer solution with pH of 3.29 was prepared (measured at 0 °C). The pH values of the solution at 25 and 50 °C were then measured. The pH meter was calibrated at each corresponding temperature (0, 25, and 50 °C) by using pH 4.01, 7.00, and 10.01 standard buffer solutions before the pH values of the polymer solution were recorded. The concentration of the polymer solution was set at 16 wt%, which is below the CGC, to ensure that no gel was formed during the studied temperature range. The pH was then adjusted to 5.10 and 5.79 at 0 °C, and the pH values at 25 and 50 °C were measured. For comparison, 30 mM KHP buffer solutions with similar pH values were prepared and measured under the same

conditions as for the polymer solutions. The results are summarized in Table C1 and C2. For pH 3.29, the pH variations of the 16 wt% polymer solution in the temperature range of 0 – 50 °C were small, only 0.09 pH units, essentially the same as those of a 30 mM KHP buffer with pH of 3.08. For pH of 5.10 and 5.79, the pH variations of 16 wt% polymer solutions in the temperature range of 0 – 50 °C were slightly larger, 0.30 and 0.40 pH units, respectively. These changes were slightly larger than those of 30 mM KHP buffers with similar pH values, 0.17 and 0.20 pH units, respectively.

Table C1. Effects of Temperature on pH Values of 16 wt% Solutions of P(TEGMA-*co*-AA)-*b*-P(DEGEA-*co*-AA) in 30 mM Aqueous KHP Buffers

Samples	0 °C	25 °C	50 °C	Δ pH
16 wt% Polymer Solution	3.29	3.27	3.36	0.09
16 wt% Polymer Solution	5.10	5.08	5.38	0.30
16 wt% Polymer Solution	5.79	5.75	6.15	0.40

Table C2. Effect of Temperature on pH Values of 30 mM Aqueous KHP Buffer

Buffer	0 °C	25 °C	50 °C	Δ pH
30 mM Aqueous KHP Buffer	3.08	3.02	3.10	0.08
30 mM Aqueous KHP Buffer	5.10	5.08	5.25	0.17
30 mM Aqueous KHP Buffer	5.80	5.85	6.00	0.20

Chapter 5. pH-Responsive Diblock Copolymer Micelle-Embedded

Agarose Hydrogels for Controlled Release of Substance

Abstract

Agarose hydrogel embedded with pH-responsive, poly(ethylene oxide) (PEO)-based diblock copolymer micelles were prepared. The hybrid hydrogels were designed to improve the functions of agarose gels, a type of soft materials widely used in biomedical applications. A well-defined pH-sensitive diblock copolymer, PEO-*b*-poly(2-(*N,N*-diisopropylamino)ethyl methacrylate), was synthesized by atom transfer radical polymerization of 2-(*N,N*-diisopropylamino)ethyl methacrylate from a PEO macroinitiator. The block copolymer micelles were formed by the solvent switching method, and their responsive properties were studied by dynamic light scattering and fluorescence spectroscopy. Hybrid hydrogels were made from 1 wt% agarose solutions that contained PEO-*b*-PDPAEMA micelles with concentrations of $0.5 - 5.0$ mg/g. The solutions were kept at 4 °C overnight to allow the formation of gels. Rheological studies showed that the gel properties were not significantly affected even when the block copolymer micelle concentration was as high as 5.0 mg/g. The pH-induced release behavior of PEO-*b*-PDPAEMA micelles in a hybrid hydrogel was studied by using fluorescence spectroscopy with Nile Red as a model drug.

5.1 Introduction

A critical challenge faced by the tissue engineering community is to properly combat the multifaceted tissue damage and synchronize tissue regeneration with wound healing. For example, when post-injury infections within the intracranial cavity occur after a traumatic brain injury,[1] a surgery might be needed to remove the infected tissue to prevent any potentially life threatening disease. However, due to the physical gap created by the surgery, neural cells cannot reconnect without the aid of regenerative medicine.[2] One of the key components in the regenerative process is an implanted scaffold in the brain cavity that acts as a synthetic extracellular matrix. Such scaffold should be biocompatible and support cell infiltration and neuron outgrowth.[3]

Hydrogels, especially agarose hydrogels, are widely used as scaffolding materials for neural tissue engineering.[2,4-8] Agarose is a biocompatible polysaccharide. The porous structure of agarose hydrogels and the highly hydrated network of interacting polymer chains provide a biomimetic environment for cellular outgrowth.[5,9] In addition, agarose hydrogels are nontoxic and degradable in the human body. However, during the tissue repair process, many challenges still remain, such as excessive inflammation and lack of growth factors. To overcome the limitations of agarose hydrogels and to improve their functions, herein we incorporate stimuli-responsive block copolymer micelles into agarose hydrogels; the micelles can be loaded with substances, for example, anti-inflammatory agents, and can be dissociated by applying a stimulus to release the payload.

Among various stimulus-responsive block copolymers that have been used for triggered release of substances, pH-sensitive polymers are arguably the most extensively investigated.[10-22] In this work, a poly(ethylene oxide) (PEO)-based diblock copolymer,

PEO-*b*-poly(2-(*N*,*N*-diisopropylamino)ethyl methacrylate) (PEO-*b*-PDPAEMA), was used. The tertiary amine groups in the second block impart the pH sensitivity. The degree of protonation of PDPAEMA, and thus the hydrophilicity/hydrophobicity balance of the PDPAEMA block, can be precisely controlled by changing the solution pH.[23-27] It is known that there is a pH difference between pathological (e.g. cancerous[28] and inflamed) and normal tissues. The pathological tissues normally have a lower pH value. One attractive feature of tertiary amine-containing polymers is that at lower pH values they become hydrophilic. This change will induce the dissociation of block copolymer micelles and subsequently the release of the payload.

PEO-*b*-PDPAEMA was synthesized by atom transfer radical polymerization of DPAEMA from a PEO macroinitiator (Scheme 5.1). The solution behavior of PEO-*b*-PDPAEMA was first studied in order to determine the critical pH value of micelle dissociation. Hybrid hydrogels embedded with PEO-*b*-PDPAEMA micelles were made by cooling 1 wt% agarose solutions that contained various concentrations of block copolymer micelles at 4 °C overnight. It was found that the rheological properties of the hydrogels were not significantly affected even when the concentration of PEO-*b*-PDPAEMA was as high as 5.0 mg/g. Nile Red was used as a model drug and loaded into the core of micelles. The controlled release behavior of Nile Red in a hybrid hydrogel was studied by fluorescence spectroscopy.
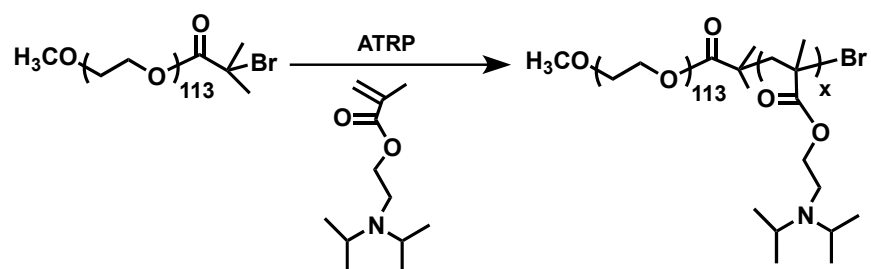
Scheme 5.1 Synthesis of Poly(ethylene glycol)-*b*-poly(2-(*N*,*N*-diisopropylamino)ethyl methacrylate) by ATRP

5.2 Experimental Section

5.2.1 Materials

Poly(ethylene glycol) monomethyl ether (PEO-OH, MW = 5000 g/mol) was purchased from Sigma Aldrich. CuBr (98%, Aldrich) was stirred in glacial acetic acid, filtered, and washed sequentially with absolute ethanol and diethyl ether. The purified CuBr was then dried in vacuum and stored in a desiccator. The monomer, 2-(*N*,*N*-diisopropylamino)ethyl methacrylate (DPAEMA), was synthesized by a one-step reaction between 2-(*N*,*N*-diisopropylamino)ethanol (99%, Aldrich) and methacryloyl chloride (Aldrich). 1,1,4,7,10,10-Hexamethyltriethylenetetramine (HMTETA, 97%) was purchased from Aldrich and used as is. *N*,*N*-dimethylformamide (DMF, extra dry), dichloromethane, tetrahydrofuran, potassium hydrogen phthalate (KHP, primary standard, p.a.), acetone (HPLC grade), and Nile Red (99%) were obtained from Acros and used as received. Diethyl ether, 1.0 M KOH solution (volumetric standard solution) and 1.0 M HCl solution (volumetric standard solution) were obtained from Fisher Scientific. SeaPrep® Agarose was purchased from Lonza. All other chemicals were purchased from either Aldrich or Fisher/Acros and used without further purification.

5.2.2 Characterization

Size exclusion chromatography (SEC) was conducted at room temperature using PL-GPC 50 Plus (an integrated GPC system from Polymer Laboratories, Inc.). The instrument was equipped with a refractive index detector, one GRAL guard column (8 × 50 mm, 10 micron particles), and two GRAL linear columns (each 8 × 300 mm, 10 micron particles, molecular weight range from 500 to 1,000,000 according to Polymer Standards Service-USA, Inc.). The system was calibrated by using polystyrene standards.

N,N-Dimethylformamide was used as the carrier solvent at a flow rate of 1.0 mL/min. The data were processed by using Cirrus[TM] GPC/SEC software (Polymer Laboratories, Inc.). The ^{1}H NMR (300 MHz) spectra were recorded on a Varian Mercury 300 NMR spectrometer and CDCl$_3$ was used as the solvent.

5.2.3 Synthesis of Macroinitiator and Block Copolymer PEO-*b*-PDPAEMA

The macroinitiator (PEO-Br) was prepared according to a literature procedure.[29] The trace amount of water in poly(ethylene glycol) monomethyl ether (PEO-OH) was removed via azeotropic distillation with dry toluene prior to the reaction between PEO-OH and excess 2-bromoisobutyryl bromide. The polymer was precipitated in diethyl ether, then dissolved in water, and extracted with methylene chloride for several times. After drying in high vacuum for 4 h, the PEO macroinitiator was used for the synthesis of PEO-*b*-PDPAEMA.

As shown in Scheme 5.1, PEO-*b*-PDPAEMA was synthesized by atom transfer radical polymerization (ATRP).[30-36] PEO-Br (1.010 g, 0.197 mmol), CuBr (40.9 mg, 0.285 mmol), 1,1,4,7,10,10-hexamethyltriethylenetetramine (HMTETA, 63.5 mg, 0.276 mmol), DPAEMA (1.624 g, 7.62 mmol), and acetone (10.000 g) were charged into a 25 mL two-necked flask, followed by three freeze-pump-thaw cycles to degas the reaction mixtures. The polymerization was monitored by SEC. The polymerization proceeded for 440 min before it was stopped. The copper complex was removed by passing the reaction mixture through a basic aluminum oxide column. The polymer was then dissolved in acetone at room temperature and precipitated in acetone that was cooled in an acetone/dry ice bath. The purification process was repeated additional four times. The block copolymer was then dried under high vacuum at 55 °C overnight before use. The

molecular weight and polydispersity index (PDI) were determined by SEC. The $M_{n,SEC}$ and PDI were 12.6 kDa and 1.06, respectively. The number of DPAEMA repeat units in the PDPAEMA block was calculated from the ^{1}H NMR spectrum.

5.2.4 Preparation of PEO-*b*-PDPAEMA Micelles in Aqueous Solution

The so-called co-solvent method was used for the preparation of PEO-*b*-PDPAEMA micelles in water.[37,38] A typical procedure is described below. PEO-*b*-PDPAEMA (88.3 mg) was dissolved in DMF (0.531 g) and stirred overnight at room temperature. A 1× phosphate buffered saline (PBS) buffer with pH of 7.4 (5.009 g) was added into the DMF solution in a dropwise fashion to induce the formation of micelles. The polymer solution was then dialyzed against the 1× PBS buffer (pH 7.4). The buffer solution was changed every hour in the first 8 h and then changed every 8 h for the next 48 h. A certain amount of a 1× PBS buffer (pH 7.4) was added to the dialyzed solution to adjust the final concentration of PEO-*b*-PDPAEMA to 10 mg/g. This stock solution was used for other experiments in this work.

5.2.5 Dynamic Light Scattering Study of PEO-*b*-PDPAEMA Micelles

The dynamic light scattering (DLS) study of PEO-*b*-PDPAEMA in water was conducted using a Brookhaven Instruments BI-200SM goniometer equipped with a PCI BI-9000AT digital correlator, a solid-state laser (model 25-LHP-928-249, λ = 633 nm), and a temperature controller at a scattering angle of 90°. The DLS samples were made by diluting the 10 mg/g stock solution with a 1× PBS buffer (pH 7.4) to 1.0 mg/g. A series of micelle solutions with different pH values were made by injecting 1.0 M HCl into the PEO-*b*-PDPAEMA solution via a microsyringe in a stepwise fashion. When a desired pH value was reached, a portion of the solution was taken out for DLS measurement. The

solutions were filtered through a Millipore hydrophilic PTFE filter (0.2 μm pore size) into borosilicate glass tubes with an inner diameter of 7.5 mm. The tubes were sealed with a PE stopper and a Teflon tape. The glass tube was then placed in the cell holder of the DLS instrument. The solution was equilibrated for 30 min at 25 °C prior to the collection of data. The correlation functions were analyzed by CONTIN program. The pH value at which block copolymer micelles were completely dissociated was determined by analyzing the plots of hydrodynamic diameter (D_h) and scattering intensity versus pH.

5.2.6 Study of pH-Induced Dissociation of PEO-*b*-PDPAEMA Micelles by Fluorescence Spectroscopy

The pH-induced dissociation of PEO-*b*-PDPAEMA micelles was also studied by fluorescence spectroscopy using Nile Red as fluorescence probe. A stock solution of Nile Red in acetone with a concentration of 0.71 mg/g (100 μL) was added into a pre-weighed vial using a microsyringe. The weight of the vial plus the solution was measured immediately. The vial was then dried under high vacuum for 3 h at 55 °C before 20.000 g of a 1 mg/g PEO-*b*-PDPAEMA solution with pH of 7.4 was added. The mixture was then sonicated for 30 min and kept in the fridge overnight prior to use. The nominal concentration of Nile Red was 6.7×10^{-6} M. The pH of the Nile Red-loaded micelle solution was adjusted by the injection of 1 M HCl solution in a step-wise fashion. Samples were taken out at different pH values for fluorescence measurements. Fluorescence emission spectra of Nile Red in these solutions were recorded using a PerkinElmer LS 55 fluorescence spectrometer equipped with a 20 kW xenon discharge lamp at room temperature. The slit width was 4 nm. The excitation wavelength was set at 543 nm and the fluorescence emission spectra were collected from 550 to 720 nm.

5.2.7 Rheological Measurements

Rheological experiments were conducted on a TA Instruments rheometer (TA AR 2000ex). A cone-plate geometry with a cone diameter of 20 mm and an angle of 2° (truncation 52 μm) was used; the temperature was controlled by the bottom Peltier plate. Agarose gels are usually prepared by cooling hot aqueous agarose solution. To mimic this process on the rheometer, a hot solution was first prepared by dissolving agarose in a 1× PBS buffer (pH 7.4) at 65 °C and then cooled to room temperature. No gelation occurred at this stage. 90 μL of the solution was loaded onto the plate of the rheometer. The solvent trap was filled with water and the solvent trap cover was used to minimize water evaporation. The gel was formed on the plate by lowering the temperature. The dynamic viscoelastic properties (dynamic storage modulus G' and loss modulus G'') were first measured at 2 °C as a function of time by oscillatory shear experiments to determine a proper cooling time. Dynamic strain sweep experiments from strain amplitude of 0.01% to 80% at frequencies of 0.5, 1.0, 2.5, and 5.0 Hz were conducted to determine the linear viscoelastic regime. The dynamic viscoelastic properties of agarose gels and gels embedded with block copolymer micelles were measured by oscillatory shear experiments performed at a fixed frequency of 1 Hz in cooling/heating ramps at a rate of 3 °C/min, and a strain amplitude of 1 %. The frequency dependences of G' and G'' of a sample at selected temperatures were obtained by frequency sweep tests from 0.1 to 100 Hz at a strain amplitude of 1 %.

5.2.8 Triggered Release of Nile Red from a Hybrid Agarose Hydrogel Embedded with Nile Red-Loaded PEO-*b*-PDPAEMA Micelles

A stock solution of Nile Red in acetone with a concentration of 0.71 mg/g (25 μL) was added into a pre-weighed vial using a microsyringe. The weight of the vial plus the solution was measured immediately. The vial was then dried under high vacuum for 3 h at 55 °C. The stock solution of PEO-*b*-PDPAEMA micelles (1.005 g, 10 mg/g) was added into the vial. The solution was diluted to a polymer concentration of 2.0 mg/g by adding a 1× PBS buffer (pH 7.4). The nominal concentration of Nile Red was 8.5×10^{-6} M. The mixture was then sonicated for 30 min and kept in the fridge overnight prior to use. A portion of the Nile Red-loaded PEO-*b*-PDPAEMA micelle solution (2.561 g) was mixed with 2.539 g of a 2.0 wt% agarose solution in the same buffer. The final concentrations of PEO-*b*-PDPAEMA micelles and agarose were 1.0 mg/g and 1.0 wt%, respectively. A portion of the mixture (2.000 g) was transferred into a glass tube and stored in a refrigerator overnight to obtain the Nile Red-loaded hybrid hydrogel. 3.000 g of a 20 mM KHP buffer (pH 3.3) was added onto the top of the hybrid agarose hydrogel. In a control experiment, a 1× PBS buffer (pH 7.4) was added onto the top of another hybrid gel formed by the same procedure. The fluorescence emission intensity of Nile Red from the gel zone was monitored as a function of time for both samples.

5.3 Results and Discussion

5.3.1 Synthesis of PEO-*b*-PDPAEMA

The pH-responsive block copolymer PEO-*b*-PDPAEMA was synthesized by atom transfer radical polymerization (ATRP) from a PEO macroinitiator, PEO-Br. The solvent

used for the polymerization and purification was acetone. Taking advantage of the difference in the solubility of PEO-*b*-PDPAEMA in acetone at different temperatures, the same solvent was used to dissolve the polymer at room temperature and to precipitate it at -78 °C in an acetone/dry ice bath. The SEC trace of the purified block copolymer PEO-*b*-PDPAEMA is shown in Figure 5.1a. The $M_{n,SEC}$ and PDI were 12.6 kDa and 1.06, respectively, indicating that the polymerization was controlled. Figure 5.1b shows the ^{1}H NMR spectrum of the obtained PEO-*b*-PDPAEMA. The degree of polymerization (DP) of PDPAEMA in the block copolymer was calculated by using the DP of PEO and the integral values of the peaks from 4.10 to 3.40 ppm (-COOC*H*$_2$- of DPAEMA units and C*H*$_2$C*H*$_2$O- of PEO) and the peak from 3.20 to 2.85 ppm (-N(C*H*CH$_3$CH$_3$)$_2$ of DPAEMA units) on the NMR spectrum. The calculated DP of PDPAEMA was 31.

5.3.2 Dynamic Light Scattering Study of pH-Induced Dissociation of PEO-*b*-PDPAEMA Micelles

We first studied the stability of PEO-*b*-PDPAEMA micelles in response to pH changes by dynamic light scattering. A 1.0 mg/g PEO-*b*-PDPAEMA micelle solution with a pH of 7.40 was prepared by the solvent switching method. To change the pH, 1.0 M HCl was injected into the micelle solution via a microsyringe in a stepwise fashion. At each pH, a small portion of the solution was taken out and filtered for DLS measurements. As shown in Figure 5.2, at pH = 7.40, the micelles had a hydrodynamic diameter of 33 nm and a single size distribution. The scattering intensity was high (~140 kcps). Upon decreasing the pH to 7.20, while the size of micelles remained the same, the scattering intensity decreased slightly. At pH = 7.00, the average hydrodynamic diameter increased to 65 nm, and two size distributions were observed. The scattering intensity decreased

188
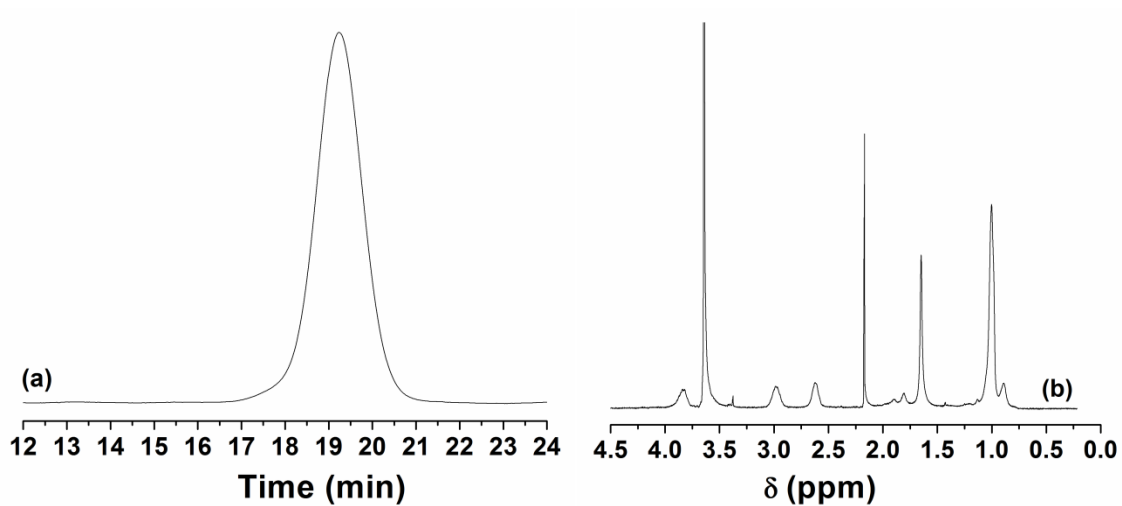
Figure 5.1 (a) SEC trace of PEO-*b*-PDPAEMA. DMF was used as solvent in the SEC analysis. (b) ^{1}H NMR spectrum of PEO-*b*-PDPAEMA. CDCl$_3$ was used as solvent in the ^{1}H NMR spectroscopy analysis.
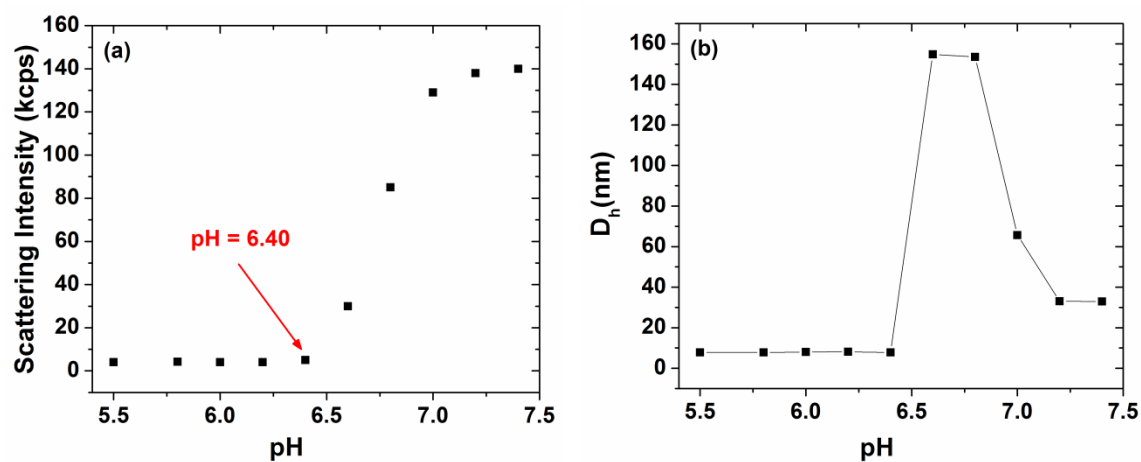
Figure 5.2 Scattering intensity at scattering angle of 90° (a) and apparent hydrodynamic size D_h (b), obtained from CONTIN analysis, as a function of pH in a dynamic light scattering study of a 1 mg/g solution of PEO-*b*-PDPAEMA in a 1× PBS buffer.

appreciably. At pH = 6.80 and 6.60, the hydrodynamic size jumped to 150 nm with a single distribution. The scattering intensity dropped sharply. When the solution pH was decreased to 6.40 and below, the scattering intensity dropped to below 5 kcps and an average size of 7.8 nm was observed. The values of these two parameters indicated that a unimer state was reached. It also clearly indicated that the micelle-to-unimer transition was complete at pH = 6.40.

The reasons for micelle dissociation and the change of the hydrodynamic size upon lowing pH are presented in the following. At high pH, the tertiary amine groups in the PDPAEMA block were deprotonated and therefore insoluble, while the PEO block remained soluble in water. The hydrophobic PDPAEMA block thus formed the core with the hydrophilic PEO block being the corona. It is worth mentioning that the self-assembly process sacrifices the entropy of single chains, but prevents a larger enthalpy penalty that results from the energetically unfavorable hydrophobe-water interactions, and therefore lowers the total free energy of the system. At low pH, the PDPAEMA block was protonated and therefore became soluble. As a result, the micelles dissociated. It was observed from the DLS study that upon lowering pH from 7.40 to 7.00, and 6.60, the hydrodynamic size changed from 33 nm (one distribution), to 65 nm (two distributions), and to 150 nm (one distribution), respectively. The change in size is likely due to the change in the hydrophobicity of PDPAEMA.[39]

5.3.3 Fluorescence Spectroscopy Study of pH-Induced Dissociation of PEO-*b*-PDPAEMA Micelles

Fluorescence spectroscopy was also employed to study the pH-induced dissociation of PEO-*b*-PDPAEMA micelles. Nile Red, which is hydrophobic, was used as the

fluorescent probe. Nile Red was loaded into the micelles of PEO-*b*-PDPAEMA. The fluorescence emission spectra of Nile Red at various pH values were recorded.

Figure 5.3 shows the emission spectra of Nile Red and the maximum emission intensity (MEI) as a function of pH. From pH 7.40 to 7.00, the emission spectra almost overlapped and the MEI dropped only very slightly. These results were in agreement with the DLS data (scattering intensities at pH = 7.40, 7.20, and 7.00) shown in Figure 5.2a. When the pH was decreased to 6.80 and 6.60, the MEI dropped sharply (Figure 5.3b). When pH reached 6.40 and below, the MEI was nearly zero, indicating that the PEO-*b*-PDPAEMA micelles were dissociated and Nile Red was completely released. Thus, the results from fluorescence spectroscopy further confirmed that the pH value for complete dissociation of micelles was 6.40.

5.3.4 Rheological Properties of Pure and Hybrid Agarose Gels

We then studied whether the incorporation of PEO-*b*-PDPAEMA micelles would affect the rheological properties of agarose hydrogels. A set of hybrid agarose hydrogels embedded with different amounts of PEO-*b*-PDPAEMA micelles was prepared. Their rheological properties were characterized. Dynamic time sweep and strain sweep experiments were first conducted to determine the gelation time and the linear viscoelastic regime of the gel. Afterwards, cooling and heating ramps as well as frequency sweep experiments were conducted for pure and hybrid agarose hydrogels to investigate the effect of the incorporation of block copolymer micelles on the properties of agarose hydrogels.

As described in the experimental section, an agarose solution was loaded onto the bottom plate of the rheometer in a liquid form at room temperature. The solution gelled
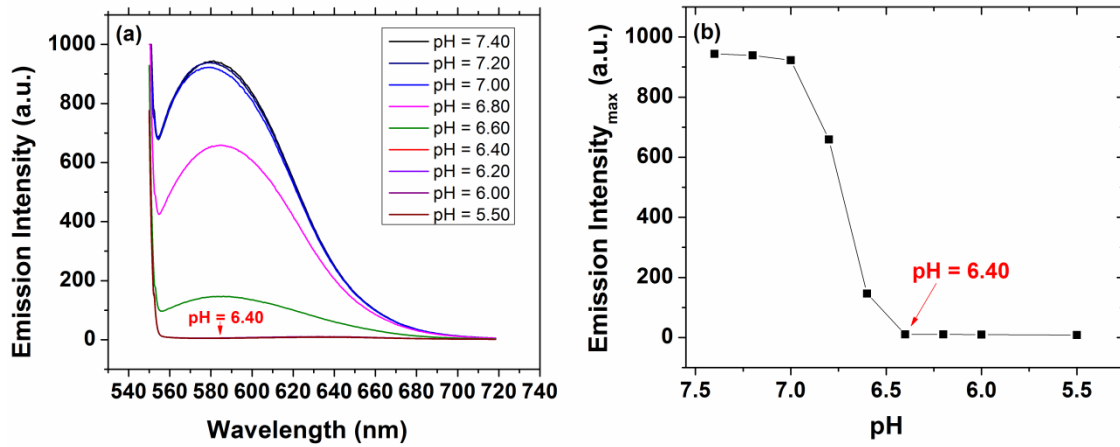
Figure 5.3 (a) Fluorescence emission spectrum of Nile Red in aqueous solutions of PEO-*b*-PDPAEMA with a concentration of 1 mg/g at various pH values. (b) Plot of maximum fluorescence intensity of Nile Red versus pH.
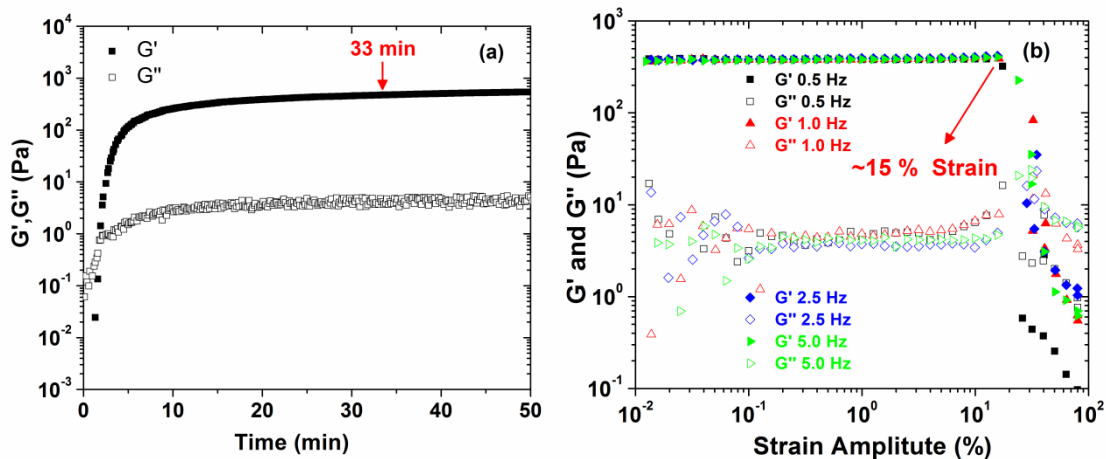
Figure 5.4 (a) Dynamic storage modulus (G') and dynamic loss modulus (G'') as a function of time for a 1 wt% agarose solution in a $1\times$ PBS buffer (pH 7.4) upon cooling the sample from 25 to 2 °C and maintaining at 2 °C. A strain amplitude of 1.0 % and a frequency of 1 Hz were used. The cooling rate was 3 °C /min. (b) Dynamic strain amplitude sweeps at frequencies of 0.5, 1.0, 2.5, and 5.0 Hz for a 1 wt% agarose hydrogel. The experiments were conducted at 2 °C after the agarose gel was formed on the bottom plate of the rheometer.

upon cooling. Figure 5.4a shows the dynamic storage modulus G' and loss modulus G'' as a function of time when the sample was cooled from 25 °C to 2 °C and kept at 2 °C. In the first several minutes, both G' and G'' increased sharply with the increase of time. G' quickly became larger than G'', indicating the formation of a gel. The temperature quickly reached 2 °C during this period. After 5 min, both G' and G'' did not increase significantly; a plateau was reached for each of them. It was found that there was essentially no change after 33 min. Therefore, we chose 33 min as the cooling time for all samples. To determine the linear viscoelastic regime, we then conducted dynamic strain sweep experiments at 0.5 Hz, 1.0 Hz, 2.5 Hz, and 5.0 Hz. The data are shown in Figure 5.4b. Clearly, the linear range was up to 15 % strain. Therefore, a 1 % strain amplitude was employed in the following dynamic experiments.

We first studied the rheological properties of a 1 wt% pure agarose gel. A 1 wt% aqueous solution of agarose was loaded onto the plate of the rheometer at 25 °C. After a short equilibration at 25 °C, the sample was cooled to 2 °C at a cooling rate of 3 °C/min and maintained at 2 °C for 25 min. A heating ramp was then started from 2 to 60 °C. The same procedure was applied to hybrid hydrogels with the same concentration of agarose but different amounts of PEO-*b*-PDPAEMA micelles (0.5, 1.0, 2.0, and 5.0 mg/g). Figure 5.5 shows the cooling and heating ramps of a pure 1 wt% agarose gel and four hybrid gels. The shapes of cooling and heating ramps of five samples are similar. If the temperature at which $G' = G''$ is taken as the melting temperature, then it is 51.5 °C for the 1 wt% pure agarose gel, 50.8 °C for the gel with 0.5 mg/g PEO-*b*-PDPAEMA micelles, 50.2 °C for the gel with 1.0 mg/g micelles, 49.2 °C for the gel with 2.0 and 5.0 mg/g of micelles. The melting temperature decreased slightly. The G' values at various
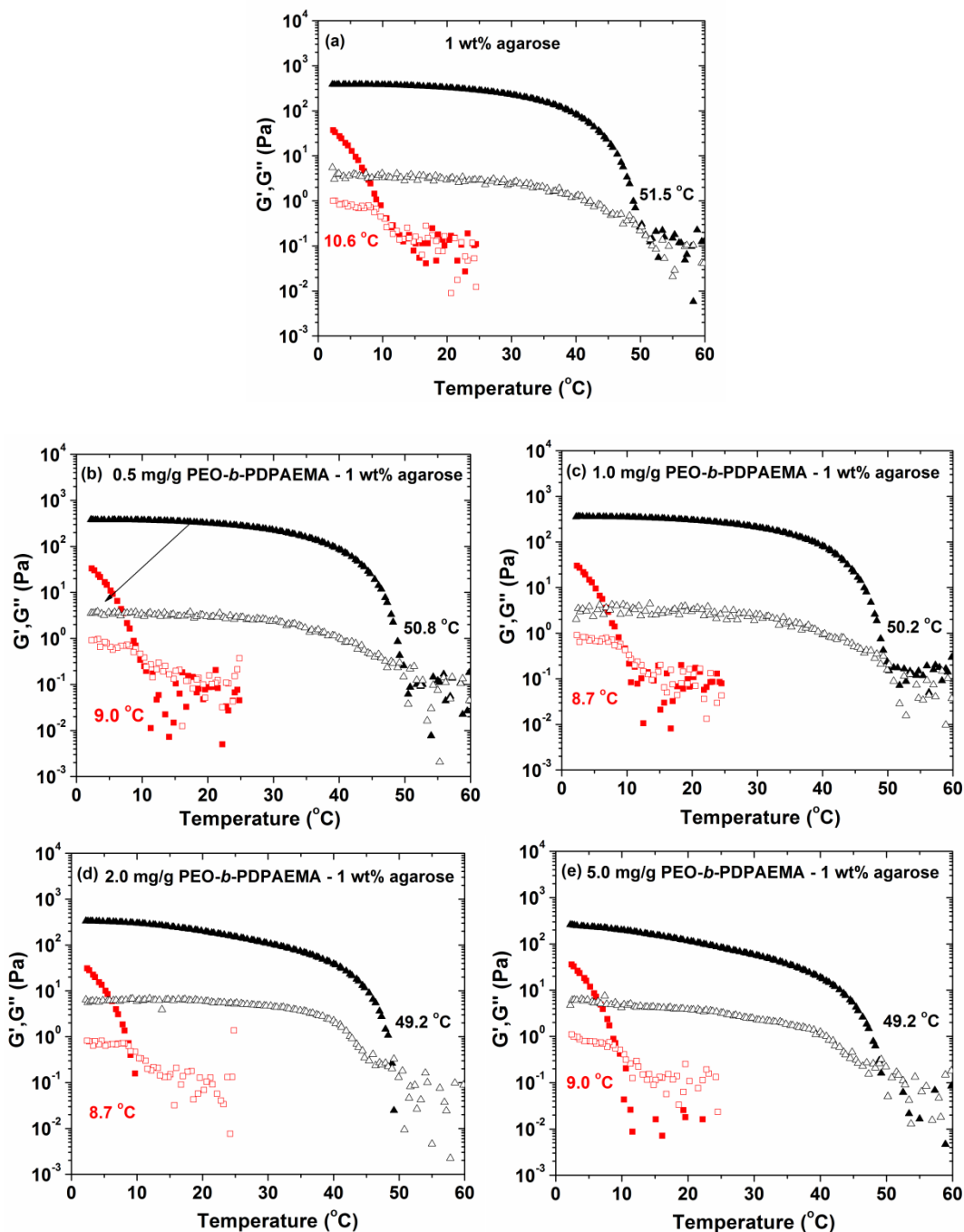
Figure 5.5 Dynamic storage modulus *G*' (solid black triangle and solid square) and loss modulus *G*'' (hollow symbols) of 1 wt% agarose gel with a concentration of PEO-*b*-PDPAEMA micelles of (a) 0, (b) 0.5, (c) 1.0, (d) 2.0, and (e) 5.0 mg/g. The samples were first cooled from 25 to 2 °C (showed in red square) and then equilibrated at 2 °C for 25 min. The whole process took about 33 min. The samples were then heated to 60 °C (showed in black triangle). A cooling/heating rate of 3 °C/min, a strain amplitude of 1.0 %, and a frequency of 1 Hz were used.

temperatures of five samples from heating curves are summarized in Table 5.1. With the concentration of PEO-*b*-PDPAEMA micelles increasing from 0, to 0.5, and to 1.0 mg/g, the *G*' values at 2, 25, and 37 °C remained essentially the same. Further increasing the micelle concentration to 2 mg/g and 5 mg/g, while *G*' values at 2 °C were comparable, the values at 25 and 37 °C decreased. This is likely due to the interaction between the PEO block of PEO-*b*-PDPAEMA and agarose.

To further investigate the effect of block copolymer micelles on the rheological property of agarose gels, frequency sweep experiments were conducted for five samples at 2 °C, 25 °C, and 37 °C. Figure 5.6 shows two sets of representative frequency sweep data of the pure agarose gel and the gel embedded with 1 mg/g micelles. The shapes of the curves of two samples at the same temperature were similar; the values of *G*' at 1 Hz were also close. The curves of other samples are not shown here due to the similarity, but the *G*' values at 1 Hz for all samples at 2, 25, and 37 °C are summarized in Table 5.2. Similar to the observations from heating ramps, *G*' decreased with increasing the concentration of PEO-*b*-PDPAEMA. However, the values at the same temperature were still comparable. These data indicated that the gel properties were not significantly affected by the incorporation of PEO-*b*-PDPAEMA with a concentration up to 5.0 mg/g.

5.3.5 pH-Induced Release of Nile Red in a Hybrid Agarose Gel Embedded with PEO-*b*-PDPAEMA Micelles

Nile Red was used a model substance to study the pH-induced release in a hybrid agarose gel embedded with PEO-*b*-PDPAEMA micelles. An aqueous solution of Nile Red-loaded PEO-*b*-PDPAEMA micelles was mixed with an agarose solution. The final solution contained 1.0 mg/g of block copolymer micelles and 1 wt% agarose. The sample

Table 5.1 *G'* Values at Different Temperatures for a Pure Agarose Hydrogel and Four Micelle-Embedded Agarose Hydrogels

PEO-*b*-PDPAEMA micelles	*G'* at 2 °C (Pa)	*G'* at 25 °C (Pa)	*G'* at 37 °C (Pa)
0 mg/g	389.6	284.5	131.2
0.5 mg/g	384.9	281.2	130.6
1 mg/g	360.5	261.0	122.2
2 mg/g	336.2	150.8	58.7
5 mg/g	262.5	83.0	29.2
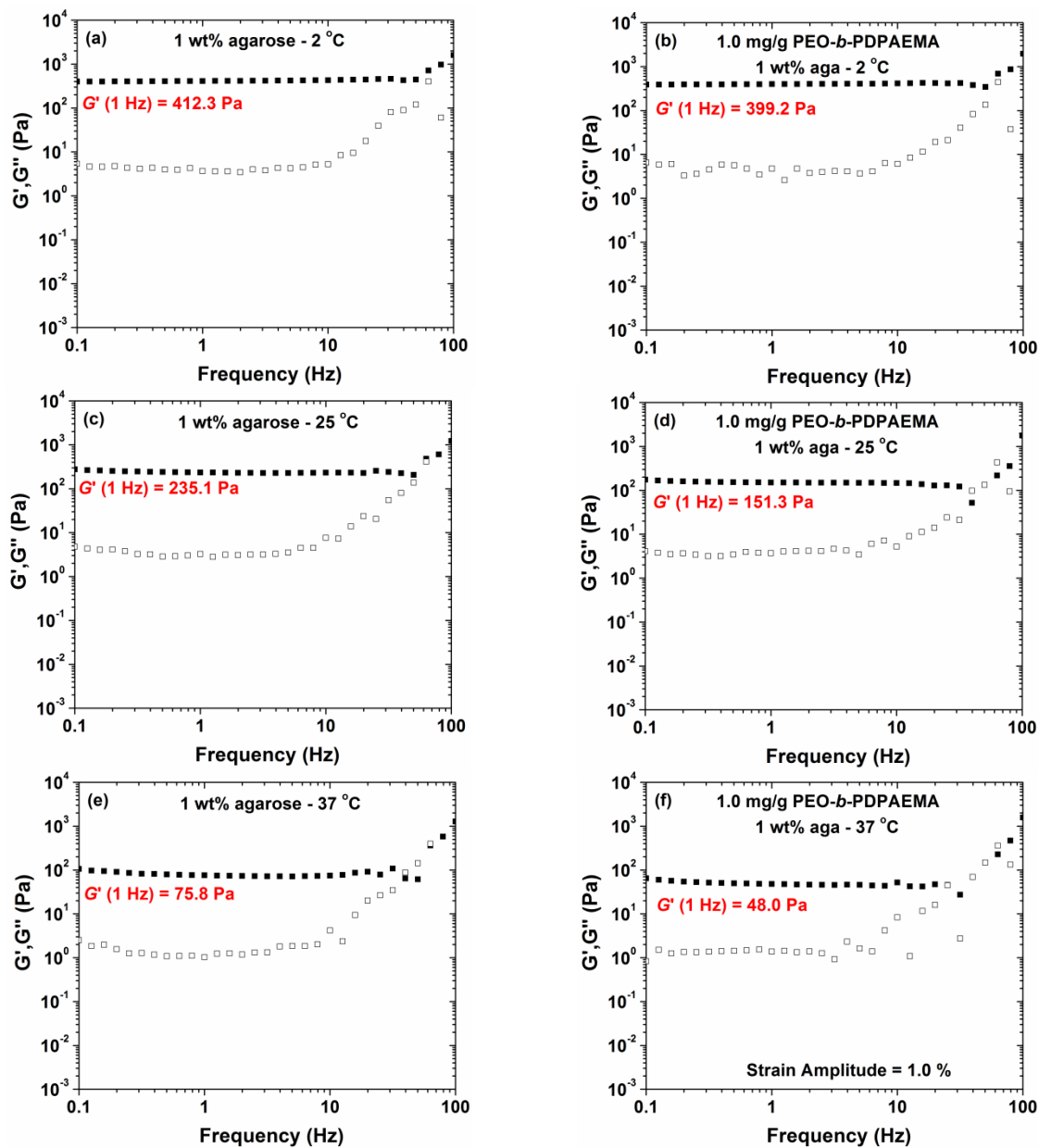
Figure 5.6 Frequency dependences of dynamic storage modulus *G'* and loss modulus *G''* experiments of a 1 wt% pure agarose hydrogel at (a) 2, (c) 25, and (e) 37 °C, and of 1 wt% hybrid agarose hydrogels embedded with 1.0 mg/g PEO-*b*-PDPAEMA micelles at (b) 2, (d) 25, and (f) 37 °C. A strain amplitude of 1 % was used.

Table 5.2 *G'* Values Determined from Frequency Sweep Experiments at Different Temperatures for a Pure Agarose Hydrogel and Four Hybrid Agarose Gels Embedded With Different Amounts of PEO-*b*-PDPAEMA Micelles

PEO-*b*-PDPAEMA micelles	*G'* at 2 °C, 1 Hz (Pa)	*G'* at 25 °C, 1 Hz (Pa)	*G'* at 37 °C, 1 Hz (Pa)
0 mg/g	412.3	235.1	75.82
0.5 mg/g	400.6	198.3	63.24
1 mg/g	399.2	151.3	48.0
2 mg/g	383.7	140.9	45.4
5 mg/g	353.2	112.0	33.7

was pink, similar to the Nile Red-loaded micelle solution. This indicated that Nile Red was still encapsulated in the core of micelles and the micelles were well dispersed in the final solution. The hybrid gel was formed by cooling the sample to 4 °C and keeping it at 4 °C overnight. The gel was pink, suggesting that the Nile Red-loaded PEO-*b*-PDPAEMA micelles were stable in the hybrid agarose hydrogel.

To demonstrate the pH-induced release of Nile Red, we designed the following experiments. Two identical Nile Red-loaded hybrid agarose hydrogels were prepared. A 20 mM KHP buffer with pH of 3.3 was added on the top of one gel, and a 1× PBS buffer (pH 7.4) was loaded onto the top of another gel for a control experiment. The fluorescence emission spectra of both samples at various times were recorded and are shown in Figure 5.7.

For the experiment with a pH = 3.30 buffer placed on top of the hydrogel, the maximum emission intensity decreased gradually over the time. The complete release of Nile Red took about 40 h, indicating that the process was controlled. Note that the sample at the beginning of the experiment was pink, but became transparent after 41 h. For the control experiment, no significant decrease in fluorescent intensity was observed, indicating that the Nile Red-loaded PEO-*b*-PDPAEMA micelles were stable during the period of study.

5.4 Conclusion

A well-defined pH-responsive block copolymer PEO-*b*-PDPAEMA was synthesized by atom transfer radical polymerization from a PEO macroinitiator. Dynamic light
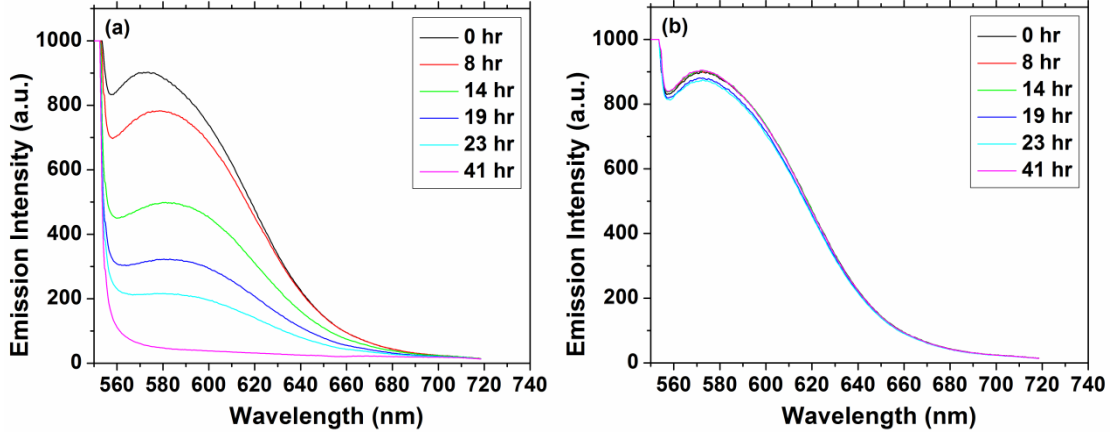
Figure 5.7 Fluorescence emission spectrum of Nile Red as a function of time for hybrid hydrogel with (a) a 20 mM pH = 3.3 KHP buffer solution and (b) a 1× pH = 7.4 PBS buffer solution placed on top.

scattering and fluorescence spectroscopy studies showed that the PEO-*b*-PDPAEMA micelles were completely dissociated when the pH decreased to 6.40. This block copolymer was used to make micelles-embedded hybrid agarose gels. Rheological measurements showed that the gel properties were not significantly affected with the incorporation of PEO-*b*-PDPAEMA micelles up to 5.0 mg/g. To demonstrate the pH-induced dissociation of block copolymer micelles and the controlled release in the hybrid hydrogel, Nile Red was used as a model compound and was loaded into the core of PEO-*b*-PDPAEMA micelles. It was found that when the gel was in contact with a pH 3.30 buffer, Nile Red was completely released after 48 h. In contrast, the Nile Red-loaded micelles were stable in the hybrid gel when a pH 7.4 buffer was placed on the top. Using this system, various substances, such as anti-inflammatory agents and neuroprotective agents, can be integrated into the agarose hydrogels to improve their functions for biomedical applications.

References

1. http://www.ninds.nih.gov/disorders/tbi/detail_tbi.htm

2. Cao, Z.; Gilbert, R. J.; He, W. *Biomacromolecules* **2009**, *10*, 2954–2959.

3. Cajal, S. R. y. *Histology of the Nervous System of Man and Vertebrates*; Oxford University Press: New York, 1995.

4. Bellamkonda, R.; Ranieri, J. P.; Bouche, N.; Aebischer, P. *J. Biomed. Mater. Res.* **1995**, *29*, 663–671.

5. Martin, B. C.; Minner, E. J.; Wiseman, S. L.; Klank, R. L.; Gilbert, R. J. *J. Neural Eng.* **2008**, *5*, 221–231.

6. Jain, A.; Kim, Y. T.; McKeon, R. J.; Bellamkonda, R. V. *Biomaterials* **2006**, *27*, 497–504.

7. Hynd, M. R.; Turner, J. N.; Shain, W. *J. Biomater. Sci., Polym. Ed.* **2007**, *18*, 1223–1244.

8. Arnott, S.; Fulmer, A.; Scott, W. E.; Dea, I. C. M.; Moorhouse, R.; Rees, D. A. *J. Mol. Biol.* **1974**, *90*, 269–284.

9. Dillon, G. P.; Yu, X. J.; Sridharan, A.; Ranieri, J. P.; Bellamkonda, R. V. *J. Biomater. Sci., Polym. Ed.* **1998**, *9*, 1049–1069.

10. Lee, E. S.; Na, K.; Bae, Y. H. *J. Controlled Release* **2003**, *91*, 103–113.

11. Bae, Y.; Fukushima, S.; Harada, A.; Kataoka, K. *Angew. Chem. Int. Ed.* **2003**, *42*, 4640–4643.

12. Lynn, D. M.; Amiji, M. M.; Langer, R. *Angew. Chem. Int. Ed.* **2001**, *40*, 1707–1710.

13. Choi, S. W.; Zhang, Y.; Xia, Y. *Angew. Chem. Int. Ed.* **2010**, *49*, 7904–7908.

14. Jeong, B.; Bae, Y. H.; Kim, S. W. *J. Controlled Release* **2000**, *63*, 155–163.

15. Wang, C.; Chen, Q.; Wang, Z.; Zhang, X. *Angew. Chem.* **2010**, *122*, 8794–8797.

16. Olson, E. S.; Jiang, T.; Aguilera, T. A.; Nguyen, Q. T.; Ellies, L. G.; Scadeng, M.; Tsien, R. Y. *Proc. Natl. Acad. Sci. USA* **2010**, *107*, 4311–4316.

17. Bernardos, A.; Aznar, E.; Marcos, M. D.; Martínez-Máñez, R.; Sancenón, F.; Soto, J.; Barat, J. M.; Amorós, P. *Angew. Chem. Int. Ed.* **2009**, *48*, 5884–5887.

18. Febvay, S.; Marini, D. M.; Belcher, A. M.; Clapham, D. E. *Nano Lett.* **2010**, *10*, 2211–2219.

19. Skirtach, A. G.; Muñoz Javier, A.; Kreft, O.; Köhler, K.; Piera Alberola, A.; Möhwald, H.; Parak, W. J.; Sukhorukov, G. B. *Angew. Chem. Int. Ed.* **2006**, *45*, 4612–4617.

20. Volodkin, D. V.; Skirtach, A. G.; Mohwald, H. *Angew. Chem. Int. Ed.* **2009**, *48*, 1807–1809.

21. Saito, G.; Swanson, J. A.; Lee, K. D. *Adv. Drug Delivery Rev.* **2003**, *55*, 199–215.

22. Li, Y. L.; Zhu, L.; Liu, Z.; Cheng, R.; Meng, F.; Cui, J. H.; Ji, S. J.; Zhong, Z. *Angew. Chem. Int. Ed.* **2009**, *48*, 9914–9918.

23. Zhou, K.; Lu, Y.; Li, J.; Shen, L.; Zhang, G.; Xie, Z.; Wu, C. *Macromolecules* **2008**, *41*, 8927–8931.

24. Riess, G. *Prog. Polym. Sci.* **2003**, *28*, 1107–1170.

25. Lee, E. S.; Shin, H. J.; Na, K.; Bae, Y. H.; *J. Controlled Release* **2003**, *90*, 363–374.

26. Kim, M. S.; Hwang, S. J.; Han, J. K.; Choi, E. K.; Park, H. J.; Kim, J. S.; Lee, D. S. *Macromol. Rapid Commun.* **2006**, *27*, 447–451.

27. Bütün, V.; Armes, S. P.; Billingham, N. C. *Polymer* **2001**, *42*, 5993–6008.

28. Gatenby, R. A.; Gillies, R. J. *Nat. Rev. Cancer* **2008**, *8*, 56–61.

29. Liu, S.; Weaver, J. V. M.; Save, M.; Armes, S. P. *Langmuir* **2002**,*18*, 8350–8357.

30. Coessens, V.; Pintauer, T.; Matyjaszewski, K. *Prog. Polym. Sci.* **2001,** *26***, 337–377.**

31. Braunecker, W. A.; Matyjaszewski, K. *Prog. Polym. Sci.* **2007,** *32***, 93–146.**

32. Wang, J. S.; Matyjaszewski, K. *Macromolecules* **1995**, *28*, 7901–7910.

33. Matyjaszewski, K.; Patten, T. E.; Xia, J. H. *J. Am. Chem. Soc.* **1997,** *119***, 674–680.**

34. Xia, J. H.; Matyjaszewski, K. *Macromolecules* **1997**, *25*, 7697–7700.

35. Shipp, D.A.; Wang, J. L.; Matyjaszewski, K. *Macromolecules* **1998**, *31*, 8005–8008.

36. Davis, K. A.; Matyjaszewski, K. *Macromolecules* **2000**, *33*, 4039–4047.

37. Zhang L.; Eisenberg, A. *J. Am. Chem. Soc.* **1996**, *118*, 3168–3181.

38. Zhang L.; Eisenberg, A. *Polym. Adv. Technol.* **1998**, *9*, 677–699.

39. Mai, Y.; Eisenberg, A. *Chem. Soc. Rev.* **2012**, *41*, 5969–5985.

Chapter 6. Conclusions and Future Work

A series of stimuli-responsive hydrophilic diblock copolymers were synthesized via "living"/controlled radical polymerization, either reversible addition-fragmentation chain transfer polymerization (RAFT) or atom transfer radical polymerization (ATRP). Their solution behaviors were characterized. Chapters 2 to 4 present that the upper temperature boundary, lower boundary, or both boundaries of the sol-gel phase diagrams of moderately concentrated aqueous solutions of doubly thermosensitive diblock copolymers can be tuned by varying the solution pH. The strategy used was to statistically incorporate a small amount of carboxylic acid groups into one or both blocks of thermosensitive diblock copolymers. The hydrophobic/hydrophilic balance of the carboxylic acid-containing block and thus its LCST can be readily modified by changing the solution pH, and thus its LCST. Since the sol-gel or gel-sol transition temperature is related to the LCST of the corresponding block, the sol-gel phase diagram can be tuned by changing the pH of the solution.

Chapter 2 presents the synthesis and characterization of poly(methoxytri(ethylene glycol) acrylate-*co*-acrylic acid)-*b*-poly(ethoxydi(ethylene glycol) acrylate) (P(TEGMA-*co*-AA)-*b*-PDEGEA)).[1] The results showed that with the increase of pH, the upper temperature boundary of the sol-gel phase diagram shifted upward while the lower temperature boundary remained unchanged. Chapter 3 shows that the lower boundary of the sol-gel phase diagram of PTEGMA-*b*-P(DEGEA-*co*-AA) in water in the moderate concentration range moved upward with the increase of pH, while the upper boundary stayed unchanged.[2] Chapter 4 shows that with the incorporation of a small amount of carboxylic acid groups into both blocks of a doubly thermosensitive diblock copolymer, both boundaries of the sol-gel phase diagram can be shifted upward with the increase of

208

pH.[3] The solution behaviors of these diblock copolymers were characterized by dynamic light scattering, differential scanning calorimetry, small-angle X-ray scattering, and rheology. Using pH change as a trigger not only allowed the sol-gel phase diagrams to be tuned precisely and continuously, but also reversibly.

Chapter 5 presents hybrid agarose hydrogels embedded with micelles of a pH-responsive diblock copolymer, poly(ethylene oxide)-*b*-poly(2-(*N*,*N*-diisopropylamino) ethyl methacrylate) (PEO-*b*-PDPAEMA). The hybrid gels were designed and developed to improve the functions of agarose gels as scaffolding materials in tissue engineering. The pH-responsive behavior of PEO-*b*-PDPAEMA was investigated by DLS and fluorescence spectroscopy. The rheological properties of pure and hybrid agarose gels were studied by rheometry. It was found that the gel properties were not significantly affected by the incorporation of PEO-*b*-PDPAEMA micelles with the concentration up to 5.0 mg/g. The pH-induced release behavior in an agarose gel embedded with 1.0 mg/g of PEO-*b*-PDPAEMA micelles was studied by using fluorescence spectroscopy and Nile Red as a model drug.

One possible project along this line of research is to investigate the effect of the molar content of carboxylic acid groups on sol-gel-sol transitions of doubly thermosensitive hydrophilic diblock copolymers. Chapter 3 shows that the sol-to-gel transition temperature of a thermo- and pH-responsive diblock copolymer with 9.1 % carboxylic acid groups in the PDEGEA block changed more sharply with the increase of pH than that of the block copolymer with 4.9 % carboxylic acid in the PDEGEA block. A systematic study can be conducted by incorporating 5 %, 10 %, 15 %, and 20 % carboxylic acid into the PDEGEA, PTEGMA, or both blocks. Their pH-responsive

behavior will be investigated. The results of the work can serve as a guideline for choosing diblock copolymers with a desired pH sensitivity.

References

1. Jin, N. X.; Woodcock, J. W., Xue, C. M.; O'Lenick, T. G.; Jiang, X. G.; Jin, S.; Dadmun, M. D.; Zhao, B. *Macromolecules* **2011**, *44*, 3556-3566.

2. Jin, N. X.; Zhang, H.; Jin, S.; Dadmun, M. D.; Zhao, B. *J. Phys. Chem. B.* **2012**, *116*, 3125-3137.

3. Jin, N. X.; Zhang, H.; Jin, S.; Dadmun, M. D.; Zhao, B. *Macromolecules* **2012**, *45*, 4790-4800.

Vita

Naixiong Jin was born in Beijing, China. He attended Peking University from 2004 to 2008, where he received his B.S. degree in Chemistry while working under Professor Hongwei Ma. After graduation, he enrolled as a graduate student in the Department of Chemistry at the University of Tennessee, Knoxville. He joined Professor Bin Zhao's research group in December, 2008 and worked on stimuli-responsive hydrophilic diblock copolymers. Naixiong Jin received a Doctor of Philosophy Degree in Chemistry from the University of Tennessee in May, 2013.